

Review

# Review on Recent Advances in the Removal of Organic Drugs by Advanced Oxidation Processes

Muhammad Umair, Tayyaba Kanwal, Vittorio Loddo, Leonardo Palmisano  and Marianna Bellardita \* 

Engineering Department, University of Palermo, Viale dell Scienze Ed. 6, 90128 Palermo, Italy; muhammad.umair01@unipa.it (M.U.); tayyaba.kanwal277@gmail.com (T.K.); vittorio.loddo@unipa.it (V.L.); leonardo.palmisano@unipa.it (L.P.)

\* Correspondence: marianna.bellardita@unipa.it

**Abstract:** In recent years, due to the high consumption of drugs both for human needs and for their growing use, especially as regards antibiotics, in the diet of livestock, water pollution has reached very high levels and attracted widespread attention. Drugs have a stable chemical structure and are recalcitrant to many treatments, especially biological ones. Among the methods that have shown high efficiency are advanced oxidation processes (AOPs) which are, among other things, inexpensive and eco-friendly. AOPs are based on the production of reactive oxygen species (ROS) able to degrade organic pollutants in wastewater. The main problem related to the degradation of drugs is their partial oxidation to compounds that are often more harmful than their precursors. In this review, which is not intended to be exhaustive, we provide an overview of recent advances in the removal of organic drugs via advanced oxidation processes (AOPs). The salient points of each process, highlighting advantages and disadvantages, have been summarized. In particular, the use of AOPs such as UV, ozone, Fenton-based AOPs and heterogeneous photocatalysis in the removal of some of the most common drugs (tetracycline, ibuprofen, oxytetracycline, lincomycin) has been reported.

**Keywords:** drug degradation; advanced oxidation processes (AOPs); reactive oxygen species (ROS); heterogeneous photocatalysis; Fenton-based AOPs; sulfate radical-based AOP



**Citation:** Umair, M.; Kanwal, T.; Loddo, V.; Palmisano, L.; Bellardita, M. Review on Recent Advances in the Removal of Organic Drugs by Advanced Oxidation Processes. *Catalysts* **2023**, *13*, 1440. <https://doi.org/10.3390/catal13111440>

Academic Editors: Albin Pintar and Gregor Žerjav

Received: 25 October 2023

Revised: 10 November 2023

Accepted: 11 November 2023

Published: 14 November 2023



**Copyright:** © 2023 by the authors. Licensee MDPI, Basel, Switzerland. This article is an open access article distributed under the terms and conditions of the Creative Commons Attribution (CC BY) license (<https://creativecommons.org/licenses/by/4.0/>).

## 1. Introduction

Water is a fundamental need of human beings, and its main sources are rivers, lakes, aquifers and the desalination of seawater which, however, is exploited in a more limited way. With population growth and industrialization, almost all water sources are contaminated mainly by agricultural and industrial waste. As a result, one of the biggest problems facing humanity in the 21st century may be the sustainable use of water. For the remediation of water pollution, scientific society is attracted to the development of sustainable and green technologies [1].

Due to the rapidly growing demand for various products to treat humans and animals, pharmaceutical companies are expanding significantly. Molecules of pharmacological importance present in drugs are widespread in the environment [2,3]. In seawater, lakes, rivers, surface waters, urban wastewater and drinking water, their concentrations have been found to range between ng and µg per liter [4–6]. Furthermore, it must be kept in mind that, due to their presence, synergistic interactions can occur in these water systems which generally significantly increase ecotoxicity [7].

In this context, drug metabolites are not completely removed, which can increase the concentration of drugs in wastewater from treatment plants [8]. Drugs are difficult to remove from water systems through traditional wastewater treatment methods due to their particularly stable structure which hinders their complete degradation and their high hydrophilic properties [9,10]. Traditional methods such as biological treatment [11], adsorption [12], nanofiltration [13] and membrane bioreactors [14] have been used for

their removal, but these methods are often not very efficient and/or give rise to a transfer of the pollutant rather than its total abatement. Therefore, alternative technologies have been developed.

Among the different methods for drug removal, advanced oxidation processes (AOPs) can be considered economical, flexible and highly efficient methods for destroying persistent organic molecules [15,16]. AOPs are generally known for in situ production of strongly oxidizing species in sufficient quantity and low selectivity such as hydroxyl radicals ( $\text{HO}^\bullet$ ),  $\text{O}_3$ ,  $\text{H}_2\text{O}_2$  and superoxide anion radicals ( $\text{O}_2^{\bullet-}$ ). These species almost always cause complete mineralization to  $\text{CO}_2$ ,  $\text{H}_2\text{O}$  and inorganic compounds of the attacked molecule and, under certain operating conditions, could be preferred from an environmental point of view [17]. For example, they are highly effective in providing clean drinking water free of organic and inorganic substances and microorganisms [18]. The main advantage of AOPs compared to other available methods, however, is that they are completely ecological not only because they do not involve the removal of pollutants from one place to another (think for example of the precipitation of pollutants by chemical substances or their adsorption) but also because they do not produce large quantities of harmful waste [19,20].

Research progress on AOPs has increased significantly over the last 30 years, mainly due to the availability of a significant variety of technologies and numerous application areas. Among the main AOPs, we can mention ozonation, electrolysis, ultrasound, the use of Fenton reagents or various types of membranes, UV-based processes and heterogeneous photocatalysis using near-ultraviolet (UV) or visible light irradiation [21]. Less common but developing methods involve ionizing radiation, microwaves [22] and ferrate reagents. AOPs have been used for a variety of purposes, including odor control, groundwater purification, soil remediation and volatile organic compound treatment, but wastewater treatment is by far the most frequently studied and developed [23,24]. The application of AOPs, however, must be carefully evaluated considering their overall sustainability, chemical input, energy use and feasibility in real systems, comparing their effectiveness and cost with other traditional processes [25].

AOPs can be used alone or in combination with other biological and physico-chemical processes, depending on the properties of the wastewater to be treated and the purposes of the treatment. In principle, process coupling is advantageous because it generally increases the efficiency of the treatment. For example, AOPs could be used as a pre-treatment step to transform originally bio-recalcitrant molecules into other more easily biodegradable species, which would then be subjected to biological post-treatment. However, for drugs containing biodegradable substances, biological pre-treatment following chemical post-treatment might also be desirable since, even if biodegradable substances can be easily eliminated initially, the effectiveness of biodegradation is not comparable to that of a chemical oxidizing treatment [26].

All AOPs involve the in-situ production of the main oxidant species and the consequent combination of these species with contaminants. Reactor design and drug composition have an impact on the formation of reactive species, which are mainly radicals. In addition to radical scavenging, other factors including hydrodynamics and mass transfer of radicals are crucial for effectively destroying drugs [27]. Different types of AOPs are illustrated in Figure 1.

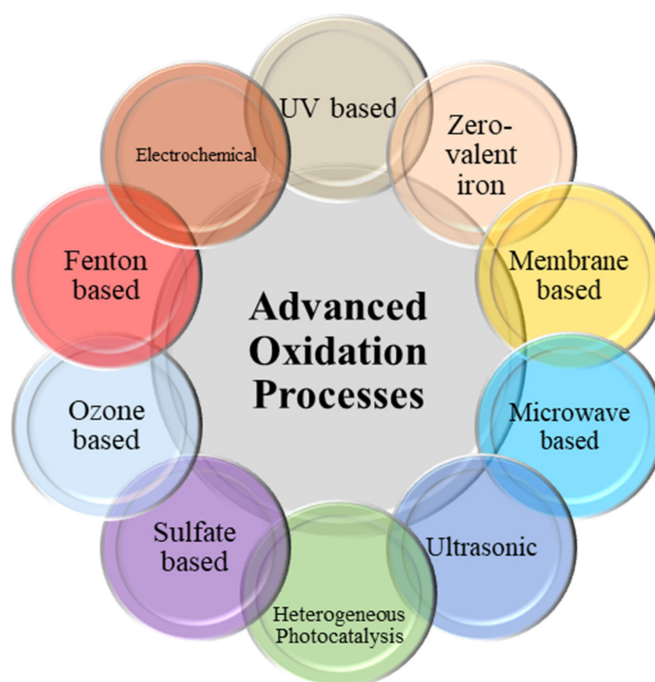


**Figure 1.** Different advanced oxidation processes.

### 1.1. UV-Based AOPs

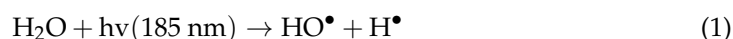
UV-based AOPs are those processes that use ultraviolet (UV) light alone or in the presence of radical promoters for the degradation of organic compounds. Radical-based UV AOPs use only UV light to generate oxidant species, but other processes use  $\text{Cl}_2$  (to generate radicals of the chlorine species and hydroxyl radicals), ozone,  $\text{H}_2\text{O}_2$  and persulfate (to generate sulfate radicals).

Low-pressure Hg vapor lamps with a partial pressure of approximately 1 Pa are the most common UV radiation sources for UV-based AOPs. The efficiency of these lamps is 25–45% in the range of the emitted wavelength. The emission spectra of low-pressure Hg lamps show two distinct lines at approximately 254 and 185 nm. The line emitted at the wavelength of 254 nm is very useful for disinfection. In fact, UV light inactivates microbes which cause damage to DNA or RNA molecules, preventing their reproduction [28].

#### 1.1.1. UV Irradiation

UV irradiation involves the direct interaction between UV light and a target pollutant and the induction of chemical reactions that can break down the pollutant into intermediate products whose subsequent decomposition eventually provides mineral end-products [29,30]. Traditionally, UV treatment has been used to disinfect drinking water with the benefit of limiting the creation of any regulated waste products of disinfection [31].

The homolysis (Equation (1)) and photochemical ionization (Equation (2)) of water are generated through UV light absorption:



The main advantages of the AOP with UV irradiation are that it requires a relatively short time to treat, and the use of chemicals is not necessary, ensuring that no residual substances are produced during the process [1]. The degradation efficiency of drugs under UV light in water depends on several factors. Different types of buffer solutions can be used to modify the pH, but this generally has an important impact on the degradation of

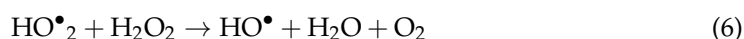
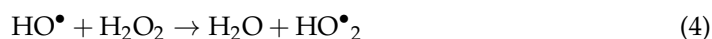
drugs as free radicals may be formed which are linked to the species constituting the buffer and interfere with the degradation mechanism [32].

### 1.1.2. UV/H<sub>2</sub>O<sub>2</sub>

UV/H<sub>2</sub>O<sub>2</sub> is the most used AOP for the degradation of drugs. H<sub>2</sub>O<sub>2</sub> present in solution gives rise to the production of two HO• radical species through the photolytic cleavage of the O-O bond (initiation step) (Equation (3)).



After the formation of two hydroxyl radicals, a chain of reactions is formed (propagation and termination steps) (Equations (4)–(9)) [33].



Some factors, i.e., pH, H<sub>2</sub>O<sub>2</sub> concentration, organic compound structure, HO• formation rate and water contents, influence the efficiency of UV/H<sub>2</sub>O<sub>2</sub> AOP. At alkaline pHs, the absorption of CO<sub>2</sub> from the air increases, so the reaction should be carried out in a closed vessel to counteract this effect. The decrease in pH has a direct effect on the concentration of carbonate and bicarbonate ions resulting from the absorption of CO<sub>2</sub>; therefore, the effectiveness of the process can increase as the amount of HO• radicals in the solution increases [1].

### 1.1.3. UV/Chlorine

The UV/chlorine process is an interesting AOP because the chlorine (Cl<sub>2</sub>) used in water is a common disinfectant and UV-activated chlorine radicals (Cl•) are formed. Chlorine dioxide (ClO<sub>2</sub>) and the hypochlorite radical (ClO•) are the two main oxidizing species [34]. This method involves the addition of a sodium salt (Na<sup>+</sup> + ClO<sup>−</sup>) to an aqueous solution, and ClO<sup>−</sup> is also present as the protonated form HClO (pK<sub>a</sub> = 7.52), depending on the pH values. This system involving an acid–base equilibrium is known as active chlorine (AC) [35]. The chlorine radical prefers to react with electron-rich molecules, so it is a more selective oxidant than the hydroxyl radical [36]. This method is generally useful for the treatment of wastewater with low pH values [37]. Indeed, pH significantly influences the molar absorption coefficient as the ratio between HOCl and ClO<sup>−</sup> can change significantly.

Below are the main equations (Equations (10)–(12)) representing the process. Under UV light irradiation of an aqueous HClO solution, HO• and Cl• radicals are obtained [38,39] (Equation (10)). These highly reactive radicals subsequently interact with HClO to form the chlorine monoxide radical (ClO•) (Equations (11) and (12)).



Various types of active species such as HO•, AC, Cl• and ClO• coexist and often act in a complementary manner for efficient degradation of the pollutant. HO•, which is a selective oxidant, reacts at approximately the same rate with the organic species present [40]. Cl•, which is more selective, reacts with electron-rich organic components via H-abstraction, one-electron oxidation and addition to unsaturated C-C bonds. Cl• is very reactive towards benzoic acid and phenol, compared to the HO• radical [41]. In conclusion, the UV/chlorine AOP is more efficient than the UV/H<sub>2</sub>O<sub>2</sub> AOP for the removal of drugs such as tolytriazole, iopamidole and benzotriazole [42].

#### 1.1.4. UV/O<sub>3</sub>

Ozone (O<sub>3</sub>) in combination with UV light irradiation increases the concentration of HO• radicals, improving drug removal efficiency. During the reaction, the by-product H<sub>2</sub>O<sub>2</sub> is formed which, however, can in turn decompose into two HO• radicals [43,44]. Equations (13) and (14) summarize these reactions:

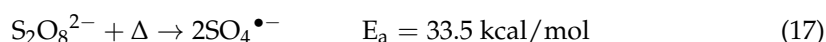
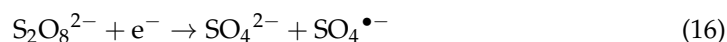
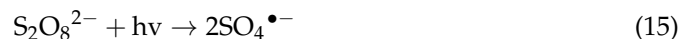


O<sub>3</sub> at extremely high concentrations can act as a radical scavenger and interact with them or give rise to secondary reactions by decomposing and inhibiting the oxidation process. It can react directly and electrophilically with the organic compounds to be broken down or indirectly through a radical reaction. However, the main reaction in the UV/O<sub>3</sub> system is the interaction of HO• with the organic pollutant because the direct oxidation rate with molecular O<sub>3</sub> is slower [45].

#### 1.1.5. UV/SO<sub>4</sub>•<sup>-</sup>

SO<sub>4</sub>•<sup>-</sup> is a strong mono-electronic oxidant that shows higher degradation efficiency than HO• under neutral and alkaline conditions due to its higher redox potential and longer lifetime [46]. These electrophilic radicals can rapidly oxidize some aromatic compounds through the abstraction of hydrogen atoms and the transfer of single electrons [47]. Compared to HO•, SO<sub>4</sub>•<sup>-</sup> can easily promote electron transfer but at a slower rate than the extraction and addition of hydrogen atoms [48]. pH is a crucial factor in oxidation in the presence of SO<sub>4</sub>•<sup>-</sup> for drug degradation. In fact, the production of HO• and sulfate radicals increases with an increase in the pH, but it must be considered that the increase in these radicals involves their interaction with OH<sup>-</sup> and causes an overall decrease in the reaction rate [49].

Sulfate radicals can be produced using peroxydisulfate (PS) or peroxymonosulfate (PMS). The radicals, in particular, can be generated from PS through its homolytic cleavage by UVC radiation (Equation (15)), in the presence of a photocatalyst which provides the photoproduced electron (Equation (16)) or heat (that can be also generated by microwaves) (Equation (17)).



#### 1.1.6. Advantages and Disadvantages of UV-Based AOPs

In Table 1 the main advantages and disadvantages of UV-based AOPs are reported.

**Table 1.** Advantages and disadvantages of UV-based AOPs.

Process	Advantages	Disadvantages	References
UV	Absence of limitation of mass transfer Disinfection No bromate formation No need for off-gas treatment Potential to use sunlight	Cost- and energy-intensive Fouling of UV lamps UV light penetration decreases in presence of iron and nitrate Interference with chemical compounds	[50]
UV/H <sub>2</sub> O <sub>2</sub>	High stability of H <sub>2</sub> O <sub>2</sub> Long-time storage ability Availability for drinking water treatment on full scale	UV light penetration is impacted by turbidity Special reactors are needed for UV light Residual H <sub>2</sub> O <sub>2</sub> must be considered	[51]
UV/chlorine	Cl• radical is a more selective oxidant than HO• radical More efficient than UV/H <sub>2</sub> O <sub>2</sub> Additional chlorine to quench residual H <sub>2</sub> O <sub>2</sub> is not needed Cost-effective Favorable at low pH	Impact on efficiency of UV light due to suspended particles	[52] [53] [1]
UV/O <sub>3</sub>	O <sub>3</sub> absorbs more UV light as compared to H <sub>2</sub> O <sub>2</sub> The presence of UV light has a disinfectant effect The residual oxidant quickly deteriorates	Intensive energy required Cost-intensive Special reactors required Stripping of volatile compounds Blocking of UV light penetration due to turbidity Mass transfer limitation due to diffusion	[51]
UV/SO <sub>4</sub> <sup>•−</sup>	Efficient at moderate pH conditions Efficient electron transfer reaction mechanism High standard reduction potential	Toxicity of by-products Presence of unreacted chemicals Metal contamination	[54] [55]

## 1.2. Ozone-Based AOPs

### 1.2.1. O<sub>3</sub>/H<sub>2</sub>O<sub>2</sub>

The combination of O<sub>3</sub> with H<sub>2</sub>O<sub>2</sub> is an efficient method for the degradation of organic drugs. This method is also known as peroxone in which the decomposition of O<sub>3</sub> takes place after the production of HO<sub>2</sub><sup>−</sup> from H<sub>2</sub>O<sub>2</sub> (Equations (18) and (19)) [56].



It is important that neither an excessive quantity nor a too-low quantity of H<sub>2</sub>O<sub>2</sub> is used because an excessive quantity can cause a decrease in HO• species with the formation of HO•<sub>2</sub> (Equation (20)) and a too-low quantity can be insufficient for oxidizing organic drugs while achieving dissociation of the H<sub>2</sub>O<sub>2</sub> molecule (Equation (21)):



### 1.2.2. Catalytic Ozonation

In this process, catalysts react with O<sub>3</sub>, increasing the degradation rate of drugs by generating HO• radicals following the decomposition of O<sub>3</sub> [57]. Homogeneous catalytic ozonation involves the use of different transition metal ions (Mn<sup>2+</sup>, Ni<sup>2+</sup>, Co<sup>2+</sup>, Cr<sup>2+</sup>,

$\text{Ag}^{2+}$ ,  $\text{Zn}^{2+}$ ,  $\text{Cd}^{2+}$ ,  $\text{Fe}^{2+}$ ,  $\text{Cu}^{2+}$ ) which function as catalysts for the degradation of organic drugs [58].

Ozone decomposition performance improves in the presence of highly stable heterogeneous catalysts which consequently can be recycled and reused without prior further treatment after the first use. Because of these advantages, heterogeneous catalytic ozonation is often used to treat aqueous effluents. In addition to the nature of the catalyst, in particular, its surface chemical–physical characteristics, and the pH of the solution, which influence the properties of the surface catalytic sites, the degradation processes of ozone in water is extremely important for the performance of catalytic ozonation [59]. The main heterogeneous catalysts used in coupling with  $\text{O}_3$  are  $\text{TiO}_2$  [60],  $\text{MgO}$  [61],  $\text{MnO}_2$  [62],  $\text{ZnO}$  [63],  $\text{SiO}_2$  [64] and  $\text{CuFe}_2\text{O}_4$  [65].

### 1.2.3. Electro-Peroxone

In recent years, researchers have been attracted to electrochemical methods for water treatment. Advantages over traditional methods are, for example, the possibility of obtaining chemicals on site and often easy maintenance and reliable performance [66].

The electro-peroxone (E-peroxone) process is a new AOP that is a combination of traditional electrolysis and ozonation.  $\text{H}_2\text{O}_2$  is produced in situ inside an electrolytic device which allows its quantity in the reaction medium to be controlled. This avoids the transport, management and storage of this chemical product which is dangerous and explosive [35]. The polluting drugs to be treated are present in a reactor equipped with a carbon-based cathode which converts the ozone (in reality it is a mixture of  $\text{O}_3$  and  $\text{O}_2$ ) coming from the generator and present in the effluent into  $\text{H}_2\text{O}_2$  through an electrochemical reaction (Equation (22)). The  $\text{H}_2\text{O}_2$  formed reacts with  $\text{O}_3$  to produce  $\text{HO}^\bullet$  radicals which play a major role in drug degradation (Equation (23)) [67–70].



### 1.2.4. Advantages and Disadvantages of Ozone-Based AOPs

In Table 2 the main advantages and disadvantages of ozone-based AOPs are reported.

**Table 2.** Advantages and disadvantages of ozone-based AOPs.

Process	Advantages	Disadvantages	References
$\text{O}_3/\text{H}_2\text{O}_2$	Highly effective Highly efficient Handling of remediation Disinfection	Bromate formation Energy- and cost-intensive Excess $\text{H}_2\text{O}_2$ may need to be managed due to potential microbial growth The concentration of $\text{O}_3\text{-H}_2\text{O}_2$ must be properly controlled	[51]
Catalytic ozonation	Low operating cost No need for pH adjustment Complete mineralization Improved $\text{O}_3$ utilization efficiency Enhanced reaction kinetics Production of $\text{HO}^\bullet$ radicals at low pH	Challenge for selection of green, cost-effective and efficient catalysts Complex synthesis of ozone catalysts Reuse of catalysts Fouling of catalysts Challenge of residual toxicity	[71] [72]
Electro-peroxone	Economical, convenient and safe method Low sludge formation Highly efficient for low reactive ozone species No secondary pollution On-site production of $\text{H}_2\text{O}_2$	Energy-intensive Lower current efficiency Not particularly efficient for pesticide degradation	[73] [74] [75] [76]

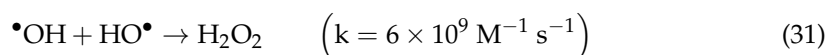
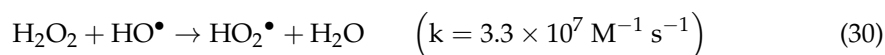
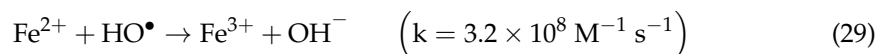
### 1.3. Fenton-Based AOPs

#### 1.3.1. Fenton-like Process

The Fenton process involves the formation of HO• radicals through a series of reactions of H<sub>2</sub>O<sub>2</sub> with Fe(II) salts. The reagent system is called the Fenton reagent [77,78] (Equations (24) and (25)).



A hydrogen atom of the organic drug to be treated (R-H) is extracted by the HO• radicals to produce an organic radical (R•) which gives rise to a chain reaction up to the final oxidation products (Equations (26)–(28)). H<sub>2</sub>O<sub>2</sub> and Fe<sup>2+</sup> should oxidize the drug to H<sub>2</sub>O and CO<sub>2</sub> (and to inorganic species deriving from the possible presence of heteroatoms in the molecule) even without the presence of HO•/R•, radicals, obviously with different kinetics. However, it must be considered that the HO• radicals produced can be further involved in subsequent reactions which have a negative effect on the oxidation reactions (Equations (29)–(31)):



The optimal pH at which one must operate with the Fenton reagent must be between 3 and 5 as under neutral and near-neutral pH conditions, Fe<sup>3+</sup> would react with HO•, producing insoluble ferric hydroxide which would separate from the solution. Consequently, the efficiency of the oxidation process would decrease, and continuous addition of Fe<sup>2+</sup> ions should be necessary.

Finally, it should be noted that there is still a different hypothesis regarding the oxidizing species and their production. Without wanting to go into detail, referring to the specific papers, we only mention the possibility of the involvement of the high-valence ferryl-oxo species Fe(IV), instead of HO• radicals, and in that case, Equation (24) can be replaced with the following Equation (32):



#### 1.3.2. Photo-Fenton

In the photo-Fenton process (PFP), under UV irradiation, the reaction of H<sub>2</sub>O<sub>2</sub> with Fe<sup>2+</sup> occurs, producing HO• radicals in quantities sufficient for oxidizing drugs. The operating mechanism of this process involves the photochemical regeneration of Fe<sup>2+</sup> ions through the photoreduction of Fe<sup>3+</sup> ions (Equation (33)). In particular, when all the Fe<sup>2+</sup> ions are used in the Fenton reaction, the Fe<sup>3+</sup> ions start to accumulate in the solution, and the reaction stops. The use of light, however, allows the cycle to continue as the Fe<sup>2+</sup> ions which are necessary for the reaction with H<sub>2</sub>O<sub>2</sub> are photochemically reformed [77,79,80].



In the case of post-treatment of raw leachate, it should be noted that the concentration of total dissolved solids (TDSs) and the degree of turbidity significantly influence the performance of UV irradiation [81].

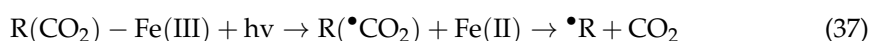
### 1.3.3. Electro-Fenton

The electro-Fenton process (EFP) is considered an efficient method for the degradation of drugs based on electrocatalytic in situ generation of hydroxyl radicals. It can be conducted in two different setups. In the first case, the ferrous ions are introduced into the reactor from the outside and H<sub>2</sub>O<sub>2</sub> is produced at the cathode (Equation (34)). In the second possible configuration, also Fe<sup>2+</sup> ions are produced in situ using cast iron sacrificial anodes (Equation (35)). EFP has some advantages over the traditional Fenton process; this method, in fact, allows better control of the process and does not require the transport or storage of H<sub>2</sub>O<sub>2</sub> [82,83]. Furthermore, the electro-Fenton process is environmentally friendly and does not produce any harmful pollutants [84]. The main weakness of EFP is the operating cost, principally the chemical cost, when used on a practical scale.



### 1.3.4. Photoelectro-Fenton

The photoelectro-Fenton process (PEFP) is a combination of photochemical and electrochemical processes with the Fenton process. This method involves UVA light and the electrochemical production of H<sub>2</sub>O<sub>2</sub> which is used for the treatment of wastewater. The photoreduction of Fe(III) occurs, producing a high amount of HO• radicals and Fe(II) (Equation (36)). Fe(III) can form complexes with some organic compounds present in solution that absorb in the near-UV and visible region. In this way, they can be decarboxylated under irradiation (Equation (37)) [85–87].



### 1.3.5. Advantages and Disadvantages of Fenton-Based AOPs

In Table 3 the main advantages and disadvantages of Fenton-based AOPs are reported.

**Table 3.** Advantages and disadvantages of Fenton-based AOPs.

Process	Advantages	Disadvantages	References
Fenton-like process	<ul style="list-style-type: none"> <li>Fe<sup>2+</sup> is non-toxic and widely available</li> <li>No formation of chlorinated products</li> <li>No limitation of mass transfer</li> <li>H<sub>2</sub>O<sub>2</sub> is easy to handle</li> <li>Complex formation enhances the coagulation of suspended solids</li> </ul>	<ul style="list-style-type: none"> <li>Sludge may formed</li> <li>Scavenging reactions may occur</li> <li>Regeneration of Fe<sup>2+</sup> is very low</li> </ul>	[88]
Photo-Fenton	<ul style="list-style-type: none"> <li>High efficiency</li> <li>Wide pH range</li> <li>Low sludge formation</li> </ul>	<ul style="list-style-type: none"> <li>Cost- and energy-intensive</li> <li>Blocking of UV radiation due to turbidity of water</li> <li>Formation of oxalate layers on the surface of lamps</li> <li>Medium- or high-pressure lamps are required</li> </ul>	[89] [90]

Table 3. Cont.

Process	Advantages	Disadvantages	References
Electro-Fenton	High oxidation efficiency High mineralization On-site production of reagents to generate H <sub>2</sub> O <sub>2</sub> Ability to treat effluents with a wide range of concentrations and ease of handling	Cost-intensive Inefficient for treatment with large-scale volumes	[91] [90]
Photoelectro-Fenton	Regeneration of Fe <sup>2+</sup> Production of HO• radicals High mineralization No need to separate the catalyst Possibility of using solar light	No commercial availability of photoanodes Visible-light-active photoanodes are required Large-scale reactors are required Cost of artificial light irradiation	[92]

#### 1.4. Ultrasonic Methods

In water, ultrasonic radiation that is emitted at values >20 kHz generates HO• radicals that induce the degradation of pollutants by means of the so-called ultrasonic method (US). A process known as acoustic cavitation is used in the US and causes bubbles to form, grow and collapse in liquids due to the extremely high temperatures and pressures created within them [93]. The US is also known as sonolysis (Equation (38)) [94].



Sonolysis is a fairly recent method for drug degradation, and therefore, it has not received much attention compared to other AOPs. There are very few publications on it. The degradation of many poorly soluble and very volatile organic drugs occurs rapidly, and consequently, this method could be useful for attacking pharmaceutical micropollutants. The efficiency of the US depends on several factors such as the type of drug, the intensity and frequency of the ultrasound, the temperature and the configuration of the reactor [26].

In Table 4 the main advantages and disadvantages of sonolysis are reported.

Table 4. Advantages and disadvantages of sonolysis.

Process	Advantages	Disadvantages	References
Sonolysis	High degradation efficiency Low energy required No need for chemicals No sludge waste Safe method Penetrability in aqueous medium Economical for small-volume treatments	Probe maintenance is required Turbidity of water Energy-intensive	[94] [95] [96]

#### 1.5. Membrane-Based AOPs (M-AOPs)

Many organic micropollutants are not mineralized completely or to any great extent using a single traditional or advanced oxidation process. To improve degradation efficiency and successfully remove organic micropollutants, the combined use of different methods operating synergistically in hybrid systems has been proposed as an alternative approach [97,98]. Membrane processes such as distillation, nanofiltration and reverse osmosis can be applied for the removal of organic drugs from water or wastewater. However, in separation using membranes, contaminants are simply transferred to a concentrated phase but are not transformed or mineralized. Furthermore, during the filtration process, the membrane can deteriorate due to fouling and obtaining retentate in large quantities [99]. Taking this into account, the coupling of filtration processes and AOPs has recently been proposed as a strategy for the treatment of polluted effluents [51].

In an M-AOP, the AOP has the primary role of degrading the target drug into less hazardous contaminants. The membrane plays a secondary role because it simply allows the passage through it of the less dangerous species obtained after the action of the AOP that, moreover, can prevent fouling and keep the membrane in the best possible operating condition.

Combined M-AOP filtration systems can be classified into different categories, depending on the type of AOP used and how the formation and oxidizing action of HO• radicals occur in the reaction medium. An interesting proposal involves using the AOP method to oxidize complex drug target molecules and then performing membrane filtration to separate the oxidized products. The type of membrane to be selected depends on the properties of the effluent and the size of the oxidized substrate to be separated, ultimately depending on the type of oxidizing reaction. The ability of membranes to couple with AOPs is still under discussion, considering in particular the polymeric ones that could be sensitive to heat, chemical attacks and irradiation, especially for long operating times [51].

In Table 5 the main advantages and disadvantages of Membrane-Based AOPs are reported.

**Table 5.** Advantages and disadvantages of membrane-based AOPs.

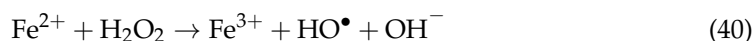
Process	Advantages	Disadvantages	References
Membrane-based AOP	Membrane captures the unoxidized contaminants and only allows safe, treated water to pass through The concentrated unoxidized contaminants on the membrane surface greatly accelerate their decomposition in the presence of AOPs By ozonating the membrane surfaces, membrane fluxes and permeability can be improved	Fouling of membranes Low stability of membranes (especially some polymeric membranes) for long irradiation times	[51] [100]

### 1.6. Electrochemical AOPs

Electrochemically based AOPs are called electrochemical advanced oxidation processes (EAOPs) and can be used for wastewater treatment. In EAOPs HO• radicals are formed directly (anodic oxidation (AO)) or indirectly via the Fenton reagent (electro-Fenton (EF)). In AO, oxidation of water occurs and produces HO• radicals at an anode having a high O<sub>2</sub> overvoltage (Equation (39)) [101].



In turn, EF involves the reaction providing HO• radicals between the Fenton reagent and H<sub>2</sub>O<sub>2</sub> which is produced electrochemically at the cathode (Equation (40)) [102].



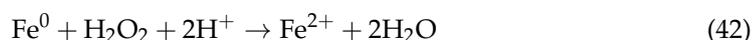
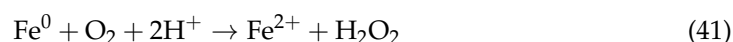
The type and quantity of reactive species created during an EAOP depend on various factors. The main ones are the composition of the polluted water, the material from which the electrodes are made and the applied potential [103]. The advantages and disadvantages of the method are shown in Table 6.

**Table 6.** Advantages and disadvantages of electrochemical AOP.

Process	Advantages	Disadvantages	References
Electrochemical AOPs	No need for light radiation	Cost- and energy-intensive Requires management of sludge-related electrocoagulant and indirect oxidation Limitation of mass transfer Poisoning effect	[51]
	Good energy efficiency		[96]
	No chemical required		
	No waste produced		
	Highly efficient as compared to other AOPs		
	Eco-friendly		
	Easy of handling		
Possibility to treat effluent with COD in the range 0.1–100 g L <sup>-1</sup>		[104]	

### 1.7. Zero-Valent Iron

Zero-valent iron (ZVI) is a very promising material, abundant, cheap, easy to produce and practically non-toxic. Therefore, it can be successfully used to degrade drugs [105,106]. The electrons that are produced directly by ZVI react with the molecules of the drug to be broken down and transform them into less dangerous contaminants. ZVI in the presence of dissolved oxygen (DO) can oxidize various organic pollutants because ZVI provides two electrons to O<sub>2</sub>, producing H<sub>2</sub>O<sub>2</sub> (Equation (41)) which can further react with two electrons also provided by ZVI and can transform into H<sub>2</sub>O (Equation (42)). The strongly oxidizing HO• radicals produced by the reaction of Fe<sup>2+</sup> and H<sub>2</sub>O<sub>2</sub> (Equation (43)), as in many other methods, are ultimately responsible for the attack on drugs and their degradation [107]:



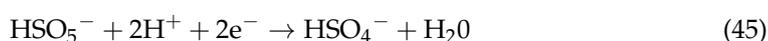
In Table 7 the advantages and disadvantages of zero-valent iron are reported.

**Table 7.** Advantages and disadvantages of zero-valent iron.

Process	Advantages	Disadvantages	References
Zero-valent iron	No sludge formation	Low stability	[108]
	Complete degradation	Fast passivation	[109]
	No formation of undesirable by-products	Limited mobility	

### 1.8. Sulfate Radical-Based AOPs

As an alternative to HO• radicals, sulfate radical (SO<sub>4</sub>•<sup>-</sup>)-based AOPs have been extensively studied for wastewater treatment. SO<sub>4</sub>•<sup>-</sup> radicals are produced from two strong oxidants, namely persulfate (also called peroxydisulfate (PS)) and peroxymonosulfate (PMS), whose oxidation potentials are 2.1 and 1.82 eV, respectively. Their decomposition is illustrated in Equations (44) and (45) [54,110]:



Persulfate, in particular, is a promising oxidant as it is quite stable at room temperature and is not very selective for drug degradation. The activation of PS and PMS to produce SO<sub>4</sub>•<sup>-</sup> radicals can occur in various ways using heat, UV light, ultrasound, alkali, transitional ions or metal oxides [111,112].

In Table 8 the advantages and disadvantages of Sulfate-Based AOPs are reported.

**Table 8.** Advantages and disadvantages of sulfate-based AOPs.

Process	Advantages	Disadvantages	References
Sulfate-based AOPs	Wide pH range (2–8)	Cost-intensive Challenge of residual sulfate ions Potential to form toxic by-products	[110] [113]
	Less need for reactants		
	High selectivity		
	High redox potential		
	Easy availability of reactant		
On large scale, safe storage of oxidants			

### 1.9. Microwave-Based AOPs

Electromagnetic radiation within the frequency range of 0.3 to 300 GHz is referred to as microwave (MW) radiation. To prevent interference with cellular phone and telecommunication frequencies, all microwave reactors used for chemical synthesis and home kitchen microwave ovens operate at 2.45 GHz [114]. In the last few years, the use of MW irradiation has been widely studied in environmental applications such as wastewater and sewage treatment, soil remediation and biomedical applications [115–117] due to its rapid and uniform heating, “hot spot” effect and nonthermal effect. Although the use of microwaves alone was found to be not very efficient for drug removal, their combination with other AOPs is very promising because can it allow the mineralization of any organic pollutant [22,118–120]. MW-based AOPs (MW-AOPs) include mainly MW-enhanced photochemistry, MW-enhanced Fenton process, MW-activated persulfate, MW-assisted ultrasonic and MW-assisted ozone [121–124], and in these cases, MW radiation enhances the formation of ROS active species (such as  $\text{HO}^\bullet$ ,  $\text{SO}_4^{\bullet-}$ ,  $\text{O}_2^{\bullet-}$ ), improving the process performance. The drawback is that MW-AOPs are currently only used on a laboratory scale, and furthermore, cost analyses have revealed their economic limitations [119].

### 1.10. Heterogeneous Photocatalysis

The heterogeneous photocatalysis AOP has been extensively studied over the past two decades and applied to drug degradation. This method appears to be more effective than other AOPs since some semiconductors are generally less expensive and non-selective, i.e., they can easily mineralize a large variety of toxic organic molecules [125,126]. The optoelectronic properties of a photocatalyst that behaves as a semiconductor depend on the energy of the conduction band (CB) and that of the valence band (VB). The energy difference between the two bands, called the bandgap, corresponds to the energy difference between the bottom of the conduction band and the top of the valence band. This value is between 1.0 and 4.0 eV in semiconductors, and therefore, thermal or light stimulation can increase the conductivity by transferring electrons from the valence band to the conduction band [1].

In heterogeneous photocatalysis, activation can be caused by irradiating the semiconductor with solar or artificial light. It must be considered that semiconductors and reagents are in two different phases. When a semiconductor is irradiated by light of an appropriate energy, the photoexcitation of electrons from the VB to the CB occurs, with the formation of positive holes in the VB. The photoproduced electrons and holes migrate to the surface of the catalyst and act as reducing and oxidizing agents, respectively. The holes can directly oxidize the species adsorbed on the surface of the photocatalyst or interact with the adsorbed water in the case of aqueous solutions producing  $\text{HO}^\bullet$  radicals. The latter, in turn, attack the polluting molecules found near the surface or adsorbed on nearby sites. The molecules can be attacked in subsequent steps and are transformed into non-toxic products until complete mineralization into  $\text{H}_2\text{O}$  and  $\text{CO}_2$  and any inorganic ions containing heteroatoms present in the degraded organic molecule [111]. The photo-

catalytic mechanism of drug degradation is reported as follows (Equations (46)–(52)) and in Figure 2:

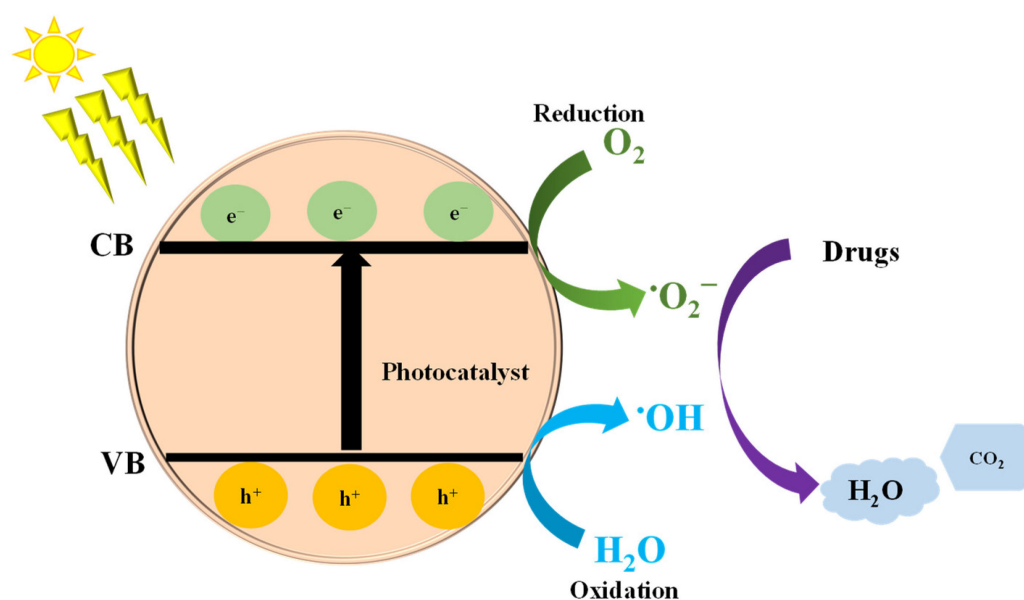
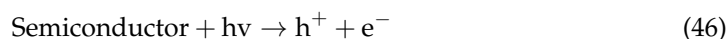


**Figure 2.** Photocatalytic mechanism of drug degradation.

$\text{O}_2^{\bullet-}$  and  $\text{HO}^\bullet$  radicals react with a drug and transform it into other less harmful products.



$\text{TiO}_2$  is the most studied and used semiconductor for drug abatement due to its high chemical and thermal stability, wide availability, non-toxicity, cost-effectiveness and corrosion resistance [126]. However,  $\text{TiO}_2$  has limitations due to its wide bandgap (3.0 eV and 3.2 eV in the case of the rutile and anatase polymorphs, respectively) and poor activity under the irradiation of sunlight (which contains only 4–5% of energetically effective photons for its excitation). Consequently, considerable efforts have been made to improve the performance of  $\text{TiO}_2$ -based photocatalysts for practical applications, mainly through modifications and/or combinations with other semiconductors [127,128].

In Table 9 the advantages and disadvantages of heterogeneous photocatalysis are reported.

**Table 9.** Advantages and disadvantages of heterogeneous photocatalysis.

Process	Advantages	Disadvantages	References
Heterogeneous photocatalysis	Active under the irradiation of near-UV light, compared to other AOPs which require shorter wavelengths Possibility for the use of sunlight as a clean and free energy source Mild operating conditions Non-toxicity of the catalysts Photochemical stability	Fouling of the catalyst The powdered photocatalyst needs to be recovered when employed as a slurry or suspension High recombination rates of photogenerated electrons and holes Mass transfer limitation Poor efficiency when using low lighting	[51] [95] [96]

### 1.11. Advanced Reduction Processes (ARPs)

Advanced reduction processes (ARPs) combine both activation methods and reducing agents to form highly reactive reducing radicals that can degrade oxidized contaminants. In order to determine the most efficient ARPs, different studies were carried out by applying several combinations of activation methods (ultraviolet light, ultrasound, electron beam and microwaves) and reducing agents (dithionite, sulfite, ferrous iron and sulfide) for the degradation of target contaminants at different pH-levels [129]. Many studies have been also carried out on reactions involving reducing free radicals [130], but only a few examples of the applications of reducing radicals to water treatment/contaminant degradation are present in the pertinent literature.

Ibrahim et al. [131], for the first time, expanded the concept of advanced reduction processes to green chemistry procedures. Indeed, they synthesized and characterized binary nanocomposites of TiO<sub>2</sub> nanotubes with CoFe<sub>2</sub>O<sub>4</sub> ferrites and used them for the photocatalytic reduction of 4-nitrophenol to 4-aminophenol. Successively, ARPs have been used to degrade chlorinated organic contaminants such as 1,2-dichloroethane [132] and for the degradation of persistent pollutants such as per- and polyfluoroalkyl substances (PFASs) in water [133]. The degradation was achieved by coupling various advanced reduction processes that combine ultraviolet (UV) irradiation with various reagents (dithionite, sulfite, sulfide, ferrous iron). ARPs are capable of reducing the toxicity of the solution but do not lead to complete mineralization of the drugs.

Yu et al. [134] applied both advanced oxidation and reduction processes to the degradation of diclofenac and compared the reaction mechanism and the residual toxicity. Some of the intermediates formed by the two processes are different. Notably, with an AOP, a less efficient reduction in toxicity is accomplished, and with ARP, a higher irradiation dose is necessary. Similar results were found during the degradation of tetracyclines [135].

## 2. Factors That Affect the Degradation Efficiency

There are many factors that influence the degradation efficiency of drugs, such as pH, the initial concentration of the molecule to be degraded, the quantity of catalyst and the temperature.

### 2.1. pH

The pH is an important factor because varying the electrical charge of the functional groups on the surface of the catalyst due to the presence of an excess of HO• (basic pH values) or an excess of H<sup>+</sup> (acidic pH values) in the solution produces various types of degradation products. In other words, therefore, changing the pH of the solution alters the surface charge of the semiconductor and shifts the potential of surface chemical reactions. In addition to the electrochemical/thermodynamic reasons, it must be considered that the reaction rate is also significantly influenced by the adsorption of drugs on the surface of the semiconductor. The degree of adsorption and the strength with which the reacting species adsorb depend greatly on the surface charges which in turn depend on the pH [136].

## 2.2. Initial Concentration of Drug

The initial concentration of the drug in the solution also plays an important role in its degradation during the photocatalytic reaction. In general, keeping the amount of catalyst constant, the degradation rate decreases as the drug concentration increases [137]. It must be kept in mind that an excessive concentration of the drug to be degraded could slow down the reaction because the molecules would not have sufficient sites available to adsorb and be attacked by oxidizing radicals.

## 2.3. Amount of Catalyst

The amount of photocatalyst also has an important influence on drug degradation. In heterogeneous photocatalysis, an increase in the degradation rate of the substrate is observed as the amount of catalyst increases. This is because a larger surface area has more active sites and therefore more HO• radicals that can contribute to drug degradation. However, after a certain limit that depends on the type of solid and the solution in which it is suspended, the degradation efficiency begins to decrease as the catalyst increases. In fact, the radiation is partially shielded due to the excessive turbidity of the solution and the formation of particle aggregates with a consequent decrease in surface area [138].

## 2.4. Temperature

The effect of temperature has a limited effect on heterogeneous photocatalysis used to degrade drugs dissolved in aqueous effluents. An increase in it can increase the recombination rate of the photoproducted charges and favor the desorption of the reactive species adsorbed on the surface, causing a decrease in the photocatalytic efficiency [125]. However, a moderate increase could favor the desorption of some types of products, increasing the efficiency of the process (especially in gas–solid systems), and in this case, there is an optimal temperature even higher than the ambient one at which the experiments should be carried out.

## 2.5. Dosage of Reactive Oxygen Species (ROS)

During the application of AOPs, the concentration of ROS influences the extent of conversion/mineralization of the drugs, the reaction mechanism, and the reaction rate. The degradation of tetracycline in the presence of increasing amounts of peroxydisulfate (PS) showed a volcano-like trend [139]. First, the degradation rate increased with the PS concentration due to the enhanced production of SO<sub>4</sub>•<sup>−</sup> radicals, but when the PS concentration became high, the TC degradation rate began to decrease because some SO<sub>4</sub>•<sup>−</sup> radicals could be scavenged by PS.

The selection of an appropriate O<sub>3</sub> amount is very important for the degradation of drugs. The increase in ozone up to a certain amount generally has a beneficial effect because it improves the generation of HO• radicals [56]. The behavior is not general and depends on the rate at which a drug is interacted with. Drugs can be easily degraded with a low dosage of ozone if they react with molecular ozone quickly, and a higher dosage is necessary if the reaction of a drug with ozone is difficult [140].

It is important also to use the optimum amount of H<sub>2</sub>O<sub>2</sub> because an excess amount can lead to the formation of unwanted by-products and a low amount does not produce enough HO• to obtain the complete mineralization.

## 2.6. Water Matrix

In an actual water matrix, different species such as natural organic matter (NOM), dissolved organic matter (DOM) and inorganic ions are abundantly present and affect the degradation of drugs in a positive or negative way [141,142]. When ionic species interact with drugs, they can be transformed into high-redox-potential radicals boosting the reaction rates, or they can function as free radical scavengers slowing down the degradation rate. Moreover, in the presence of a catalyst, they can compete with organic compounds for the

same adsorption sites. Depending on the existence of promoting and inhibiting compounds, the water matrix may be crucial.

### 3. Strategies for Improving the Efficiency of AOPs: Use of Nanomaterials and/or Coupling with Conventional Techniques

Nanotechnology is very promising for treating polluted aqueous effluents and in general for environmental remediation through the development of AOPs. In fact, the notable reduction of toxic by-products is favored, and this is essential to meet water quality standards [143]. Furthermore, nanotechnology can offer economic advantages over conventional techniques, thanks to industrial production and new methods that use inexpensive raw materials and reduce energy use. In particular, the use of nanoparticles which increase the efficiency of the treatment is envisaged [144]. The beneficial role of the nanoparticles is mainly due to the increase in surface area, although the quantum size effect cannot be neglected, which can be summarized very briefly in the fact that if the particle size of a semiconductor decreases to the nanometric level, a widening of the bandgap occurs with a consequent shift of the light absorption to higher energy (blue shift) [145].

Dendritic polymers, metal/metal oxide nanoparticles, zeolites and carbon-based nanomaterials are essential for wastewater degradation, as they contain multi-branched chains and can more efficiently adsorb organic pollutants and heavy metals.

Nanomaterials combined with AOPs offer great potential to achieve a significant improvement in water treatment by not only removing contaminants but also transforming them into non-harmful compounds or compounds that can be easily degraded. However, most AOPs combined with nanomaterial-based methods are still under investigation, and further investigation and development are needed to increase their potential [146].

In the next paragraphs, we will report very briefly on some innovative oxidation processes for the treatment of contaminated water which may also involve the use of nanomaterials. They are characterized by relatively low costs and high efficiency [147].

#### 3.1. UV/H<sub>2</sub>O<sub>2</sub> Processes

The UV/H<sub>2</sub>O<sub>2</sub> process in the presence of nanomaterials is a promising technology for the abatement of organic pollutants in water since the small size of the nanomaterials increases the degradation efficiency due to the increase in surface area [148].

In fact, the UV/H<sub>2</sub>O<sub>2</sub> process, due to its low molar absorption coefficient, cannot effectively degrade pollutants as complete mineralization is often not achieved. Moreover, combining this process, for example, with TiO<sub>2</sub> nanoparticles, which function as a photocatalyst, can significantly improve efficiency [149]. Notably, the UV/H<sub>2</sub>O<sub>2</sub>/TiO<sub>2</sub> process, when combined with ZnO nanoparticles, increases the degradation rate even further with the production of a higher amount of active radical species [150].

It should be noted, however, that the presence of nanoparticles, which are difficult to separate from the system due to their small size, can complicate the execution of the process and can constitute a further element of pollution. Another drawback when ZnO is used in water is the anodic photo-oxidation to which this material is subjected which depends on the pH and causes the formation of soluble ionic species of zinc in the system to be purified.

#### 3.2. Persulfate-Based Processes

Sulfate radicals are effective for removing organic pollutants from aqueous solutions. The use of magnetic iron oxide nanoparticles (MNPs) to obtain sulfate radicals from persulfate is a promising technology due to their wide availability and not only their magnetic characteristics but also their specific structural and catalytic properties. Furthermore, the excellent ferromagnetic behavior of Fe<sub>3</sub>O<sub>4</sub> makes it easily separable from the solution [151]. Other nanomaterials such as ferrite-carbon aerogel, cobalt, iron, Co<sub>3</sub>O<sub>4</sub>/graphene oxide, CoFe<sub>2</sub>O<sub>4</sub>/titanate nanotubes, Co-MnO<sub>4</sub> and  $\alpha$ -MnO<sub>2</sub> are proposed as promising heterogeneous catalysts for persulfate activation [144].

### 3.3. Coupling of AOPs with Conventional Water Treatment Techniques

While it is clear that several AOPs are effective at removing drugs, most AOPs are generally considered to be expensive techniques. To address this problem, the combination of advanced oxidation treatments with conventional water treatment technologies is suggested in some studies, although practical applications for large volumes of real effluent have not yet been seen [152].

Coupling of AOPs has been reported to improve the quality of the effluent prior to discharge to the environment, as demonstrated by a recent study demonstrating that the effluent is safer when ozone and sonolysis are coupled for the degradation of amoxicillin in water [152].

Furthermore, the coupling of heterogeneous photocatalysis with membrane technology constitutes another interesting example in terms of studies. The membrane, in fact, can perform the function of keeping the pollutant in the presence of the photocatalyst for longer during its degradation, preventing its permeation or the loss of the photocatalyst if the system is continuous. Another possibility is to allow the permeation of a useful intermediate with high added value before its further oxidation in the reagent system [153]. For this type of coupling, it is essential to appropriately choose the type of membrane and photocatalyst in relation to the process to be performed [154–156].

## 4. Use of AOPs for Drug Degradation

### 4.1. Tetracycline

The elimination of tetracycline (TC) by AOPs has been by far the most studied due to the widespread use of this molecule (it has been found in wastewater, surface water and groundwater at  $\text{ng L}^{-1}$  to  $\mu\text{g L}^{-1}$  levels) and its high stability and resistance in aqueous wastewater [157]. For these reasons, very often, the use of a single method is not effective in eliminating TC, and the coupling of different technologies is necessary [158,159]. The main problem related to the degradation of drugs is their partial oxidation to compounds which are often more harmful than their precursors. Unfortunately, in many papers, the degradation of drugs is evaluated but not their complete mineralization. The most used AOP methods are UV, UV/H<sub>2</sub>O<sub>2</sub> treatments and heterogeneous photocatalysis.

The first photochemical oxidation of TC was reported in 1979 by Davies et al. [160], who studied the behavior of TC under UV light irradiation. The authors demonstrated that the process proceeds in several steps through the photo-deamination of TC followed by the interaction of the formed tetracycline radical with molecular oxygen forming a peroxy radical, which abstracts a hydrogen atom, giving rise to a hydroperoxide. Finally, the hydroperoxide decomposes, losing water. Figure 3 presents a scheme showing the possible degradation route of TC and some of the intermediates that can be formed during its degradation. López-Peñalver et al. [161] investigated the aqueous degradation of TC in the presence of UV and UV/H<sub>2</sub>O<sub>2</sub> by changing the initial concentration and initial solution pH and by adding H<sub>2</sub>O<sub>2</sub>. The degradation rate turned out to be dependent on the initial concentration and pH; TC degradation by UV radiation alone was low, and the addition of H<sub>2</sub>O<sub>2</sub> before UV treatment increased the quantum yield of the reaction, also reducing the final TOC concentration and the toxicity of the by-products.

Photo-Fenton degradation of TC has been successfully carried out by using a magnetically recoverable MnFe<sub>2</sub>O<sub>4</sub>/MXene hierarchical heterostructure [159]. The uniform dispersion of MnFe<sub>2</sub>O<sub>4</sub> nanoparticles within MXene nanosheets enhanced the visible light utilization and avoided the agglomeration of the MnFe<sub>2</sub>O<sub>4</sub> particles. A TC degradation efficiency of 93.8% was reached at pH = 3 starting from a drug concentration of 10 mg L<sup>-1</sup>.

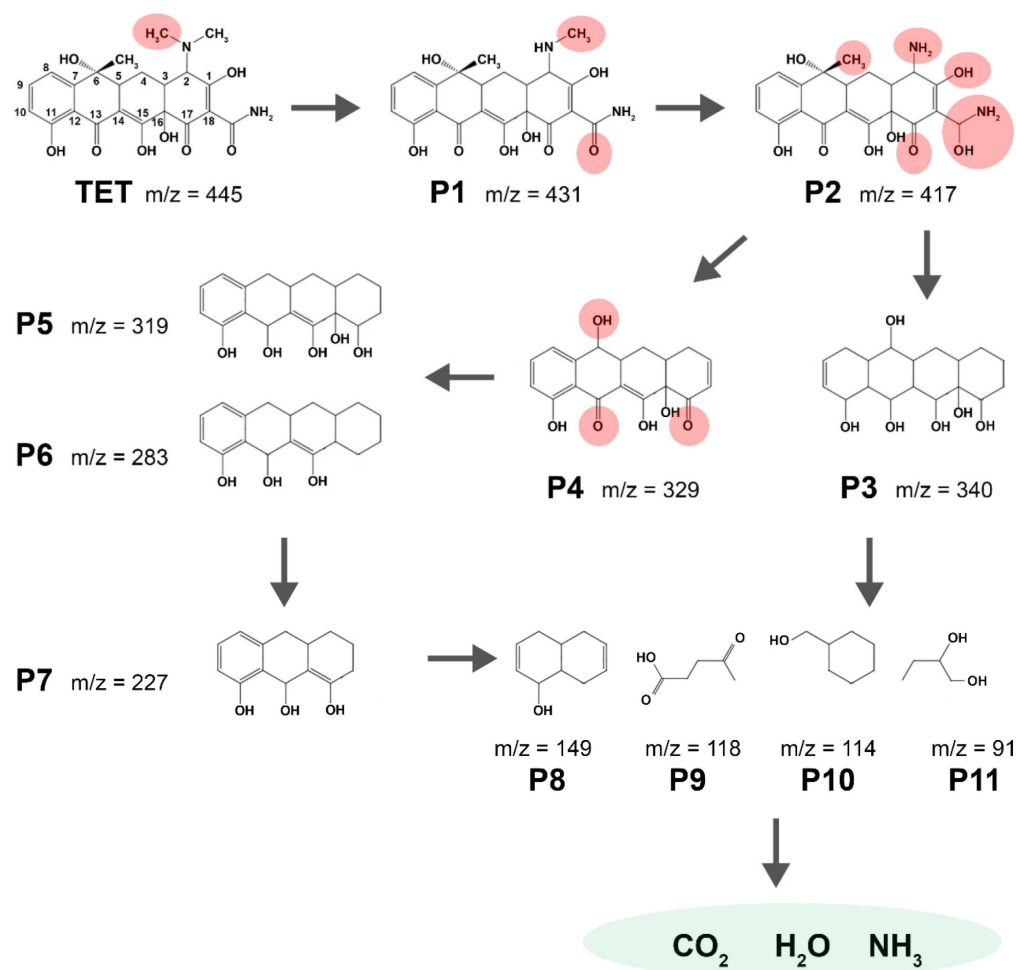


**Figure 3.** Scheme showing the possible degradation route of TC [162].

The photo-Fenton method has been used effectively for the complete mineralization of various types of antibiotics. As seen in more detail in Section 1.3.2, hydroxide radicals are produced due to the reaction between hydrogen peroxide and ferrous salt. In particular, this treatment allowed the removal of  $24 \text{ mg L}^{-1}$  of TC with a residual TOC concentration of  $5 \text{ mg L}^{-1}$  and  $2 \text{ mg L}^{-1}$  under black-light and solar irradiation, respectively, according to Bautiz and Nogueraiv [163].

The photo-Fenton treatment of  $40 \text{ mg L}^{-1}$  of TC solution under UV irradiation in the presence of  $\text{H}_2\text{O}_2$  (48% of stoichiometric dose) and  $\text{Fe}^{2+}$  ( $5 \text{ mg L}^{-1}$ ) allowed the total degradation of the drug and 77% TC mineralization [164]. An innovative 3D porous hydrogel composed of  $\alpha\text{-FeOOH/rGO}$  (reduced graphene oxide) was able to generate reactive oxygen species in the absence of  $\text{H}_2\text{O}_2$ , eliminating 97.3% of TC in a Fenton-like process [165].

Liu et al. [166] compared the results of the degradation of TC obtained by UV irradiation, electro-Fenton and photoelectro-Fenton by using Pt gauze as an anode, a  $\text{Fe}_3\text{O}_4\text{-graphite}$  system as a cathode with an applied current density of  $70 \text{ mA/cm}^2$  and  $\text{Na}_2\text{SO}_4$  as electrolyte. A synergistic effect was noticed in the photoelectro-Fenton system (see Figure 4) between the two different technologies with a mineralization degree of ca. 84%. This finding demonstrates that the coupling of different technologies is an effective strategy for enhancing efficiency.

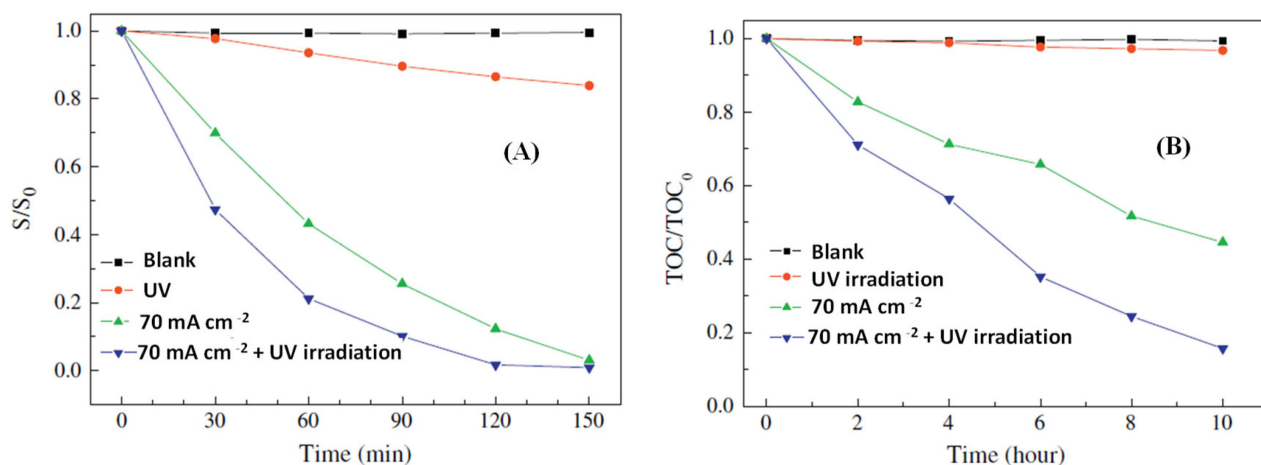


**Figure 4.** Effect of the different processes on tetracycline degradation (A) and mineralization (B) [166].

Ao et al. [167] applied the UV-activated peroxymonosulfate ( $\text{SO}_4^{\bullet-}$ ) process to TC degradation both in synthetic home-prepared and real wastewater systems. PMS ( $\text{HSO}_5^-$ ) was used to generate the  $\text{SO}_4^{\bullet-}$  radicals under irradiation with a medium-pressure UV (MPUV) lamp, and the effect of PMS dose, pH and addition of some anions was evaluated together with the ecotoxicity and mutagenicity of the transformation products (TPs). As shown in Figure 5A, the genotoxicity of the solution first increases and then decreases as the irradiation is increased. Very low values are reached at the end of the treatment. The higher degradation rate in the real wastewater solutions with respect to the lab-prepared one (Figure 5B) has been attributed to the presence of anions like  $\text{Cl}^-$ ,  $\text{HCO}_3^-$  and  $\text{CO}_3^{2-}$  in the former.

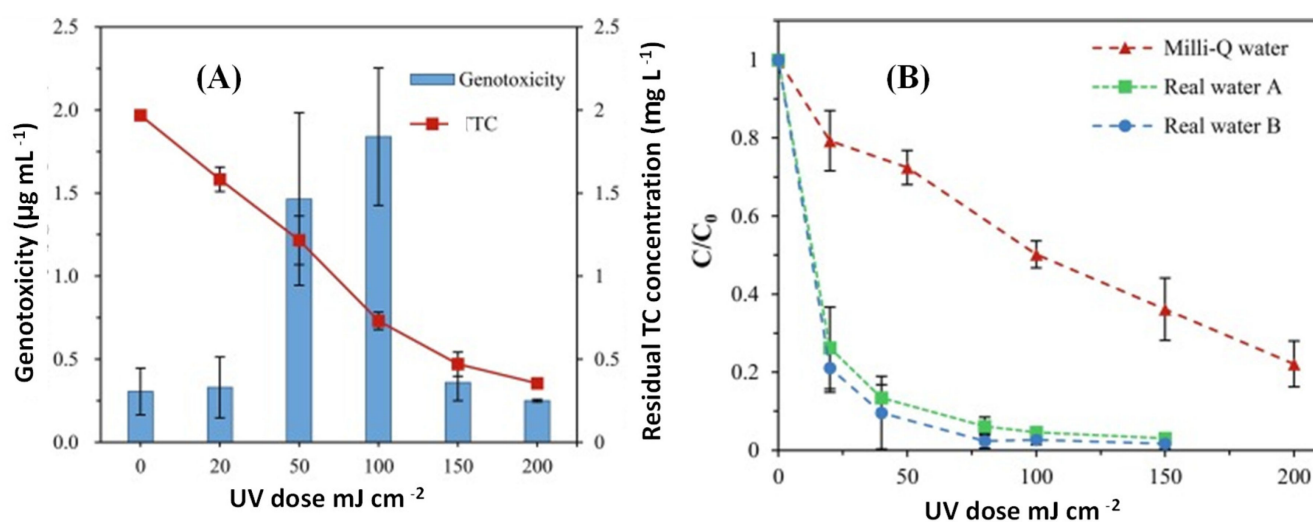


**Figure 5.** (A) Variation in genotoxicity of TC during MPUV/PMS process; (B) comparison of TC degradation in different systems [167].

Using  $4 \text{ mM S}_2\text{O}_8^{2-}$  (PS) activated by ultrasound irradiation results in 96.5% removal of TC and 74% and 61.2% removal of chemical oxygen demand and total organic carbon, respectively [168]. Moreover, in this case, the TC degradation rate was higher in drinking water than in ultrapure water.

Ultrasound irradiation combined with  $\text{Fe}_3\text{O}_4$  was very effective in the activation of PS for TC degradation, allowing 89% removal of the drug in just 90 min under the optimal operation conditions (TC initial concentration  $100 \text{ mg L}^{-1}$ , persulfate concentration  $200 \text{ mM}$ , initial pH 3.7,  $\text{Fe}_3\text{O}_4$  concentration  $1.0 \text{ g L}^{-1}$  and ultrasound power at  $80 \text{ W}$ ) [169].

Thermal activation of PS at 70 °C has also been described as a rapid and simple approach to activate the PS system, with almost complete elimination of TC within 30 min at 70 °C and ca. 70% at 40 °C within 240 min [170].

Natural bornite ( $\text{Cu}_5\text{FeS}_4$ ), in which Cu(I) and Fe(III) ions are present abundantly, was efficient in persulfate activation for TC degradation [171]. The removal efficiency was 81.6% and the mineralization percentage was 48.7% in 180 min. Indeed, both of these ionic species can be used to efficiently trigger PS activation for TC degradation. Also, ferromanganese oxides (FMOs) displayed high activity in activating peroxymonosulfate (PMS) for TC degradation, allowing 94.3% of TC and ca. 55% of TOC removal after 30 min starting from an initial concentration of TC of  $5 \text{ mg L}^{-1}$  [172]. Electron spin resonance measurements revealed that Mn-oxides with active surface sites controlled by Fe are responsible for the generation of  $\text{SO}_4^{\bullet-}$  radicals and the latter has a preponderant role compared to  $\text{HO}^{\bullet}$  radicals in TC degradation. Similar results were found by using magnetic  $\text{Ni}_{0.6}\text{Fe}_{2.4}\text{O}_4$  for activating PS: a TC removal of 86% in 35 min was achieved starting from a concentration of  $20 \text{ mg L}^{-1}$  [173].

Gao et al. [174] investigated the TC degradation mechanism of MW-activated PS. The effects of various experimental parameters such as TC and PS concentrations, initial pH and MW power were studied. Experiments carried out in the presence of scavengers revealed that sulfate radicals have a predominant role compared to hydroxyl radicals. By using the MW alone, the degradation of TC (initial concentration  $20 \text{ mg L}^{-1}$ ) was low as its removal was only 10.3%; 99.4% of TC was instead degraded within 5 min in the MW-PS process. Moreover, compared with conventional heating processes, MW heating raised the degradation rates. When the MW power was varied from 500 to 700 W, the TC removal efficiency increased.

Ozonation is one of the most popular treatment methods because it can degrade complex substances into simpler by-products. However, due to the slow mass transfer rate of ozone from the gas phase to the liquid phase and high cost, it has some drawbacks. For this reason, ozonation is often used in combination with other processes, including  $\text{O}_3/\text{H}_2\text{O}_2$ ,  $\text{O}_3/\text{UV}$ ,  $\text{O}_3/\text{ultrasound}$  and catalytic ozonation. Using only ozonation, complete removal of TC (TC solution 0.5 mM) was achieved in just 4–6 min, but about 40% mineralization was reached after 2h [175].

After 20 min of ozonation in an internal loop-lift reactor,  $2.08 \text{ mmol L}^{-1}$  was almost totally converted [176]. Moreover, after 90 min of ozonation, 35% of the COD was removed, and practically no residual acute toxicity was detected. Complete mineralization and decreased toxicity of by-products were achieved during TC removal by applying ultrasound in the presence of ozone and a goethite catalyst ( $\text{US/goethite/O}_3$ ) [177].

Combined processes including  $\text{O}_3/\text{activated carbon}$ ,  $\text{O}_3/\text{H}_2\text{O}_2$  and  $\text{O}_3/\text{biological treatment}$  were employed to achieve complete TC mineralization avoiding the formation of toxic intermediates [178]. When a  $\text{US/Fe}_3\text{O}_4/\text{O}_3$  combined system was used,  $100 \text{ mg L}^{-1}$  of TC was nearly removed after 20 min, with a COD reduction of ca. 42% [179]. This COD reduction reached ca. 89% after 120 min, accompanied by a biological degradability ratio of 0.694. The system exhibited low energy consumption, excellent stability and reusability. Ultrasound-enhanced TC ozonation has been also studied using a rectangular air-lift reactor. The technique removes 91% of the COD and reduces the acute toxicity from initial values of 95% to 60% after 90 min of reaction [180].

The photocatalytic method has been widely employed for the treatment of wastewater containing TC. Figure 6 shows the number of papers published since 2000, the year the first paper appeared (source: Scopus, Elsevier (October 2023) relating to the entry “Photocatalytic degradation of tetracycline”). Due to the huge number of publications, only the most representative have been selected in this review.

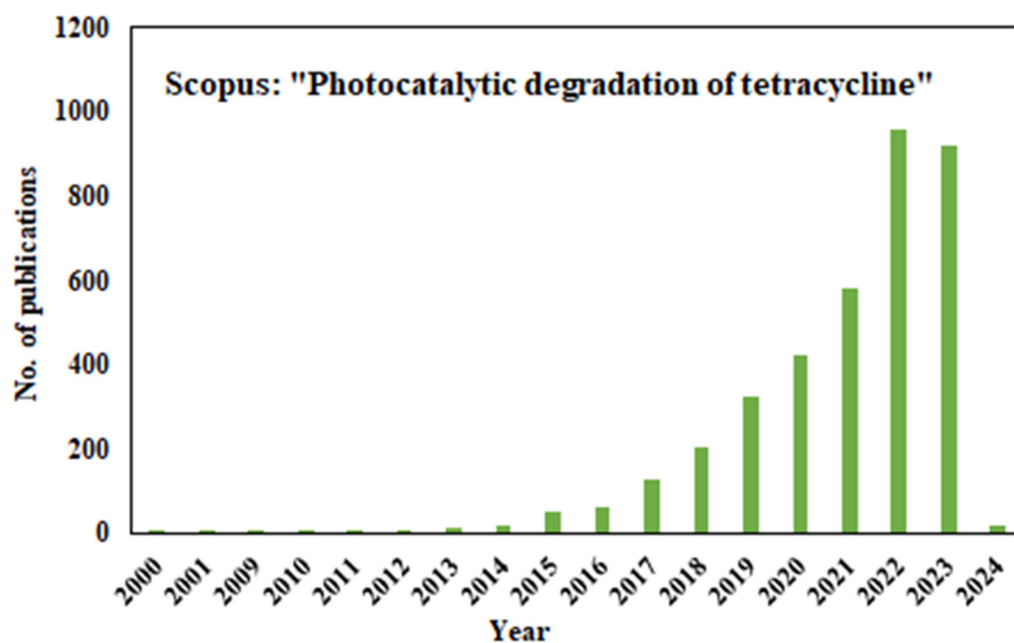


**Figure 6.** Number of papers published since 2000 on the photocatalytic degradation of tetracycline.

Different photocatalysts and setup configurations (irradiation sources, reactor geometry, experimental conditions, etc.) have been tested for TC removal by evaluating sometimes only the TC disappearing or also its mineralization. Table 10 reports a comparison of different photocatalytic systems for photocatalytic TC degradation. The reported results highlight the good efficiency of the reported systems in TC degradation under different experimental conditions. Only some papers reported data related to TC mineralization, and good TOC removal was found only in a few cases. A direct comparison of the results is not possible due to the different experimental conditions used by the authors.

**Table 10.** Results related to TC degradation with different photocatalytic systems.

Photocatalyst	Irradiation	TC Conc.	Photo Catalyst Conc.	TC Degradation	Ref.
TiO <sub>2</sub>	Ultraviolet	32.44 mg L <sup>-1</sup>	0.5 g L <sup>-1</sup>	100% 50% mineralization	[181]
C–N–S tri-doped TiO <sub>2</sub>	Visible light	5.0 mg L <sup>-1</sup>	0.5 g L <sup>-1</sup>	99%, 180 min 26% mineralization	[182]
α-Fe <sub>2</sub> O <sub>3</sub> /TiO <sub>2</sub>	500 W halogen	29.9 mg L <sup>-1</sup>	0.614 g L <sup>-1</sup>	97.5%	[183]
Cu <sub>2</sub> O–TiO <sub>2</sub> Cu <sub>2</sub> O coupled with TiO <sub>2</sub> nanotubes	Visible light	100 mg L <sup>-1</sup>	1.5 g L <sup>-1</sup>	100%, 60 min	[184]
MWCNT/TiO <sub>2</sub> nano-composite	UVC irradiation	10 mg L <sup>-1</sup>	0.2 g L <sup>-1</sup>	100%, 100 min 37.3% mineralization	[185]
TiO <sub>2</sub> @g-C <sub>3</sub> N <sub>4</sub>	Xenon lamp	20 mg L <sup>-1</sup>	0.1 g L <sup>-1</sup>	100%	[186]
Graphitic carbon nitride	Visible light	10 mg L <sup>-1</sup>	1 g/L	77%, 120 min	[187]
5-PANI/CuFe <sub>2</sub> O <sub>4</sub>	UV-Vis	49.94 mg L <sup>-1</sup>	0.1 g L <sup>-1</sup>	86%, 120 min 95% mineralization	[188]
Bi <sub>2</sub> Ti <sub>2</sub> O <sub>7</sub> (BTO)	Visible light	25 mg L <sup>-1</sup>	0.1 g L <sup>-1</sup>	88.2%, 150 min	[189]
CuO/Fe <sub>2</sub> O <sub>3</sub>	UV	20 mg L <sup>-1</sup>	0.05 g L <sup>-1</sup>	88%, 50 min	[190]

Table 10. Cont.

Photocatalyst	Irradiation	TC Conc.	Photo Catalyst Conc.	TC Degradation	Ref.
ZnO/ $\gamma$ -Fe <sub>2</sub> O <sub>3</sub>	UV-visible light	30 mg L <sup>-1</sup>	0.01 g L <sup>-1</sup>	88.52%, 150 min	[191]
Black graphitic carbon nitride (CN-B)	UV-Vis	30 mg L <sup>-1</sup>	0.05 g L <sup>-1</sup>	92%, 120 min	[192]
AgI/BiVO <sub>4</sub>	300 W xenon lamp	20 mg L <sup>-1</sup>	0.03 g L <sup>-1</sup>	94.91%, 60 min 90.5% mineralization	[193]
UiO-66-NDC/P-C <sub>3</sub> N <sub>4</sub>	UV-visible light	30 mg L <sup>-1</sup>	1 g L <sup>-1</sup>	95%, 120 min 49% mineralization	[194]
3% SnO <sub>2</sub> /g-C <sub>3</sub> N <sub>4</sub>	Visible light	30 mg L <sup>-1</sup>	0.5 g L <sup>-1</sup>	95.90%, 120 min	[195]
[(L1(Ag <sub>4</sub> I <sub>7</sub> )]CH <sub>3</sub> CN	Visible light	20 mg L <sup>-1</sup>	0.01 g L <sup>-1</sup>	97.91%, 180 min	[196]
ZnO/NiFe <sub>2</sub> O <sub>4</sub> /Co <sub>3</sub> O <sub>4</sub>	Natural solar light	30 mg L <sup>-1</sup>	0.02 g L <sup>-1</sup>	98%, 20 min 90% mineralization	[197]
Bi <sub>2</sub> Sn <sub>2</sub> O <sub>7</sub> /Bi <sub>2</sub> MoO <sub>6</sub>	300 W xenon lamp	20 mg L <sup>-1</sup>	0.035 g L <sup>-1</sup>	98.7%, 100 min 56.4% mineralization	[198]
MIL-88A	Visible light	200 mg L <sup>-1</sup>	0.25 g L <sup>-1</sup>	99.8%	[139]
UiO-66-NH <sub>2</sub> @WO <sub>3</sub> /CC	Visible light	20 mg L <sup>-1</sup>	0.02 g L <sup>-1</sup>	100%, 60 min	[199]

In addition to traditional TiO<sub>2</sub>-based photocatalytic systems, new catalysts have been prepared with the aim of having more active samples under visible light irradiation. Below, along with some titania-based photocatalysts, some of the new systems used for tetracycline removal are described.

Palominos et al. [200] performed the degradation of TC in aqueous suspensions containing ZnO or TiO<sub>2</sub> under simulated solar light irradiation. The photocatalytic oxidation of the antibiotic tetracycline (TC) was performed in an aqueous suspension containing TiO<sub>2</sub> or ZnO under simulated solar light. ZnO showed a slightly higher activity than TiO<sub>2</sub>, and runs carried out in the presence of appropriate scavengers revealed that in the presence of TiO<sub>2</sub>, the TC degradation occurs essentially by direct hole oxidation, and hydroxyl radicals played a secondary role, whilst when using ZnO, the oxidation is primarily driven by hydroxyl radicals.

Magnetic g-C<sub>3</sub>N<sub>4</sub>@MnFe<sub>2</sub>O<sub>4</sub>-graphene coupled systems with a relatively high specific surface area (SSA) and rapid separation of photoproduced e<sup>-</sup>/h<sup>+</sup> pairs were able to remove 91.5% of TC under visible light illumination in the presence of persulfate in a photo-Fenton-like reaction [201]. The photocatalyst was recovered by applying an external magnetic field and reused numerous times without loss of activity.

Doping with Co<sup>2+</sup> slows down the rapid recombination of the e<sup>-</sup>/h<sup>+</sup> pair in TiO<sub>2</sub> nanosheets. Co-TiO<sub>2</sub>/rGO nanocomposites synthesized by coating co-doped TiO<sub>2</sub> with rGO sheets using a one-pot hydrothermal method remove 60% of TC (initial concentration 30 mg L<sup>-1</sup>) in 180 min under visible light with five-cycle repeatability [202]. A heterojunction core-shell structure consisting of a Co-TiO<sub>2</sub> nanofiber core and a g-C<sub>3</sub>N<sub>4</sub> shell showed excellent photocatalytic performance with 90.8% TC removal and disinfection activity against *E. coli* [203]. This photocatalyst is advantageous due to its excellent chemical stability and non-toxicity of g-C<sub>3</sub>N<sub>4</sub> with a moderate bandgap (2.7 eV). In a heterojunction with a flower shape, high-surface-area BiOCl/TiO<sub>2</sub> proves excellent for use in photocatalysis, resulting in 82% removal of TC during 10 min of illumination [204].

Black TiO<sub>2</sub> is considered an emerging photocatalyst different from white stoichiometric TiO<sub>2</sub> [16,205]. Black anatase-TiO<sub>2</sub> was effective for visible light photodegradation of TC, allowing ca. 66% removal after 240 min [16].

Calcite coating, CaCO<sub>3</sub> (CAL), is widely recommended to limit hole-electron recombination and improve the reusability of TiO<sub>2</sub> nanoparticles. A CAL/TiO<sub>2</sub> nanocomposite

produced by the sol–gel method shows TC mineralization greater than 90% under UV irradiation [206]. Ilmenite, a mixture of NiO and TiO<sub>2</sub>, is obtained by co-precipitation of NiTiO<sub>3</sub> and TiO<sub>2</sub> to form a nanocomposite with a heterojunction [207]. It has a visible band-gap energy and efficiently produces H<sub>2</sub> in addition to removing 58% of TC in just two hours. Mixed metal oxides (MMOs) showed increased visible light absorption and charge transfer. Zn/Fe-MMO, for example, is a composite with a layered double hydroxide structure and effectively removes 88% of TC in 2 h of visible light irradiation [208]. The TC removal ability of another MMO, namely TiO<sub>2</sub>-Fe<sub>2</sub>O<sub>3</sub>, is 79.75% [209]. Ternary Ag<sub>x</sub>O/FeO<sub>x</sub>/ZnO nanotubes were effective in the photocatalytic removal of TC under visible light irradiation [210]. The high activity has been ascribed both to interactions of light with the local magnetized domains in the Fe-containing composites and to efficient interfacial charge transfer between the different semiconductors. Moreover, the magnetic separation of the catalyst after the reaction reduces the cost of the separation of the photocatalyst from the reaction medium and makes the process advantageous compared to conventional methods.

The combination of Bi<sub>2</sub>O<sub>3</sub> and g-C<sub>3</sub>N<sub>4</sub> produced an effective core–shell material with a TC removal of 80.2% starting from an initial TC concentration of 10 mg L<sup>-1</sup> with the use of a 250 W xenon lamp with a 420 nm cut-off filter [211]. Tun et al. [212] compared the photoactivity of Bi<sub>2</sub>O<sub>3</sub>, Bi<sub>2</sub>O<sub>3</sub>/montmorillonite and Ag-loaded Bi<sub>2</sub>O<sub>3</sub>/montmorillonite composites towards TC degradation under visible light irradiation. The ternary Ag-Bi<sub>2</sub>O<sub>3</sub>/montmorillonite sample exhibited superior outstanding activity due to the increased specific surface area, enhanced visible light absorption and photoproduced charge separation. Up to 90% TC removal efficiency was obtained in just 60 min of irradiation starting from a 20 mg L<sup>-1</sup> TC initial concentration. The high activity has been ascribed to the surface plasmon resonance (SPR) which occurs on Ag nanoparticles. Similar results were found by Heidari et al. [213]. They compared the activity of Bi<sub>2</sub>Sn<sub>2</sub>O<sub>7</sub>, gC<sub>3</sub>N<sub>4</sub>, Bi<sub>2</sub>Sn<sub>2</sub>O<sub>7</sub>-C<sub>3</sub>N<sub>4</sub>, Ag/Bi<sub>2</sub>Sn<sub>2</sub>O<sub>7</sub>, Ag/C<sub>3</sub>N<sub>4</sub> and Ag/Bi<sub>2</sub>Sn<sub>2</sub>O<sub>7</sub>-C<sub>3</sub>N<sub>4</sub> photocatalysts towards TC degradation. The most active sample was Ag/Bi<sub>2</sub>Sn<sub>2</sub>O<sub>7</sub>-C<sub>3</sub>N<sub>4</sub>, eliminating 89.1% of TC (20 mg L<sup>-1</sup>) over 90 min under simulated solar light irradiation. The high activity has been attributed to both the formation of a type-II heterojunction between Bi<sub>2</sub>Sn<sub>2</sub>O<sub>7</sub> and gC<sub>3</sub>N<sub>4</sub> and a surface plasmonic resonance on Ag nanoparticles. Bi<sub>24</sub>O<sub>31</sub>Br<sub>10</sub> nanosheets with controllable thickness exhibited high photocatalytic activity under solar light irradiation towards TC degradation under visible light irradiation [214]. Starting from an initial concentration of 20 mg L<sup>-1</sup>, more than 95% of TC was degraded within 90 min. Ag/Ag<sub>2</sub>S@BiOI nanowires were shown to be very effective in TC removal (100 mg L<sup>-1</sup>), allowing its almost complete degradation within 60 min under simulated solar light irradiation [215]. Cytotoxicity tests revealed that this new catalyst is harmless or less harmful to humans after exposure in the visible region.

Reduced graphene oxide@ZnAlTi (rGO@ZnAlTi) photocatalysts have been applied for the oxidation of TC (10 mg L<sup>-1</sup>) in the visible light range [216]. Graphene behaves like an electron donor and improves the adsorption of TC on the composite's surface. A removal efficiency of ca. 90% was realized in 120 min, along with a TOC abatement of ca. 80% within 270 min.

The photocatalytic treatment of TC may cause incomplete mineralization and is insufficient for higher pollutant concentrations. Its integration with adsorption technology or other AOPs can serve to obtain complete mineralization. The effectiveness of adsorption for the removal of antibiotics depends on the type of sorbent and properties such as SSA, porosity and pore diameter. Excellent TC removal is achieved with carbon-based materials, metal oxides, MOFs, clays, minerals, and composites [217].

Some Bi-containing semiconductors, such as BiOCl coupled to CdS nanoparticles, reveal both high adsorption capacity and photocatalytic removal efficiency under visible light towards TC (20 mg L<sup>-1</sup>) degradation, resulting in 91.2% removal after 60 min [218]. The suggested mechanism is chelated TC adsorption followed by photocatalytic degradation.

Zhang et al. [139] coupled a Fe-based metal–organic framework (MIL-88A) with sulfate radical (SR)-based AOPs for TC degradation under visible light starting from an initial

concentration of  $100 \text{ mg L}^{-1}$ . Thanks to a synergistic effect, TC was practically totally degraded within 80 min (Figure 7).

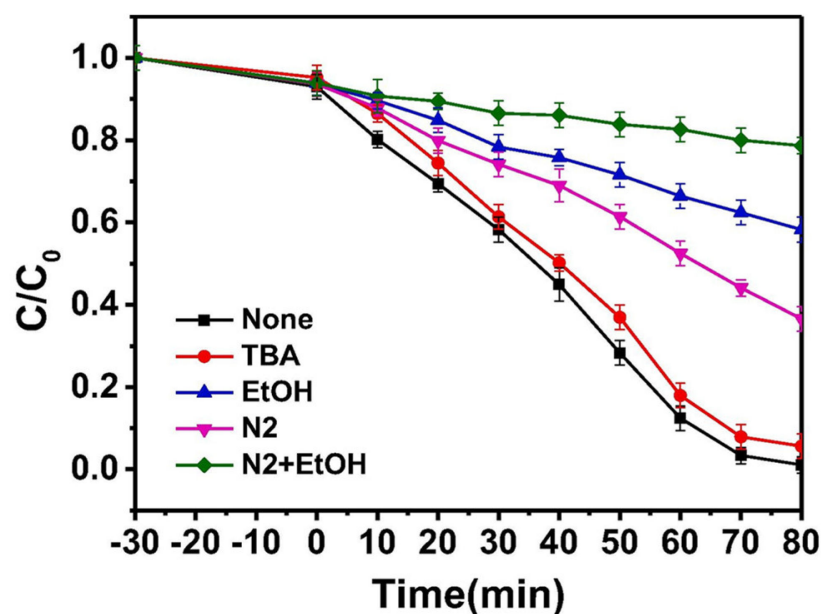


**Figure 7.** Degradation of TC by different processes. Reaction conditions: TC ( $200 \text{ mg L}^{-1}$ ), MIL-88A ( $0.25 \text{ g L}^{-1}$ ), PS ( $4.0 \text{ mM}$ ), initial pH 3.45 [139].

#### 4.2. Ibuprofen

Ibuprofen (IBP), also known as 2-[4-(2-methylpropyl)phenyl] propanoic acid, is a non-steroidal anti-inflammatory drug typically used as an analgesic, anti-inflammatory and antipyretic. Different AOPs have been employed for its degradation in water solution.

The ultrasonic method (US) gave good results in IBP removal with an IBP degradation of 98% in 30 min starting from an initial concentration of  $21 \text{ mg L}^{-1}$  with an applied power of 80 W [219]. The degradation rate was higher in both the presence of air and oxygen, acid media being the most favorable. BOD<sub>5</sub> and COD measures indicated that, although some dissolved organic carbon remained, IBP was transformed into biodegradable by-products which could be destroyed in a subsequent biological step.

The activation of PDS, PMS and H<sub>2</sub>O<sub>2</sub> at various ultrasonic frequencies was investigated [220]. A stock solution for IBP was prepared by dissolving 0.1 g of powder in methanol. Synthetic wastewater containing IBP was prepared by mixing deionized water with IBP stock solution. PS, PMS and H<sub>2</sub>O<sub>2</sub> were added to the solution. Batch tests were conducted to determine the oxidative elimination of IBP. They were also used to investigate how IBP was degraded in the US-PS, US-PDS and US-H<sub>2</sub>O<sub>2</sub> systems. It was reported that the IBP degradation followed pseudo-first-order kinetics regardless of the method used. The rate constant for IBP decomposition was found to be the highest at a frequency of 1000 kHz. US alone was efficient for IBP degradation, and the addition of PS, PMS and H<sub>2</sub>O<sub>2</sub> improved the decomposition efficiency of IBP.

Direct photolysis by UV light ( $\lambda = 254 \text{ nm}$ ) and UV/H<sub>2</sub>O<sub>2</sub> processes were assessed for the oxidation of IBP in synthetic solutions (initial concentration  $9.90\text{--}34.24 \text{ mg L}^{-1}$ ) [221]. The effects of drug concentration, pH and H<sub>2</sub>O<sub>2</sub> concentration were investigated (Figure 8). By varying the IBP initial concentration, an average efficiency of 82.63% was obtained after 270 min, and the oxidation was higher at pH 6. As  $pK_a = 4.9$  is for IBU, it is mainly present in its dissociated form at pH 6, and this finding suggests its higher reactivity with respect to the protonated species. The optimum amount of H<sub>2</sub>O<sub>2</sub> was  $10 \text{ mg L}^{-1}$ , which obtained 97.39% removal after 75 min. TOC and COD measurements revealed the partial mineralization of IBP both after UV and UV/H<sub>2</sub>O<sub>2</sub> treatment.

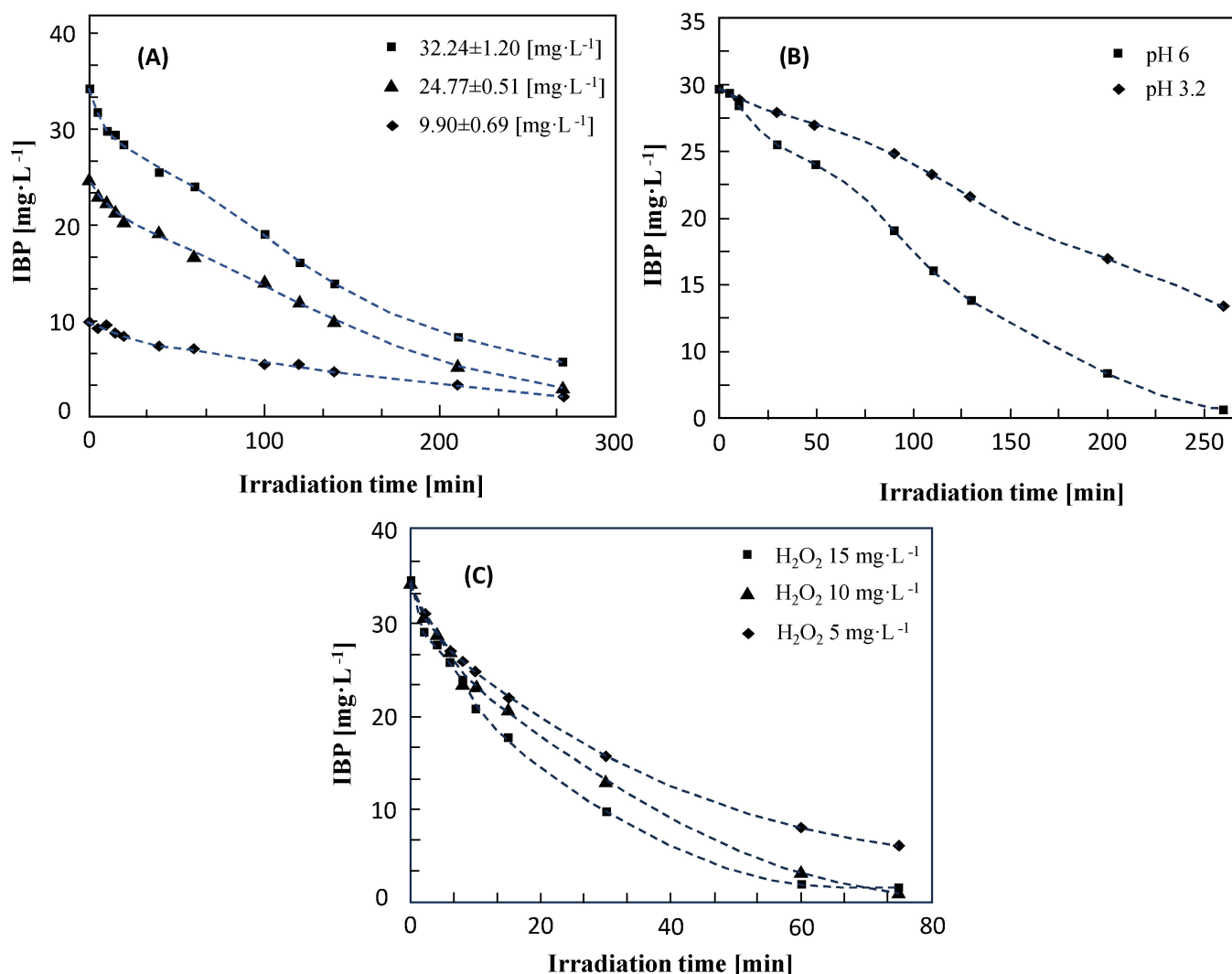


**Figure 8.** Influence of initial IBP concentration (A), pH (B) and  $\text{H}_2\text{O}_2$  concentration (C) on IBP removal by UV/ $\text{H}_2\text{O}_2$  process.

Adityosulindro et al. [222] used a heterogeneous Fenton process in the presence of a Fe-zeolite catalyst. The Fe-ZSM5 catalyst was effective in removing  $20 \text{ mg L}^{-1}$  IBP in pure water, with 88% degradation but only 27% TOC removal after 180 min at natural  $\text{pH} = 4.3$ . The drug decay followed a pseudo-first-order reaction with an activation energy of  $53 \text{ kJ mol}^{-1}$ . A few years later, the same research group [223] compared the degradation of IBP under UV, UV/ $\text{H}_2\text{O}_2$ , photo-Fenton and sono-photo-Fenton processes by varying the drug concentration and the irradiation source. In particular, two lamps were used: lamp L1, 254 nm, 6 W, and visible light lamp L2, 360–740 nm, 150 W. Applying the photo-Fenton process, by using both lamps, a complete degradation of IBP was obtained after 3 h while the mineralization was 82% with lamp L1 and 59% with lamp L2. The coupling of the L2-photo-Fenton process with ultrasound has a beneficial effect only at low Fe concentrations.

The degradation of IBP by the UV/chlorine and UV/ $\text{H}_2\text{O}_2$  AOPs follows pseudo-first-order kinetics, with the UV/chlorine AOP having a rate constant 3.3 times higher than that of UV/ $\text{H}_2\text{O}_2$  at  $\text{pH} 6$ . The degradation is sensitive to the dosage of chlorine and to the  $\text{pH}$  of the solution (decreasing at  $\text{pH} 9$ ), but not to the temperature or the concentration of chloride ions. Increasing  $\text{pH}$  decreases the first-order rate constant and increases the contribution of reactive chlorine species [38].

The UV–Vis/H<sub>2</sub>O<sub>2</sub> process was effective in the degradation of IBP (initial concentration 0.87 mM), allowing ca. 40% of degradation after 2 h [224]. With the addition of 1.2 mM of Fe(II) in the presence of 0.32 mM of H<sub>2</sub>O<sub>2</sub>, the complete degradation was reached with a mineralization degree of 40%.

Quero-Pastor et al. [225] studied the degradation of IBP (1 mg L<sup>-1</sup>) by ozonation, also evaluating the residual toxicity of the solution after the treatment. Under the best operational condition, an almost complete conversion was reached after 20 min of treatment, but no mineralization was observed. The results of toxicity tests revealed that the intermediates are more toxic than the starting drug. Almeida et al. [226] evaluated the effects of single ozonation, oxidation in the presence of H<sub>2</sub>O<sub>2</sub> and the combination of the two processes on IBP degradation (initial concentration 20 mg L<sup>-1</sup>), mineralization and residual toxicity. When single ozonation was used, IBP was immediately removed, but no important TOC removal was reached. The addition of H<sub>2</sub>O<sub>2</sub> did not present substantial enhancements; when O<sub>3</sub> and H<sub>2</sub>O<sub>2</sub> were combined, a mineralization of 70% was accomplished after 180 min of reaction.

The investigation of IBP degradation by the UV/Fe<sup>3+</sup>/Oxone process revealed that the efficiency depends on the operating parameters, and the best results were obtained at pH = 3 and with an optimal molar ratio of Fe<sup>3+</sup>/Oxone/IBP equal to 2:2:1 [227]. Electroperoxone treatment resulted in effective IBP removal, enhancing both its degradation and mineralization [228]. With an initial IBP concentration of 20 mg L<sup>-1</sup>, O<sub>3</sub> gas phase concentration of 40 mg L<sup>-1</sup>, current of 300 mA and pH = 7, IBP was completely degraded after 5 min and mineralized after 60 min.

The degradation of IBP by heterogeneous photocatalysis has been widely investigated in the presence of different photocatalysts by changing the experimental conditions and coupling photocatalysis with other technologies. In the presence of bare TiO<sub>2</sub>, 0.03 g of photocatalyst was effective in totally degrading IBP (concentration 10<sup>-4</sup> M) in 5 min at pH = 5 under UV irradiation [229].

Candido et al. [230] reported that UV light irradiation of TiO<sub>2</sub> suspended in 1 L of IBP solution (1.0 mg L<sup>-1</sup>) at 25 °C and at pH = 7.8 produced, after 1 h, 92% and 78% removal of IBP and TOC in pure water and 64% and 35% in spring water, respectively. Ecotoxicity tests using some bioindicators of environmental conditions revealed that the solution had residual acute effects after the treatment.

Khalaf et al. [231] demonstrated that a synthetic solution of IBP (initial concentration 25 mg·L<sup>-1</sup>) can be successfully treated under irradiation in the presence of photoactive glass coated with TiO<sub>2</sub>. Moreover, the immobilization of TiO<sub>2</sub> on glass substrates avoided the recovery problems encountered when the photocatalyst is used as powder.

Agócs et al. [232] obtained 81% degradation of IBP (50 µM) in pure water after 60 min of treatment in the presence of nanometric TiO<sub>2</sub>, stabilized with cyclodextrins, under UV irradiation. In tap water, the degradation was slower due to loss of efficiency of the oxidizing agents.

The activity of TiO<sub>2</sub> Degussa P25 under UV LED irradiation towards IBP degradation was evaluated in pure water and municipal and pharmaceutical wastewaters by measuring IBP degradation, mineralization and biotoxicity [233]. The process was effective in treating pure water and wastewater deriving from the pharmaceutical industry and less efficient in municipal wastewater, probably due to its complex composition. The degradation was higher at pH near 5.0 due to the enhanced electrostatic attractions between TiO<sub>2</sub> and IBP. For all the matrices, a reduction of 40% in acute toxicity was observed.

Jiménez-Salcedo et al. [234] compared the uses of TiO<sub>2</sub> nanoparticles under UV light and g-C<sub>3</sub>N<sub>4</sub> nanosheets under visible light irradiation for IBP degradation. The authors observed a higher efficiency of TiO<sub>2</sub> with respect to g-C<sub>3</sub>N<sub>4</sub>, although the use of a higher-energy light must be considered. The initial IBP concentration was 5 µg mL<sup>-1</sup>. With TiO<sub>2</sub>, the complete degradation of IBP was achieved in 10 min, whilst more than 3 h was necessary with g-C<sub>3</sub>N<sub>4</sub>; in both cases, no complete mineralization was accomplished.

By using monoclinic  $\text{BiVO}_4$  under simulated solar light irradiation [235], an IBP conversion of 90% was reached after 25 min starting from an initial concentration of the drug of  $10 \text{ mg L}^{-1}$ . No information about the mineralization has been reported by the authors.

By coupling ozonation with photocatalysis in the presence of  $\text{SrWO}_4/\text{ZnO}$ , an IBP removal efficiency of 93% and a 55% BOD elimination were obtained under UV irradiation starting from an initial drug concentration of  $0.1 \text{ mg L}^{-1}$  [236].

Fidelis et al. [237] studied the degradation of IBP by combining different methods: ozonation, photolytic ozonation, photocatalysis and photocatalytic ozonation (Figure 9). The single methods afforded a good IBP removal rate but a low mineralization degree. A synergistic effect was instead noticed in photocatalytic ozonation, with a complete degradation of IBP after 12 min and a 98% TOC reduction in 30 min of reaction.

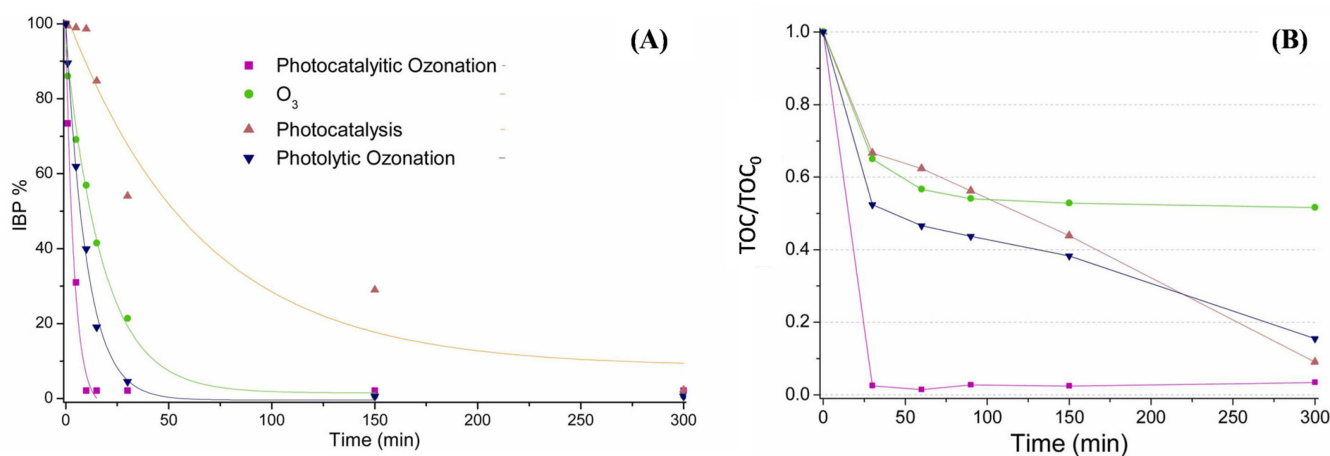


**Figure 9.** IBP (A) and TOC (B) removal with the different processes [237].

#### 4.3. Oxytetracycline

The broad-spectrum antibiotic oxytetracycline (OTC) has notable biodegradability but has bioaccumulation and persistence properties and consequently is extremely harmful to human health.

Its abatement (initial concentration  $5 \text{ mg L}^{-1}$ ) has been studied both in synthetic (ultrapure water) and real wastewater matrices using hybrid systems that combine microfiltration (MF) with photolysis (UVA/MF) or heterogeneous photocatalysis in the presence of a  $\text{TiO}_2\text{-P25}$  photocatalyst [238]. A photocatalytic membrane reactor (PMR) has been tested using  $\text{TiO}_2\text{-P25}$  nanoparticles both in suspension and immobilized on a nanoengineered membrane (NEM). A higher photocatalyst loading results in higher OTC removal efficiency (90% in 30 min), but a greater decrease in permeate flux because a denser  $\text{TiO}_2/\text{P25}$  cake layer formed. The presence of NEM led to the improvement of the antifouling properties and also a decrease in the permeate flux.

Photo-Fenton catalytic activity for OTC degradation was tested with a  $\text{MnFe}_2\text{O}_4/\text{g-C}_3\text{N}_4$  heterojunction composite which exhibited excellent catalytic activity as approximately 80.5% was removed in 10 min. OTC breakdown was primarily started by  $\text{h}^+$  oxidation, with  $\text{HO}^\bullet$  and  $\text{O}_2^{\bullet-}$  playing only minor supporting roles [239]. The hypothesized reaction mechanism is reported in Figure 10. Through  $\text{h}^+$  attacks, OTC molecules are oxidized, producing different intermediates by eliminating groups like  $-\text{OH}$ ,  $-\text{NH}_2$ ,  $-\text{CH}_3$  and  $-\text{CONH}_2$  and breaking the benzene ring. The intermediates are further degraded by  $\text{h}^+$ ,  $\text{HO}^\bullet$  and  $\text{O}_2^{\bullet-}$  and form aliphatic compounds, tiny organic acids,  $\text{CO}_2$  and water.

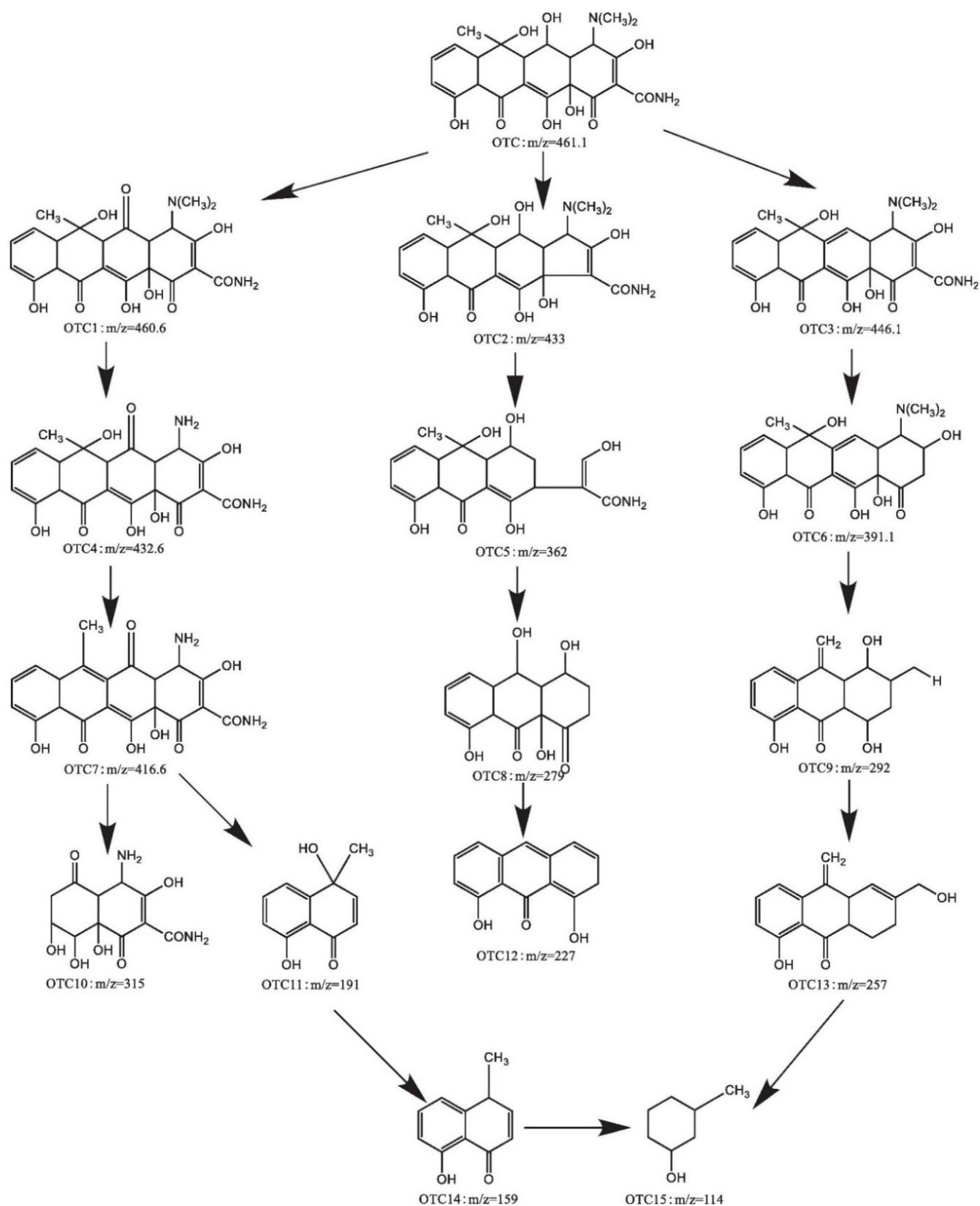


**Figure 10.** Possible degradation pathways of OTC in the photo-Fenton catalytic system [239].

The photocatalytic method using persulfate (PS) and  $\text{Fe}_3\text{O}_4/\text{MIL-101}(\text{Fe})$  allowed the occurrence of 87.1% degradation of  $70 \text{ mg L}^{-1}$  of OTC in 60 min [240]. MWCNTs- $\text{CuNiFe}_2\text{O}_4$  nanomaterials were utilized to effectively remove OTC from an aqueous

solution in the presence of persulfate following the mechanism shown in Figure 11 [241]. Excellent adsorption characteristics toward OTC were shown by the MWCNTs-CuNiFe<sub>2</sub>O<sub>4</sub> combination, which also successfully activated potassium persulfate (KPS) for drug removal. By using a catalyst concentration of 10 mg L<sup>-1</sup> with an initial concentration of OTC equal to 300 mg L<sup>-1</sup>, 88.6% degradation was achieved. SO<sub>4</sub><sup>•-</sup> and HO<sup>•</sup> radical-capturing agents such as ethanol and isopropyl alcohol were used to investigate the reaction mechanism. The outcomes showed that the presence of these quenching agents reduced the removal effectiveness of MWCNTs-CuNiFe<sub>2</sub>O<sub>4</sub>, confirming the active role of these radicals in the degradation process.

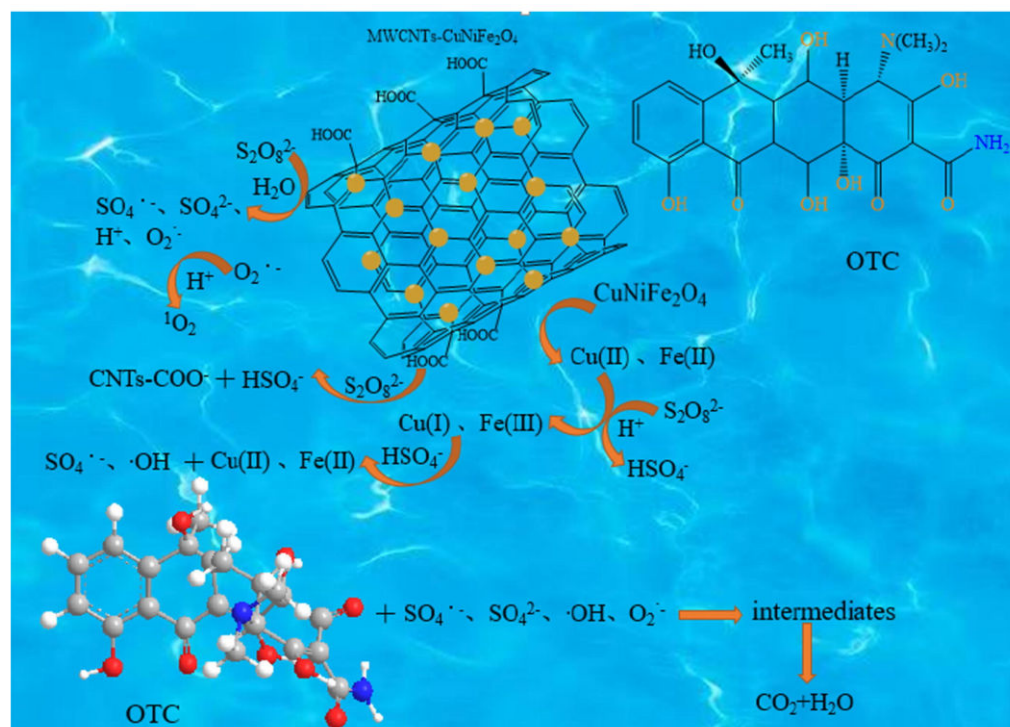


**Figure 11.** Mechanism of degradation of OTC by using MWCNTs-CuNiFe<sub>2</sub>O<sub>4</sub>/KPS system [241].

Ozonation was also proved to be beneficial for the degradation of OTC. Li et al. [242] investigated how ozonation affected OTC degradation at various pH levels. Chemical oxygen demand (COD), the concentration of oxytetracycline and the BOD<sub>5</sub>/COD ratio were used to measure the effectiveness of the ozonation process. Using bioluminescence assays, the hazardous potential of OTC degradation was also investigated. The findings suggested that in pharmaceutical wastewater containing a high OTC concentration, ozonation as a partial step in a combined treatment concept can boost biodegradability.

#### 4.4. Lincomycin

Lincomycin is an antibiotic found in water effluents. Its structure is shown in Figure 12.

TiO<sub>2</sub>-based nanomaterials, including TNAs (TiO<sub>2</sub> nanotube arrays), TNWs/TNAs (TiO<sub>2</sub> nanowires on nanotube arrays), Au-TNAs and Au-TNWs/TNAs, were developed for enhanced photocatalytic degradation of antibiotics in aquaculture wastewater. TNWs/TNAs showed higher activity than TNAs due to larger surface area [243]. Au-TNWs/TNAs showed the highest activity under UV-VIS or VIS irradiation, exhibiting 100% efficiency in 20 min (lincomycin concentration 500 ng mL<sup>-1</sup>) with reaction rates of 0.26 min<sup>-1</sup> and 0.096 min<sup>-1</sup>, respectively. The high activity of Au-TNWs/TNAs can be ascribed to the synergistic effects between the high surface area and the surface plasmonic effect of Au nanoparticles. Augugliaro et al. [244] reported that lincomycin is broken down by photocatalytic oxidation in aqueous suspensions of Degussa P25 polycrystalline TiO<sub>2</sub>, using

a hybrid system consisting of a solar photoreactor and a membrane module. The initial lincomycin concentration was 20  $\mu\text{M}$ . The reported kinetics are pseudo-first-order with high membrane rejection for lincomycin and its oxidation products.

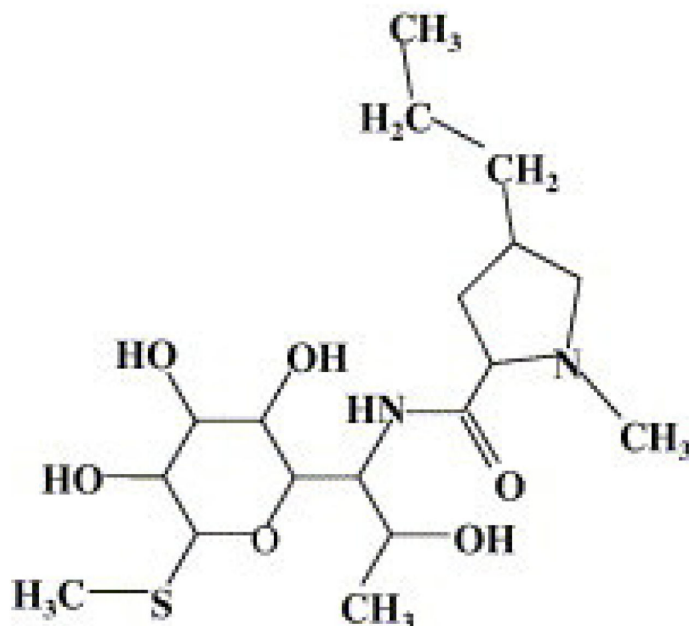


**Figure 12.** Structure of lincomycin.

As a highly effective metal-free photocatalyst, graphitic carbon nitride ( $\text{g}/\text{C}_3\text{N}_4$ ) shows promising behavior for the degradation of drugs. Adjusting the energy band, improving charge extraction and adding a cocatalyst enhances the  $\text{g}/\text{C}_3\text{N}_4$  photocatalytic activities and increases both the degradation rate and conversion degree of lincomycin under visible light irradiation [245]. Carbon quantum dots (CDs) were added as cocatalysts to improve the formation of  $\text{O}_2^{\bullet-}$ ; graphene oxide (rGO) was employed to improve the charge mobility. The most active improved photocatalyst was CD-rGO-O-g/ $\text{C}_3\text{N}_4$ , which exhibited a tenfold increase in degradation rate when compared to the original  $\text{g}/\text{C}_3\text{N}_4$ . Starting from an initial concentration of the drug of  $100 \text{ mg L}^{-1}$ , 99% degradation was achieved after 180 min. The active species, such as  $\text{O}_2^{\bullet-}$ ,  $\text{HO}^\bullet$  and  $\text{h}^+$ , contribute differently to the degradation in each of the photocatalysts.

Metal–organic framework (MOF)-based photocatalytic treatment of lincomycin using Basolite F300 as a catalyst in the presence of two oxidants ( $\text{H}_2\text{O}_2$ ,  $\text{S}_2\text{O}_8^{2-}$ ) was reported by Kontogiannis et al. [246]. The results showed that the drug elimination was completed within 2 h, and the oxidant concentration ( $0\text{--}300 \text{ mg L}^{-1}$ ) affected the process rate. The best concentration for attaining maximum degradation was  $100 \text{ mg/L}$  for both oxidants. After 120 min, just 8% of MOFs were degraded according to photolysis studies. The photocatalyst Basolite<sup>®</sup> F300 was activated using  $\text{H}_2\text{O}_2$  as an oxidant in order to study the photocatalytic process. MIL-100 surface iron sites showed Fenton-type activity, which synergistically increased degradation. When  $\text{H}_2\text{O}_2$  was added, the rate of degradation increased to 95% in 90 min, indicating catalyst activation and a conceivable heterogeneous photo-Fenton reaction involving Fe-sites and  $\text{H}_2\text{O}_2$ . The mechanism of the reaction pathway is shown below in Figure 13.

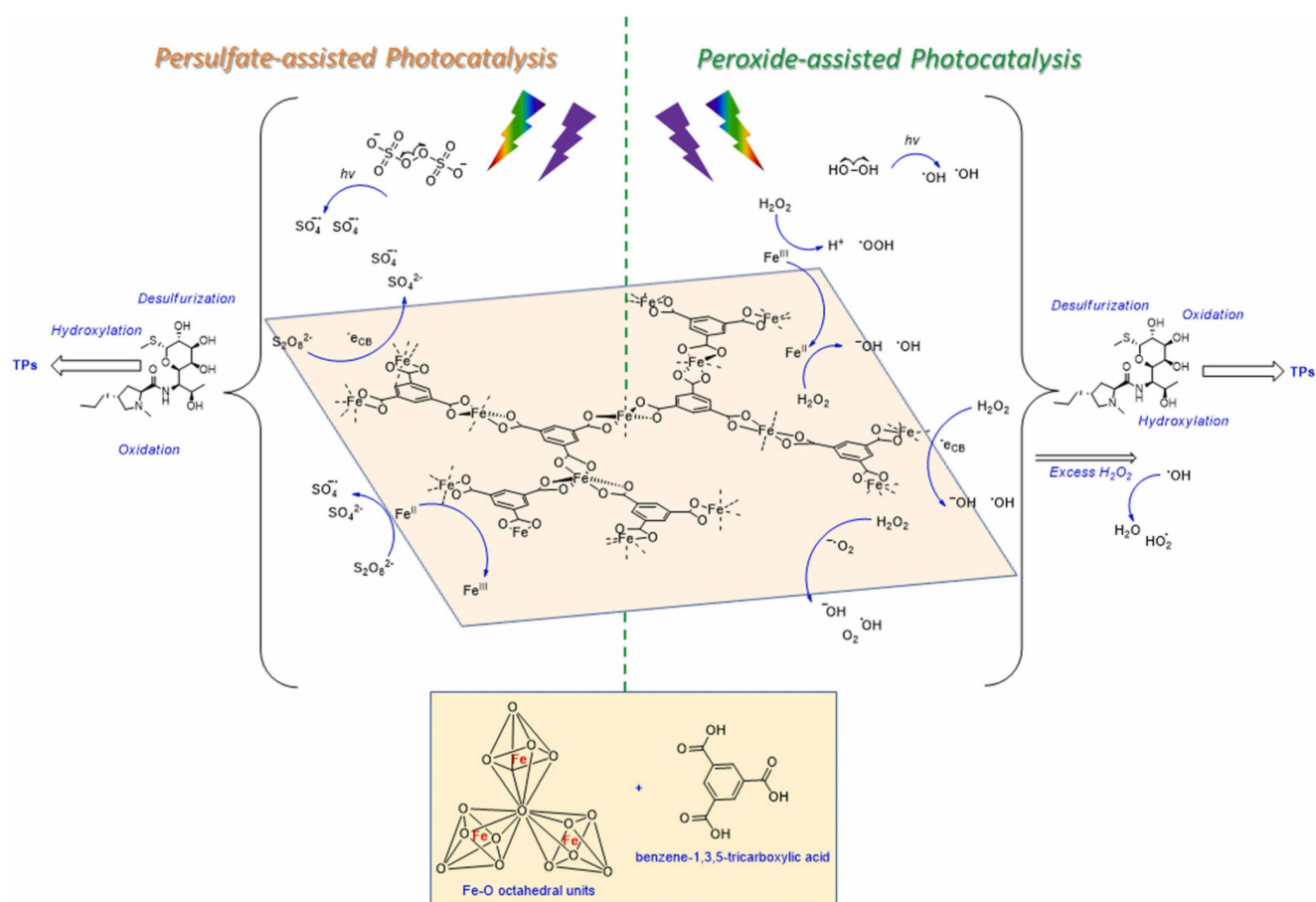


**Figure 13.** Mechanistic reaction pathways taking place on Basolite F300 as a catalyst activated by hydrogen peroxide or persulfate [246].

A Zr-based metal–organic framework (MOF), known as VNU-1, with increased pore size and improved optical properties, was prepared and used as a photocatalyst for the degradation of antibiotics [247]. The prepared sample was as active as well-known P25 in the removal of lincomycin, and a contemporary TOC decreasing to 95% was accomplished. After five cycles, the catalyst maintained its high photodegradation performance (e.g., 100% photodegradation in 10 min).

In perspective, good results can be obtained by combining a series of measures that enhance the photocatalytic activity, such as the doping of structured materials. Using nanowires on an Au-TiO<sub>2</sub> nanotube array causes 83% degradation of lincomycin in 20 min upon irradiation with visible light. This result can be attributed to the nanowires having a larger surface area than TiO<sub>2</sub> nanotubes [248].

#### 4.5. Amoxicillin

Çağlar Yılmaz et al. [249] compared the activity of commercial TiO<sub>2</sub> P25 and lab-prepared bare and Co-doped TiO<sub>2</sub> towards the degradation of amoxicillin (AMX) under UV-C and visible irradiation. Co-TiO<sub>2</sub> was the most active photocatalyst, allowing the complete elimination of 100 mg L<sup>-1</sup> of AMX after 240 min under UV-C irradiation and after 300 min under visible light. TiO<sub>2</sub> nanoparticles loaded on graphene oxide (GO/TiO<sub>2</sub>) removed more than 99% of AMX (initial concentration 50 mg L<sup>-1</sup>) under UV light irradiation using a lamp with an intensity of 36 W [250]. Photoproducted holes were the main active species in degrading AMX, and TOC analyses revealed a good mineralization degree, obtaining a COD and TOC removal of 91.25% and 89.7%, respectively. The photocatalysts showed good stability, recyclability and efficiency in reducing the initial toxicity of the solution.

Nanostructured photocatalysts consisting of titanium dioxide doped with iron and nitrogen ( $\text{Fe}^{3+}\text{-TiO}_{2-x}\text{N}_x$ ) synthesized using the sol-gel (SG) method and microwave (MW) technology, were tested for their ability to break down amoxicillin (AMX) [251]. Higher activity was observed for the materials manufactured using the SG approach, and degradation efficiencies of 58.61% for SG and 46.12% for MW samples were observed after 240 min of visible light at pH 3.5.

Al-Musawi et al. [252] carried out the photocatalytic degradation of AMX by using a  $\text{Fe}_2\text{O}_3$ /bentonite/ $\text{TiO}_2$  nanocomposite under both visible LED light and UV irradiation. The reaction rate followed a pseudo-first-order kinetics, and starting from an AMX concentration of  $25 \text{ mg L}^{-1}$ , under UV light, a complete degradation of the drug was obtained in 60 min, while under visible light, a removal percentage of 98.8% was observed in 90 min.

The electrophotocatalytic treatment of an AMX aqueous solution ( $100 \text{ mg L}^{-1}$ ) was studied by measuring the chemical oxygen demand (COD) [253]. The degradation of the drug was 79% after 120 min of irradiation.

Elmolla and Chaudhuri [254] compared Fenton, photo-Fenton, UV/ $\text{ZnO}$  and  $\text{TiO}_2$  photocatalysis processes in the degradation of AMX. All methods were effective in AMX oxidation, and, except for UV/ $\text{ZnO}$ , an enhancement of the residual solution biodegradability was measured by the  $\text{BOD}_5/\text{COD}$  ratio evaluation. The best results were obtained by the photo-Fenton process.

#### 4.6. Erythromycin

Erythromycin (ERY) is a penicillin medication that can remain in nature for up to a year, preserving its antibiotic activity. The inefficiency of conventional ERY degradation methods has prompted the development of cutting-edge technologies such as AOPs [255].

Chu et al. [256] studied ERY removal using PS activated by gamma radiation in different systems. The degradation rate follows the order deionized water > groundwater > secondary treated municipal wastewater, and in the deionized water, ERY was eliminated with a TOC removal of 25%.

Albornoz et al. [257] carried out ERY degradation by direct photolysis and by using photocatalysts such as  $\text{TiO}_2$ ,  $\text{Ti}_{1-x}\text{Sn}_x\text{O}_2$  and a commercial  $\text{TiO}_2$  mesh under UV-A irradiation. Under direct photolysis, only a low degree of degradation and mineralization was observed with the formation of low-molecular-weight carboxylic acids (Figure 14). In the presence of photocatalysts, the best results (complete degradation after 4 h) were obtained with the sample  $\text{Ti}_{1-x}\text{Sn}_x\text{O}_2$  due to the formation of a type-II heterojunction between  $\text{TiO}_2$  and  $\text{SnO}_2$ .

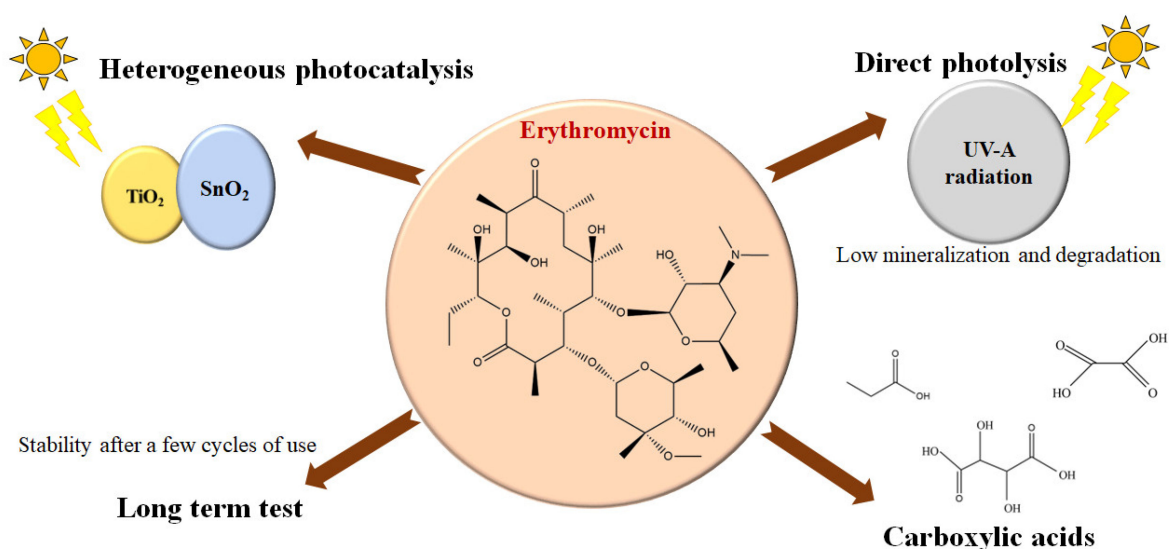


Figure 14. Photolytic and photocatalytic degradation of erythromycin.

Photocatalytic mineralization of ERY in aqueous TiO<sub>2</sub> suspensions using commercially available TiO<sub>2</sub> catalysts was also reported in the literature [258]. The most effective catalyst was Degussa P25, which reduced 90% of total organic carbon after 90 min of reaction with an ERY initial concentration of 10 mg L<sup>-1</sup>.

Vignesh et al. [259] reported that when both zinc phthalocyanine and TiO<sub>2</sub> nanoparticles were used, a significant improvement in photocatalytic activity was demonstrated in comparison to pure TiO<sub>2</sub>. A 74% degradation of ERY was achieved in 3 h by irradiation with visible light, while the undoped material degraded only 31.6% of the antibiotic under the same experimental conditions.

A composite g-C<sub>3</sub>N<sub>4</sub>/CdS photocatalyst showed good activity towards ERY degradation under simulated solar light irradiation [260]. Starting from an initial concentration of 50 mg L<sup>-1</sup>, ca. 80% of the drug was converted in 1h. The high activity has been ascribed to the formation of a Z-scheme between g-C<sub>3</sub>N<sub>4</sub> and CdS with an efficient charge separation.

The activity of CaCO<sub>3</sub> (calcite) towards ERY (initial concentration 30 mg L<sup>-1</sup>) removal was explored under both UV and solar light irradiation by Mohsin et al. [261]. After 2 h of UV irradiation, 73% of conversion was reached, while 6 h was necessary under sunlight to remove 93% of ERY. Moreover, under sunlight irradiation, a reduction of 78.5%, 77.6% and 64.5% in COD, BOD and TOC was achieved, respectively. The photocatalyst showed good stability, maintaining its activity unchanged after three cycles.

γ-Fe<sub>2</sub>O<sub>3</sub>/SiO<sub>2</sub> composites allowed ca. 87% ERY degradation after 6 min of UV-C (λ = 254 nm) irradiation starting from a concentration of 6 mg L<sup>-1</sup> of the drug [262]. The high activity is due to the high absorbent properties of silica combined with the good photocatalytic performance of γ-Fe<sub>2</sub>O<sub>3</sub> under sunlight.

#### 4.7. Sulfonamide

Sulfonamide antibiotics are widely used in human and veterinary medicine and as herbicides in agriculture [263]. They are very dangerous for the environment because they present a very stable structure that is difficult to break down with traditional processes.

P-doped TiO<sub>2</sub>-αFe<sub>2</sub>O<sub>3</sub> mixed oxide catalysts were used together with K<sub>2</sub>S<sub>2</sub>O<sub>8</sub> for photocatalytic degradation of a sulfonamide mixture containing sulfadiazine (SDZ), sulfamerazine (SMRZ) and sulfamethazine (SMTZ) (5 mg L<sup>-1</sup> each) in a coupled process [264]. In 300 min under visible light irradiation, 69% mineralization was achieved.

Using 0.05 g Bi<sub>2</sub>O<sub>3</sub>-TiO<sub>2</sub>/PAC catalysts, a 250 mL solution containing 20 mg L<sup>-1</sup> of three different sulfonamides, namely sulfamethoxazole (SMX), sulfamethazine (SMT) and sulfadiazine (SDZ), was treated under solar light irradiation [265]. The degradation was ca. 100% for SMX after 30 min and ca. 100% for SDZ and 75% for SMT after 60 min of reaction. Tests carried out in the presence of trapping agents revealed that h<sup>+</sup> was the main active species in degrading SMX whilst O<sub>2</sub><sup>•-</sup> played the main role in the oxidation of SMT and SDZ.

Batista and Nogueira [266] investigated the parameters influencing the photo-Fenton degradation of two antibiotics belonging to sulfonamide family, namely sulfadiazine (SDZ) and sulfathiazole (STZ). The addition of Fe(III)-oxalate improved the drugs' oxidation with respect to free iron, and at pH = 5 in the presence of H<sub>2</sub>O<sub>2</sub>, the complete degradation occurred in 8 min.

O<sub>3</sub>, H<sub>2</sub>O<sub>2</sub> and O<sub>3</sub>/H<sub>2</sub>O<sub>2</sub> processes were compared in the degradation of sulfonamides such as sulfamethoxazole (SMX), sulfasalazine (SSZ), metronidazole (MNZ) and sulfamethazine (SMT) [267].

The best results were found utilizing the O<sub>3</sub>/H<sub>2</sub>O<sub>2</sub> process due to a synergistic effect between the two methods, and a maximum degradation efficiency of 98.10%, 89.34%, 86.29% and 58.70%, was obtained for SSZ, SMX, SMT and MNZ, respectively, under optimum experimental conditions.

#### 4.8. Ciprofloxacin

$\text{Ag}_3\text{PO}_4$  nanoparticles deposited onto  $\text{TiO}_2$  nanotube arrays gave rise to a heterojunction that displayed high photocatalytic activity in degrading ciprofloxacin (CIP) under solar light irradiation [268]. Starting from an initial concentration of  $10 \text{ mg L}^{-1}$ , ciprofloxacin was destroyed by 78.4% in a 60 min period of irradiation. Liu et al. [269] compared the degradation of CIP (initial concentration  $20 \text{ mg L}^{-1}$ ) by using  $\text{TiO}_2$  P25 and lab-made  $\text{TiO}_2$  nanosheets and composite  $\text{TiOF}_2/\text{TiO}_2$  flower-shaped nanosheets under simulated solar light irradiation. Different  $\text{TiOF}_2/\text{TiO}_2$  samples were prepared by the hydrothermal method at different temperatures: 140, 160, 180 and  $200 \text{ }^\circ\text{C}$ . Composite nanosheets synthesized at  $160 \text{ }^\circ\text{C}$  were the most active samples due to the formation of an efficient heterojunction allowing a decrease in the recombination rate of the photogenerated charges and an enhancement of the charge transfer (Figure 15). The  $\text{TiOF}_2/\text{TiO}_2$  nanosheets allowed a 93.7% degradation of the antibiotic after 90 min of irradiation.

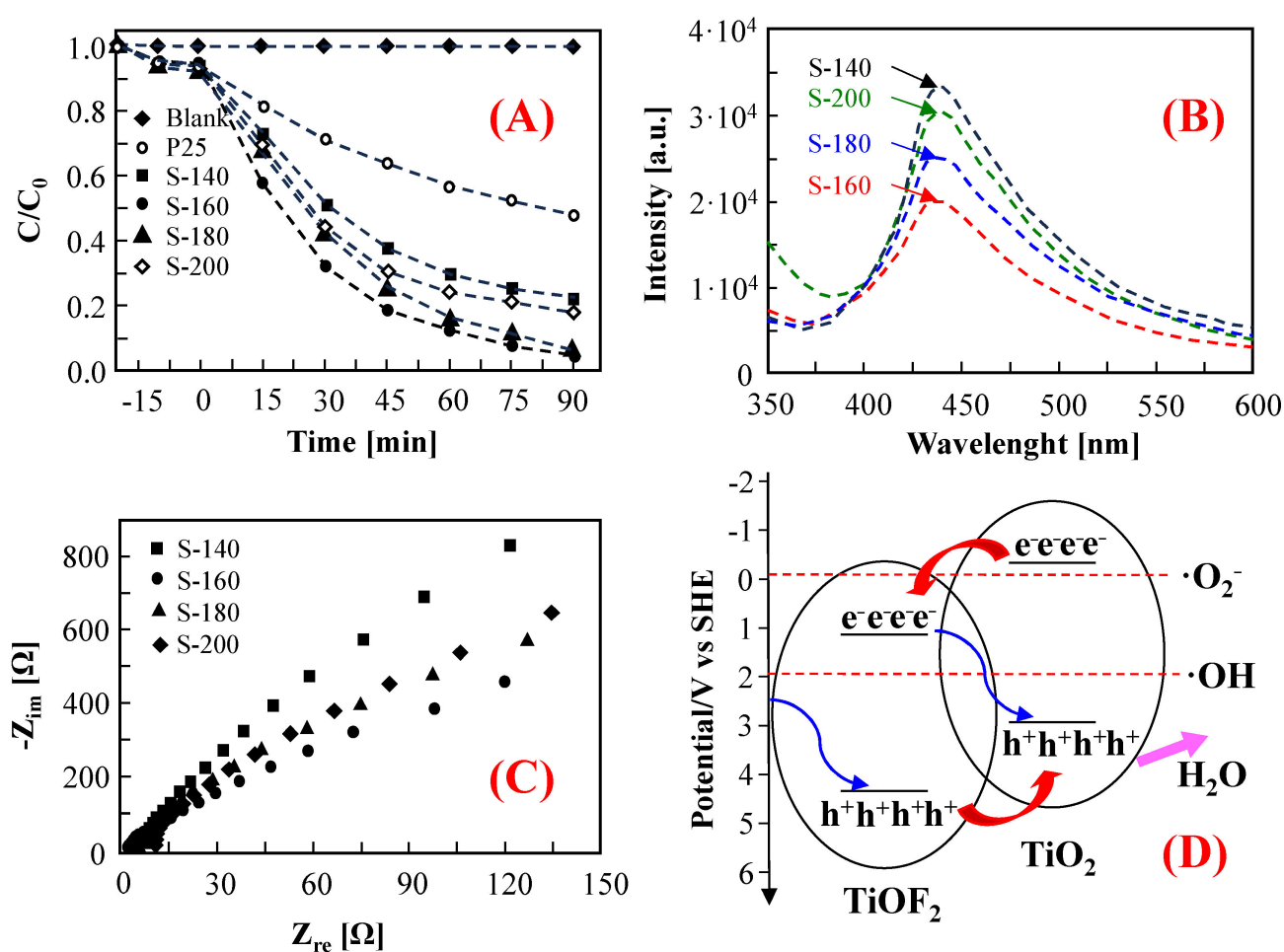


**Figure 15.** (A) Photocatalytic degradation of ciprofloxacin, (B) photoluminescence spectra, (C) electrochemical impedance spectroscopy measures and (D) heterojunction scheme.

El-Kemary et al. [270] investigated the photocatalytic activity of synthesized  $\text{ZnO}$  nanoparticles for the degradation of CIP under UV light irradiation in an aqueous solution at different pHs. The degradation process of CIP showed a pseudo-first-order reaction, and 50% degradation was observed after 60 min at  $\text{pH} = 10$  and  $\text{pH} = 7$ .

Wen et al. [271] reported that upon exposure to visible light,  $\text{CeO}_2\text{-Ag}/\text{AgBr}$  composite photocatalysts with a Z-scheme arrangement demonstrated improved photocatalytic activity for the degradation of CIP. Accelerated interfacial charge transfer and better photogenerated electron–hole pair separation were credited with the improved performance.

Zn-doped Cu<sub>2</sub>O synthesized by a solvothermal method exhibited excellent photoactivity towards the degradation of 20 mg L<sup>-1</sup> of CIP, removing about 94.6% of it after 240 min [272]. Runs carried out in the presence of specific trapping agents revealed that the main active species responsible for the drug degradation were HO• radicals and h<sup>+</sup>.

Photo-Fenton activity of rGO-ZnFe<sub>2</sub>O<sub>4</sub> towards CIP degradation was boosted by the thermal effect inducing H<sub>2</sub>O<sub>2</sub> activation [273]. The integrated process showed excellent photoactivity thanks to a synergistic effect and displayed a superior performance when compared to a solely photo-Fenton or thermal-Fenton process in lowering the H<sub>2</sub>O<sub>2</sub> activation barrier and speeding up the production and spread of radicals.

Ge et al. [274] reported that LaFeO<sub>3</sub>/polystyrene (LFO/PS) photo-Fenton catalysts, prepared using ultrasound-assisted sol-gel and hydrothermal methods, were highly efficient (98.38%) for antibiotic degradation under the following experimental conditions: CIP concentration 10 mg L<sup>-1</sup>, H<sub>2</sub>O<sub>2</sub> 5 mmol L<sup>-1</sup> and pH = 9.00. Moreover, the TOC removal efficiency reached 76.44%. Finally, Gupta and Garg [275] carried out CIP degradation using a classical Fenton process in synthetic wastewater containing an initial concentration of the drug of 100 mg L<sup>-1</sup>. Under the best experimental conditions, after 1 h, CIP degradation and TOC removal were 70% and 55%, respectively.

## 5. Challenges

As reported in this review, the use of a single AOP for the removal of drugs from wastewater may be, in many cases, insufficient to remove both the original drugs and their intermediates. Coupling of different AOPs can overcome this problem by allowing a more efficient decontamination of the effluents. Under appropriate experimental conditions, the use of integrated AOP systems is also convenient from an economical point of view because the pollutants can generally be mineralized, and less energy is needed. However, it is important to evaluate the quality of the treated water by considering its residual toxicity after the application of combined AOPs. Moreover, experiments in actual conditions must be incremented because the presence of specific chemical species can positively or negatively influence the performance of the process.

As the combined AOP treatments are still at the initial stage, in-depth research for cost reduction after a rigorous economic assessment deserves much attention and can provide positive surprises in the future. One possible benefit can be the use of solar light as an energy source in the activation of the different involved species.

## 6. Conclusions

The presence of pharmaceutical residues in wastewater is continuously growing due to increasing use, and their removal represents one of the emerging concerns regarding environmental protection and restoration. These compounds are present in a large variety, and they are extremely stable, very complex and highly persistent in the aquatic environment. Treatment using AOPs has been revealed to be effective for the removal of different drugs both in lab-prepared and real wastewater effluents due to the formation of highly reactive and unselective radicals which are the oxidizing species. In general, for almost all drugs, a good degradation efficiency was found in short treatment times with various AOPs. A weak point of some of these technologies is the low degree of mineralization of the drugs and the occurrence of only a partial oxidation giving rise to intermediates that are often more dangerous than the original compounds. Furthermore, many of the reported investigations have been conducted at laboratory or pilot scales, and large-scale application is still limited. This is probably due to the high operating (especially energetic) cost of most of the combined AOP processes.

**Author Contributions:** Writing—Original Draft Preparation, M.U.; Writing—Original Draft Preparation, T.K.; Funding Acquisition, Visualization, V.L.; Supervision, Writing—Review and Editing, L.P.; Conceptualization, Supervision, Writing—Review and Editing, M.B. All authors have read and agreed to the published version of the manuscript.

**Funding:** “SAMOTHRACE” (MUR, PNRR-M4C2, ECS\_00000022), spoke 3-Università degli Studi di Palermo “S2-COMMs-Micro and Nanotechnologies for Smart & Sustainable Communities.

**Data Availability Statement:** No additional data are available.

**Acknowledgments:** The authors thank SiciliAn MicronanOTech Research And Innovation Center for financial support.

**Conflicts of Interest:** The authors declare no conflict of interest.

## References

1. Inamuddin; Asiri, A.M. *Correction to: Sustainable Green Chemical Processes and Their Allied Applications*; Springer Nature: Cham, Switzerland, 2020; ISBN 9783030422837.
2. Changotra, R.; Rajput, H.; Dhir, A. Natural Soil Mediated Photo Fenton-like Processes in Treatment of Pharmaceuticals: Batch and Continuous Approach. *Chemosphere* **2017**, *188*, 345–353. [[CrossRef](#)] [[PubMed](#)]
3. Wols, B.A.; Hofman-Caris, C.H.M.; Harmsen, D.J.H.; Beerendonk, E.F. Degradation of 40 Selected Pharmaceuticals by UV/H<sub>2</sub>O<sub>2</sub>. *Water Res.* **2013**, *47*, 5876–5888. [[CrossRef](#)] [[PubMed](#)]
4. Wang, J.; Chu, L.; Wojnárovits, L.; Takács, E. Occurrence and Fate of Antibiotics, Antibiotic Resistant Genes (ARGs) and Antibiotic Resistant Bacteria (ARB) in Municipal Wastewater Treatment Plant: An Overview. *Sci. Total Environ.* **2020**, *744*, 140997. [[CrossRef](#)] [[PubMed](#)]
5. Wang, J.; Wang, S. Removal of Pharmaceuticals and Personal Care Products (PPCPs) from Wastewater: A Review. *J. Environ. Manag.* **2016**, *182*, 620–640. [[CrossRef](#)] [[PubMed](#)]
6. Jodeh, S.; Abdelwahab, F.; Jaradat, N.; Warad, I.; Jodeh, W. Adsorption of Diclofenac from Aqueous Solution Using Cyclamen Persicum Tubers Based Activated Carbon (CTAC). *J. Assoc. Arab. Univ. Basic Appl. Sci.* **2016**, *20*, 32–38. [[CrossRef](#)]
7. Roberts, P.H.; Thomas, K.V. The Occurrence of Selected Pharmaceuticals in Wastewater Effluent and Surface Waters of the Lower Tyne Catchment. *Sci. Total Environ.* **2006**, *356*, 143–153. [[CrossRef](#)]
8. Mirzaei, R.; Yunesian, M.; Nasseri, S.; Gholami, M.; Jalilzadeh, E.; Shoeibi, S.; Mesdaghinia, A. Occurrence and Fate of Most Prescribed Antibiotics in Different Water Environments of Tehran. *Iran. Sci. Total Environ.* **2018**, *619–620*, 446–459. [[CrossRef](#)]
9. Szabó, R.K.; Megyeri, C.S.; Illés, E.; Gajda-Schrantz, K.; Mazellier, P.; Dombi, A. Phototransformation of Ibuprofen and Ketoprofen in Aqueous Solutions. *Chemosphere* **2011**, *84*, 1658–1663. [[CrossRef](#)]
10. Tran, H.T.T.; Kosslick, H.; Ibad, M.F.; Fischer, C.; Bentrup, U.; Vuong, T.H.; Nguyen, L.Q.; Schulz, A. Photocatalytic Performance of Highly Active Brookite in the Degradation of Hazardous Organic Compounds Compared to Anatase and Rutile. *Appl. Catal. B* **2017**, *200*, 647–658. [[CrossRef](#)]
11. Liu, W.; Sutton, N.B.; Rijnaarts, H.H.M.; Langenhoff, A.A.M. Anaerobic Biodegradation of Pharmaceutical Compounds Coupled to Dissimilatory Manganese (IV) or Iron (III) Reduction. *J. Hazard. Mater.* **2020**, *388*, 119361. [[CrossRef](#)]
12. Taoufik, N.; Elmchauri, A.; Anouar, F.; Korili, S.A.; Gil, A. Improvement of the Adsorption Properties of an Activated Carbon Coated by Titanium Dioxide for the Removal of Emerging Contaminants. *J. Water Process Eng.* **2019**, *31*, 100876. [[CrossRef](#)]
13. De Souza, D.I.; Dottein, E.M.; Giacobbo, A.; Siqueira Rodrigues, M.A.; De Pinho, M.N.; Bernardes, A.M. Nanofiltration for the Removal of Norfloxacin from Pharmaceutical Effluent. *J. Environ. Chem. Eng.* **2018**, *6*, 6147–6153. [[CrossRef](#)]
14. Nguyen, L.N.; Hai, F.I.; McDonald, J.A.; Khan, S.J.; Price, W.E.; Nghiem, L.D. Continuous Transformation of Chiral Pharmaceuticals in Enzymatic Membrane Bioreactors for Advanced Wastewater Treatment. *Water Sci. Technol.* **2017**, *76*, 1816–1826. [[CrossRef](#)] [[PubMed](#)]
15. Taoufik, N.; Boumya, W.; Achak, M.; Sillanpää, M.; Barka, N. Comparative Overview of Advanced Oxidation Processes and Biological Approaches for the Removal Pharmaceuticals. *J. Environ. Manag.* **2021**, *288*, 112404. [[CrossRef](#)] [[PubMed](#)]
16. Wu, S.; Li, X.; Tian, Y.; Lin, Y.; Hu, Y.H. Excellent Photocatalytic Degradation of Tetracycline over Black Anatase-TiO<sub>2</sub> under Visible Light. *Chem. Eng. J.* **2021**, *406*, 126747. [[CrossRef](#)]
17. Khan, A.H.; Khan, N.A.; Ahmed, S.; Dhingra, A.; Singh, C.P.; Khan, S.U.; Mohammadi, A.A.; Changani, F.; Yousefi, M.; Alam, S.; et al. Application of Advanced Oxidation Processes Followed by Different Treatment Technologies for Hospital Wastewater Treatment. *J. Clean. Prod.* **2020**, *269*, 122411. [[CrossRef](#)]
18. Abdel-Raouf, N.; Al-Homaidan, A.A.; Ibraheem, I.B.M. Microalgae and Wastewater Treatment. *Saudi J. Biol. Sci.* **2012**, *19*, 257–275. [[CrossRef](#)] [[PubMed](#)]
19. Zhang, T.; Liu, Y.; Rao, Y.; Li, X.; Yuan, D.; Tang, S.; Zhao, Q. Enhanced Photocatalytic Activity of TiO<sub>2</sub> with Acetylene Black and Persulfate for Degradation of Tetracycline Hydrochloride under Visible Light. *Chem. Eng. J.* **2020**, *384*, 123350. [[CrossRef](#)]
20. Ayoub, K.; van Hullebusch, E.D.; Cassir, M.; Bermond, A. Application of Advanced Oxidation Processes for TNT Removal: A Review. *J. Hazard. Mater.* **2010**, *178*, 10–28. [[CrossRef](#)]
21. Loddo, V.; Bellardita, M.; Camera-Roda, G.; Parrino, F.; Palmisano, L. Heterogeneous Photocatalysis: A Promising Advanced Oxidation Process. In *Current Trends and Future Developments on (Bio-) Membranes: Photocatalytic Membranes and Photocatalytic Membrane Reactors*; Elsevier Inc.: Amsterdam, The Netherlands, 2018; pp. 1–43. ISBN 9780128135495.
22. Nascimento, U.M.; Azevedo, E.B. Microwaves and Their Coupling to Advanced Oxidation Processes: Enhanced Performance in Pollutants Degradation. *J. Environ. Sci. Health A Tox Hazard. Subst. Environ. Eng.* **2013**, *48*, 1056–1072. [[CrossRef](#)]

23. Deng, Y.; Zhao, R. Advanced Oxidation Processes (AOPs) in Wastewater Treatment. *Curr. Pollut. Rep.* **2015**, *1*, 167–176. [[CrossRef](#)]
24. Vogelpohl, A. Applications of AOPs in Wastewater Treatment. *Water Sci. Technol.* **2007**, *55*, 207–211. [[CrossRef](#)] [[PubMed](#)]
25. Wang, D.; Junker, A.L.; Sillanpää, M.; Jiang, Y.; Wei, Z. Photo-Based Advanced Oxidation Processes for Zero Pollution: Where Are We Now? *Engineering* **2023**, *23*, 19–23. [[CrossRef](#)]
26. Klavarioti, M.; Mantzavinos, D.; Kassinos, D. Removal of Residual Pharmaceuticals from Aqueous Systems by Advanced Oxidation Processes. *Environ. Int.* **2009**, *35*, 402–417. [[CrossRef](#)]
27. Pandis, P.K.; Kalogirou, C.; Kanellou, E.; Vaitsis, C.; Savvidou, M.G.; Sourkouni, G.; Zorpas, A.A.; Argiris, C. Key Points of Advanced Oxidation Processes (AOPs) for Wastewater, Organic Pollutants and Pharmaceutical Waste Treatment: A Mini Review. *ChemEngineering* **2022**, *6*, 8. [[CrossRef](#)]
28. Blatchley, E.R.; Shen, C.; Scheible, O.K.; Robinson, J.P.; Ragheb, K.; Bergstrom, D.E.; Rokjer, D. Validation of Large-Scale, Monochromatic UV Disinfection Systems for Drinking Water Using Dyed Microspheres. *Water Res.* **2008**, *42*, 677–688. [[CrossRef](#)]
29. Doll, T.E.; Frimmel, F.H. Fate of Pharmaceuticals—Photodegradation by Simulated Solar UV-Light. *Chemosphere* **2003**, *52*, 1757–1769. [[CrossRef](#)]
30. Saritha, P.; Aparna, C.; Himabindu, V.; Anjaneyulu, Y. Comparison of Various Advanced Oxidation Processes for the Degradation of 4-Chloro-2 Nitrophenol. *J. Hazard. Mater.* **2007**, *149*, 609–614. [[CrossRef](#)]
31. Pereira, V.J.; Weinberg, H.S.; Linden, K.G.; Singer, P.C. UV Degradation Kinetics and Modeling of Pharmaceutical Compounds in Laboratory Grade and Surface Water via Direct and Indirect Photolysis at 254 nm. *Environ. Sci. Technol.* **2007**, *41*, 1682–1688. [[CrossRef](#)]
32. Chen, S.; Hou, Y.; Rong, Y.; Tu, L.; Yu, Z.; Sun, J.; Lan, D.; Li, Z.; Zhu, H.; Wang, S. Hydroxyl Radical and Carbonate Radical Facilitate Chlortetracycline Degradation in the Bio-Photoelectrochemical System with a Bioanode and a Bi<sub>2</sub>O<sub>3</sub>/CuO Photocathode Using Bicarbonate Buffer. *Chemosphere* **2022**, *296*, 134040. [[CrossRef](#)]
33. Bilal, M.; Rizwan, K.; Adeel, M.; Iqbal, H.M.N. Hydrogen-Based Catalyst-Assisted Advanced Oxidation Processes to Mitigate Emerging Pharmaceutical Contaminants. *Int. J. Hydrogen Energy* **2022**, *47*, 19555–19569. [[CrossRef](#)]
34. Guo, K.; Wu, Z.; Shang, C.; Yao, B.; Hou, S.; Yang, X.; Song, W.; Fang, J. Radical Chemistry and Structural Relationships of PPCP Degradation by UV/Chlorine Treatment in Simulated Drinking Water. *Environ. Sci. Technol.* **2017**, *51*, 10431–10439. [[CrossRef](#)]
35. Brillas, E. A Critical Review on Ibuprofen Removal from Synthetic Waters, Natural Waters, and Real Wastewaters by Advanced Oxidation Processes. *Chemosphere* **2022**, *286*, 131849. [[CrossRef](#)] [[PubMed](#)]
36. Fang, J.; Fu, Y.; Shang, C. The Roles of Reactive Species in Micropollutant Degradation in the UV/Free Chlorine System. *Environ. Sci. Technol.* **2014**, *48*, 1859–1868. [[CrossRef](#)] [[PubMed](#)]
37. Watts, M.J.; Linden, K.G. Chlorine Photolysis and Subsequent OH Radical Production during UV Treatment of Chlorinated Water. *Water Res.* **2007**, *41*, 2871–2878. [[CrossRef](#)] [[PubMed](#)]
38. Xiang, Y.; Fang, J.; Shang, C. Kinetics and Pathways of Ibuprofen Degradation by the UV/Chlorine Advanced Oxidation Process. *Water Res.* **2016**, *90*, 301–308. [[CrossRef](#)] [[PubMed](#)]
39. Kishimoto, N. State of the Art of UV/Chlorine Advanced Oxidation Processes: Their Mechanism, Byproducts Formation, Process Variation, and Applications. *J. Water Environ. Technol.* **2019**, *17*, 302–335. [[CrossRef](#)]
40. Lee, Y.; von Gunten, U. Oxidative Transformation of Micropollutants during Municipal Wastewater Treatment: Comparison of Kinetic Aspects of Selective (Chlorine, Chlorine Dioxide, FerrateVI, and Ozone) and Non-Selective Oxidants (Hydroxyl Radical). *Water Res.* **2010**, *44*, 555–566. [[CrossRef](#)]
41. Grebel, J.E.; Pignatello, J.J.; Mitch, W.A. Effect of Halide Ions and Carbonates on Organic Contaminant Degradation by Hydroxyl Radical-Based Advanced Oxidation Processes in Saline Waters. *Environ. Sci. Technol.* **2010**, *44*, 6822–6828. [[CrossRef](#)]
42. Wang, D.; Bolton, J.R.; Hofmann, R. Medium Pressure UV Combined with Chlorine Advanced Oxidation for Trichloroethylene Destruction in a Model Water. *Water Res.* **2012**, *46*, 4677–4686. [[CrossRef](#)]
43. Mota, A.L.N.; Albuquerque, L.F.; Beltrame, L.T.C.; Chiavone-Filho, O.; Machulek, A.; Nascimento, C.A.O. Brazilian Journal of Petroleum and Gas Advanced Oxidation Processes and Their Application in the Petroleum Industry: A Review. *Braz. J. Pet. Gas* **2008**, *2*, 122–142.
44. Poyatos, J.M.; Muñoz, M.M.; Almecija, M.C.; Torres, J.C.; Hontoria, E.; Osorio, F. Advanced Oxidation Processes for Wastewater Treatment: State of the Art. *Water Air Soil Pollut.* **2010**, *205*, 187–204. [[CrossRef](#)]
45. Garoma, T.; Gurol, M.D. Degradation of Tert-Butyl Alcohol in Dilute Aqueous Solution by an O<sub>3</sub>/UV Process. *Environ. Sci. Technol.* **2004**, *38*, 5246–5252. [[CrossRef](#)]
46. Ghauch, A.; Tuqan, A.M. Oxidation of Bisoprolol in Heated Persulfate/H<sub>2</sub>O Systems: Kinetics and Products. *Chem. Eng. J.* **2012**, *183*, 162–171. [[CrossRef](#)]
47. Lee, J.; Von Gunten, U.; Kim, J.H. Persulfate-Based Advanced Oxidation: Critical Assessment of Opportunities and Roadblocks. *Environ. Sci. Technol.* **2020**, *54*, 3064–3081. [[CrossRef](#)] [[PubMed](#)]
48. Lutze, H.V.; Bircher, S.; Rapp, I.; Kerlin, N.; Bakkour, R.; Geisler, M.; Von Sonntag, C.; Schmidt, T.C. Degradation of Chlorotriazine Pesticides by Sulfate Radicals and the Influence of Organic Matter. *Environ. Sci. Technol.* **2015**, *49*, 1673–1680. [[CrossRef](#)] [[PubMed](#)]
49. Guan, Y.H.; Ma, J.; Li, X.C.; Fang, J.Y.; Chen, L.W. Influence of pH on the Formation of Sulfate and Hydroxyl Radicals in the UV/Peroxymonosulfate System. *Environ. Sci. Technol.* **2011**, *45*, 9308–9314. [[CrossRef](#)]
50. Fast, S.A.; Gude, V.G.; Truax, D.D.; Martin, J.; Magbanua, B.S. A Critical Evaluation of Advanced Oxidation Processes for Emerging Contaminants Removal. *Environ. Process.* **2017**, *4*, 283–302. [[CrossRef](#)]

51. Rosman, N.; Salleh, W.N.W.; Mohamed, M.A.; Jaafar, J.; Ismail, A.F.; Harun, Z. Hybrid Membrane Filtration-Advanced Oxidation Processes for Removal of Pharmaceutical Residue. *J. Colloid Interface Sci.* **2018**, *532*, 236–260. [[CrossRef](#)]
52. Khajouei, G.; Finklea, H.O.; Lin, L.S. UV/Chlorine Advanced Oxidation Processes for Degradation of Contaminants in Water and Wastewater: A Comprehensive Review. *J. Environ. Chem. Eng.* **2022**, *10*, 107508. [[CrossRef](#)]
53. Tian, F.X.; Ye, W.K.; Xu, B.; Hu, X.J.; Ma, S.X.; Lai, F.; Gao, Y.Q.; Xing, H.B.; Xia, W.H.; Wang, B. Comparison of UV-Induced AOPs (UV/Cl<sub>2</sub>, UV/NH<sub>2</sub>Cl, UV/ClO<sub>2</sub> and UV/H<sub>2</sub>O<sub>2</sub>) in the Degradation of Iopamidol: Kinetics, Energy Requirements and DBPs-Related Toxicity in Sequential Disinfection Processes. *Chem. Eng. J.* **2020**, *398*, 125570. [[CrossRef](#)] [[PubMed](#)]
54. Nidheesh, P.V.; Divyapriya, G.; Ezzahra Titchou, F.; Hamdani, M. Treatment of Textile Wastewater by Sulfate Radical Based Advanced Oxidation Processes. *Sep. Purif. Technol.* **2022**, *293*, 121115. [[CrossRef](#)]
55. Ricardo, I.A.; Paniagua, C.E.S.; Alberto, E.A.; Starling, M.C.V.M.; Agüera, A.; Trovó, A.G. A Critical Review of Trends in Advanced Oxidation Processes for the Removal of Benzophenone-3, Fipronil, and Propylparaben from Aqueous Matrices: Pathways and Toxicity Changes. *J. Water Process Eng.* **2022**, *49*, 102973. [[CrossRef](#)]
56. Rekhate, C.V.; Srivastava, J.K. Recent Advances in Ozone-Based Advanced Oxidation Processes for Treatment of Wastewater—A Review. *Chem. Eng. J. Adv.* **2020**, *3*, 100031. [[CrossRef](#)]
57. Qin, H.; Chen, H.; Zhang, X.; Yang, G.; Feng, Y. Efficient Degradation of Fulvic Acids in Water by Catalytic Ozonation with CeO<sub>2</sub>/AC. *J. Chem. Technol. Biotechnol.* **2014**, *89*, 1402–1409. [[CrossRef](#)]
58. Guo, Y.; Yang, L.; Wang, X. The Application and Reaction Mechanism of Catalytic Ozonation in Water Treatment. *J. Environ. Anal. Toxicol.* **2012**, *2*, 1000150. [[CrossRef](#)]
59. Kasprzyk-Hordern, B.; Ziółek, M.; Nawrocki, J. Catalytic Ozonation and Methods of Enhancing Molecular Ozone Reactions in Water Treatment. *Appl. Catal. B* **2003**, *46*, 639–669. [[CrossRef](#)]
60. Cheng, S.W.; Li, Y.H.; Yuan, C.S.; Tsai, P.Y.; Shen, H.Z.; Hung, C.H. An Innovative Advanced Oxidation Technology for Effective Decomposition of Formaldehyde by Combining Iron Modified Nano-TiO<sub>2</sub> (Fe/TiO<sub>2</sub>) Photocatalytic Degradation with Ozone Oxidation. *Aerosol Air Qual. Res.* **2018**, *18*, 3220–3233. [[CrossRef](#)]
61. Mashayekh-Salehi, A.; Moussavi, G.; Yaghmaeian, K. Preparation, Characterization and Catalytic Activity of a Novel Mesoporous Nanocrystalline MgO Nanoparticle for Ozonation of Acetaminophen as an Emerging Water Contaminant. *Chem. Eng. J.* **2017**, *310*, 157–169. [[CrossRef](#)]
62. Nawaz, F.; Xie, Y.; Cao, H.; Xiao, J.; Wang, Y.; Zhang, X.; Li, M.; Duan, F. Catalytic Ozonation of 4-Nitrophenol over an Mesoporous α-MnO<sub>2</sub> with Resistance to Leaching. *Catal. Today* **2015**, *258*, 595–601. [[CrossRef](#)]
63. Huang, W.J.; Fang, G.C.; Wang, C.C. A Nanometer-ZnO Catalyst to Enhance the Ozonation of 2,4,6-Trichlorophenol in Water. *Colloids Surf. A Physicochem. Eng. Asp.* **2005**, *260*, 45–51. [[CrossRef](#)]
64. Biard, P.F.; Werghi, B.; Soutrel, I.; Orhand, R.; Couvert, A.; Denicourt-Nowicki, A.; Roucoux, A. Efficient Catalytic Ozonation by Ruthenium Nanoparticles Supported on SiO<sub>2</sub> or TiO<sub>2</sub>: Towards the Use of a Non-Woven Fiber Paper as Original Support. *Chem. Eng. J.* **2016**, *289*, 374–381. [[CrossRef](#)]
65. Qi, F.; Chu, W.; Xu, B. Comparison of Phenacetin Degradation in Aqueous Solutions by Catalytic Ozonation with CuFe<sub>2</sub>O<sub>4</sub> and Its Precursor: Surface Properties, Intermediates and Reaction Mechanisms. *Chem. Eng. J.* **2016**, *284*, 28–36. [[CrossRef](#)]
66. Guo, Y.; Zhao, E.; Wang, J.; Zhang, X.; Huang, H.; Yu, G.; Wang, Y. Comparison of Emerging Contaminant Abatement by Conventional Ozonation, Catalytic Ozonation, O<sub>3</sub>/H<sub>2</sub>O<sub>2</sub> and Electro-Peroxone Processes. *J. Hazard. Mater.* **2020**, *389*, 121829. [[CrossRef](#)] [[PubMed](#)]
67. Turkey, O.; Ersoy, Z.G.; Barişçi, S. Review—The Application of an Electro-Peroxone Process in Water and Wastewater Treatment. *J. Electrochem. Soc.* **2017**, *164*, E94–E102. [[CrossRef](#)]
68. Yao, W.; Wang, X.; Yang, H.; Yu, G.; Deng, S.; Huang, J.; Wang, B.; Wang, Y. Removal of Pharmaceuticals from Secondary Effluents by an Electro-Peroxone Process. *Water Res.* **2016**, *88*, 826–835. [[CrossRef](#)]
69. Bakheet, B.; Yuan, S.; Li, Z.; Wang, H.; Zuo, J.; Komarneni, S.; Wang, Y. Electro-Peroxone Treatment of Orange II Dye Wastewater. *Water Res.* **2013**, *47*, 6234–6243. [[CrossRef](#)]
70. Wang, Y.; Yu, G.; Deng, S.; Huang, J.; Wang, B. The Electro-Peroxone Process for the Abatement of Emerging Contaminants: Mechanisms, Recent Advances, and Prospects. *Chemosphere* **2018**, *208*, 640–654. [[CrossRef](#)]
71. Priyadarshini, M.; Das, I.; Ghangrekar, M.M.; Blaney, L. Advanced Oxidation Processes: Performance, Advantages, and Scale-up of Emerging Technologies. *J. Environ. Manag.* **2022**, *316*, 115295. [[CrossRef](#)]
72. Shi, Y.; Xiong, Z.; Zhou, P.; Liu, Y.; Yu, S.; Xie, Z.; Wu, X.; Zheng, Y.; Shi, Y.; Xiong, Z. Review of Advanced Oxidation Processes for Treating Hospital Sewage to Achieve Decontamination and Disinfection. *Chin. Chem. Lett.* **2023**, *35*, 108714. [[CrossRef](#)]
73. Bavasso, I.; Montanaro, D.; Petrucci, E. Ozone-Based Electrochemical Advanced Oxidation Processes. *Curr. Opin. Electrochem.* **2022**, *34*, 101017. [[CrossRef](#)]
74. Shokri, A. Employing Electro-Peroxone Process for Degradation of Acid Red 88 in Aqueous Environment by Central Composite Design: A New Kinetic Study and Energy Consumption. *Chemosphere* **2022**, *296*, 133817. [[CrossRef](#)] [[PubMed](#)]
75. Dubey, S.; Joshi, A.; Trivedi, R.; Pal, D.; Prajapati, A.K. Electro-Peroxone Treatment of Rice Grain Based Distillery Biodigester Effluent: COD and Color Removal. *Water Resour. Ind.* **2021**, *25*, 100142. [[CrossRef](#)]
76. Rodríguez-Peña, M.; Mena, I.F.; Pérez, J.A.B.; Barrera-Díaz, C.E.; Rodrigo, M.A. Does Electro-Peroxonation Improve Performance of Electro-Ozonation? *J. Environ. Chem. Eng.* **2022**, *10*, 107578. [[CrossRef](#)]

77. Aramyan, S.M. Advances in Fenton and Fenton Based Oxidation Processes for Industrial Effluent Contaminants Control—A Review. *Int. J. Environ. Sci. Nat. Resour.* **2017**, *2*, 1–18. [[CrossRef](#)]
78. Santos, M.C.; Antonin, V.S.; Souza, F.M.; Aveiro, L.R.; Pinheiro, V.S.; Gentil, T.C.; Lima, T.S.; Moura, J.P.C.; Silva, C.R.; Lucchetti, L.E.B.; et al. Decontamination of Wastewater Containing Contaminants of Emerging Concern by Electrooxidation and Fenton-Based Processes—A Review on the Relevance of Materials and Methods. *Chemosphere* **2022**, *307*, 135763. [[CrossRef](#)]
79. Pacheco-Álvarez, M.; Picos Benítez, R.; Rodríguez-Narváez, O.M.; Brillas, E.; Peralta-Hernández, J.M. A Critical Review on Paracetamol Removal from Different Aqueous Matrices by Fenton and Fenton-Based Processes, and Their Combined Methods. *Chemosphere* **2022**, *303*, 134883. [[CrossRef](#)]
80. O'Dowd, K.; Pillai, S.C. Photo-Fenton Disinfection at near Neutral PH: Process, Parameter Optimization and Recent Advances. *J. Environ. Chem. Eng.* **2020**, *8*, 104063. [[CrossRef](#)]
81. Umar, M.; Aziz, H.A.; Yusoff, M.S. Trends in the Use of Fenton, Electro-Fenton and Photo-Fenton for the Treatment of Landfill Leachate. *Waste Manag.* **2010**, *30*, 2113–2121. [[CrossRef](#)]
82. Brillas, E.; Sirés, I.; Oturan, M.A. Electro-Fenton Process and Related Electrochemical Technologies Based on Fenton's Reaction Chemistry. *Chem. Rev.* **2009**, *109*, 6570–6631. [[CrossRef](#)]
83. Ismail, S.A.; Ang, W.L.; Mohammad, A.W. Electro-Fenton Technology for Wastewater Treatment: A Bibliometric Analysis of Current Research Trends, Future Perspectives and Energy Consumption Analysis. *J. Water Process Eng.* **2021**, *40*, 101952. [[CrossRef](#)]
84. Ghoneim, M.M.; El-Desoky, H.S.; Zidan, N.M. Electro-Fenton Oxidation of Sunset Yellow FCF Azo-Dye in Aqueous Solutions. *Desalination* **2011**, *274*, 22–30. [[CrossRef](#)]
85. Babuponnusami, A.; Muthukumar, K. Advanced Oxidation of Phenol: A Comparison between Fenton, Electro-Fenton, Sono-Electro-Fenton and Photo-Electro-Fenton Processes. *Chem. Eng. J.* **2012**, *183*, 1–9. [[CrossRef](#)]
86. GilPavas, E.; Dobrosz-Gómez, I.; Gómez-García, M.Á. Optimization of Solar-Driven Photo-Electro-Fenton Process for the Treatment of Textile Industrial Wastewater. *J. Water Process Eng.* **2018**, *24*, 49–55. [[CrossRef](#)]
87. Babuponnusami, A.; Muthukumar, K. A Review on Fenton and Improvements to the Fenton Process for Wastewater Treatment. *J. Environ. Chem. Eng.* **2014**, *2*, 557–572. [[CrossRef](#)]
88. Cuerda-Correa, E.M.; Alexandre-Franco, M.F.; Fern, C. Antibiotics from Water. *An Overview. Water* **2019**, *12*, 102.
89. Wang, B.; Song, Z.; Sun, L. A Review: Comparison of Multi-Air-Pollutant Removal by Advanced Oxidation Processes—Industrial Implementation for Catalytic Oxidation Processes. *Chem. Eng. J.* **2021**, *409*, 128136. [[CrossRef](#)]
90. Gautam, P.; Kumar, S.; Lokhandwala, S. Advanced Oxidation Processes for Treatment of Leachate from Hazardous Waste Landfill: A Critical Review. *J. Clean. Prod.* **2019**, *237*, 117639. [[CrossRef](#)]
91. Oturan, M.A. Outstanding Performances of the BDD Film Anode in Electro-Fenton Process: Applications and Comparative Performance. *Curr. Opin. Solid. State Mater. Sci.* **2021**, *25*, 100925. [[CrossRef](#)]
92. Nidheesh, P.V.; Trelu, C.; Vargas, H.O.; Mousset, E.; Ganiyu, S.O.; Oturan, M.A. Electro-Fenton Process in Combination with Other Advanced Oxidation Processes: Challenges and Opportunities. *Curr. Opin. Electrochem.* **2023**, *37*, 101171. [[CrossRef](#)]
93. Arefi-Oskoui, S.; Khataee, A.; Safarpour, M.; Orooji, Y.; Vatanpour, V. A Review on the Applications of Ultrasonic Technology in Membrane Bioreactors. *Ultrason. Sonochemistry* **2019**, *58*, 104633. [[CrossRef](#)] [[PubMed](#)]
94. Madhavan, J.; Theerthagiri, J.; Balaji, D.; Sunitha, S. Ultrasound: An Overview. *Molecules* **2019**, *24*, 1–18.
95. Zhou, N.; Liang, R.; Hu, A. *Nanotechnology for Water Treatment and Purification*; Springer Nature: Cham, Switzerland, 2014; Volume 22, ISBN 978-3-319-06577-9.
96. Zhang, Y.; Shaad, K.; Vollmer, D.; Ma, C. Treatment of Textile Wastewater Using Advanced Oxidation Processes—A Critical Review. *Water* **2021**, *13*, 3515. [[CrossRef](#)]
97. Grandclément, C.; Seyssiecq, I.; Piram, A.; Wong-Wah-Chung, P.; Vanot, G.; Tiliacos, N.; Roche, N.; Doumenq, P. From the Conventional Biological Wastewater Treatment to Hybrid Processes, the Evaluation of Organic Micropollutant Removal: A Review. *Water Res.* **2017**, *111*, 297–317. [[CrossRef](#)] [[PubMed](#)]
98. Mohapatra, D.P.; Kirpalani, D.M. Advancement in Treatment of Wastewater: Fate of Emerging Contaminants. *Can. J. Chem. Eng.* **2019**, *97*, 2621–2631. [[CrossRef](#)]
99. da Silva, T.L.; Costa, C.S.D.; da Silva, M.G.C.; Vieira, M.G.A. Overview of Non-Steroidal Anti-Inflammatory Drugs Degradation by Advanced Oxidation Processes. *J. Clean. Prod.* **2022**, *346*, 131226. [[CrossRef](#)]
100. Pan, Z.; Song, C.; Li, L.; Wang, H.; Pan, Y.; Wang, C.; Li, J.; Wang, T.; Feng, X. Membrane Technology Coupled with Electrochemical Advanced Oxidation Processes for Organic Wastewater Treatment: Recent Advances and Future Prospects. *Chem. Eng. J.* **2019**, *376*, 120909. [[CrossRef](#)]
101. Chaplin, B.P. Critical Review of Electrochemical Advanced Oxidation Processes for Water Treatment Applications. *Environ. Sci. Process. Impacts* **2014**, *16*, 1182–1203. [[CrossRef](#)]
102. Oturan, M.A.; Brillas, E. Electrochemical Advanced Oxidation Processes (EAOPs) for Environmental Applications. *Port. Electrochim. Acta* **2007**, *25*, 1–18. [[CrossRef](#)]
103. Ganiyu, S.O.; Martínez-Huitle, C.A.; Oturan, M.A. Electrochemical Advanced Oxidation Processes for Wastewater Treatment: Advances in Formation and Detection of Reactive Species and Mechanisms. *Curr. Opin. Electrochem.* **2021**, *27*, 100678. [[CrossRef](#)]
104. Sirés, I.; Brillas, E.; Oturan, M.A.; Rodrigo, M.A.; Panizza, M. Electrochemical Advanced Oxidation Processes: Today and Tomorrow. *A Review. Environ. Sci. Pollut. Res.* **2014**, *21*, 8336–8367. [[CrossRef](#)] [[PubMed](#)]

105. Cuervo Lumbaque, E.; Lopes Tiburtius, E.R.; Barreto-Rodrigues, M.; Sirtori, C. Current Trends in the Use of Zero-Valent Iron (Fe<sup>0</sup>) for Degradation of Pharmaceuticals Present in Different Water Matrices. *Trends Environ. Anal. Chem.* **2019**, *24*, e00069. [[CrossRef](#)]
106. Li, Q.; Chen, Z.; Wang, H.; Yang, H.; Wen, T.; Wang, S.; Hu, B.; Wang, X. Removal of Organic Compounds by Nanoscale Zero-Valent Iron and Its Composites. *Sci. Total Environ.* **2021**, *792*, 148546. [[CrossRef](#)]
107. Fu, F.; Dionysiou, D.D.; Liu, H. The Use of Zero-Valent Iron for Groundwater Remediation and Wastewater Treatment: A Review. *J. Hazard. Mater.* **2014**, *267*, 194–205. [[CrossRef](#)] [[PubMed](#)]
108. Mahmoud, M.E.; Abdelwahab, M.S. One-Step Synthesis of Zero-Valent Sn Nanoparticles and Potential Microwave Remediation of Lead from Water. *Mater. Res. Bull.* **2021**, *134*, 111090. [[CrossRef](#)]
109. Guan, X.; Sun, Y.; Qin, H.; Li, J.; Lo, I.M.C.; He, D.; Dong, H. The Limitations of Applying Zero-Valent Iron Technology in Contaminants Sequestration and the Corresponding Countermeasures: The Development in Zero-Valent Iron Technology in the Last Two Decades (1994–2014). *Water Res.* **2015**, *75*, 224–248. [[CrossRef](#)]
110. Giannakis, S.; Lin, K.Y.A.; Ghanbari, F. A Review of the Recent Advances on the Treatment of Industrial Wastewaters by Sulfate Radical-Based Advanced Oxidation Processes (SR-AOPs). *Chem. Eng. J.* **2021**, *406*, 127083. [[CrossRef](#)]
111. Cardoso, I.M.F.; Cardoso, R.M.F.; Esteves da Silva, J.C.G. Advanced Oxidation Processes Coupled with Nanomaterials for Water Treatment. *Nanomaterials* **2021**, *11*, 2045. [[CrossRef](#)]
112. Xiao, R.; Luo, Z.; Wei, Z.; Luo, S.; Spinney, R.; Yang, W.; Dionysiou, D.D. Activation of Peroxymonosulfate/Persulfate by Nanomaterials for Sulfate Radical-Based Advanced Oxidation Technologies. *Curr. Opin. Chem. Eng.* **2018**, *19*, 51–58. [[CrossRef](#)]
113. Scaria, J.; Nidheesh, P.V. Comparison of Hydroxyl-Radical-Based Advanced Oxidation Processes with Sulfate Radical-Based Advanced Oxidation Processes. *Curr. Opin. Chem. Eng.* **2022**, *36*, 100830. [[CrossRef](#)]
114. Kappe, C.O. Controlled Microwave Heating in Modern Organic Synthesis. *Angew. Chem. Int. Ed.* **2004**, *43*, 6250–6284. [[CrossRef](#)] [[PubMed](#)]
115. Jones, D.A.; Lelyveld, T.P.; Mavrofidis, S.D.; Kingman, S.W.; Miles, N.J. Microwave Heating Applications in Environmental Engineering—A Review. *Resour. Conserv. Recycl.* **2002**, *34*, 75–90. [[CrossRef](#)]
116. Bose, S.; Kumar, M. Microwave-Assisted Persulfate/Peroxymonosulfate Process for Environmental Remediation. *Curr. Opin. Chem. Eng.* **2022**, *36*, 100826. [[CrossRef](#)]
117. Liu, X.; Huang, F.; Yu, Y.; Zhao, P.; Zhou, Y.; He, Y.; Xu, Y.; Zhang, Y. Ofloxacin Degradation over Cu–Ce Tyre Carbon Catalysts by the Microwave Assisted Persulfate Process. *Appl. Catal. B* **2019**, *253*, 149–159. [[CrossRef](#)]
118. Wang, F.; Wu, C.; Li, Q. Treatment of Refractory Organics in Strongly Alkaline Dinitro Diazophenol Wastewater with Microwave Irradiation-Activated Persulfate. *Chemosphere* **2020**, *254*, 126773. [[CrossRef](#)]
119. Verma, P.; Samanta, S.K. Microwave-Enhanced Advanced Oxidation Processes for the Degradation of Dyes in Water. *Environ. Chem. Lett.* **2018**, *16*, 969–1007. [[CrossRef](#)]
120. Gao, Y.; Zou, D. Efficient Degradation of Levofloxacin by a Microwave–3D ZnCo<sub>2</sub>O<sub>4</sub>/Activated Persulfate Process: Effects, Degradation Intermediates, and Acute Toxicity. *Chem. Eng. J.* **2020**, *393*, 124795. [[CrossRef](#)]
121. Cao, M.; Xu, P.; Tian, K.; Shi, F.; Zheng, Q.; Ma, D.; Zhang, G. Recent Advances in Microwave-Enhanced Advanced Oxidation Processes (MAOPs) for Environmental Remediation: A Review. *Chem. Eng. J.* **2023**, *471*, 144208. [[CrossRef](#)]
122. Wang, H.; Zhao, Z.; Zhang, X.; Dong, W.; Cao, Z.; He, L.; Wang, X. Rapid Decomplexation of Ni-EDTA by Microwave-Assisted Fenton Reaction. *Chem. Eng. J.* **2020**, *381*, 122703. [[CrossRef](#)]
123. Hu, L.; Zhang, G.; Wang, Q.; Wang, X.; Wang, P. Effect of Microwave Heating on Persulfate Activation for Rapid Degradation and Mineralization of P-Nitrophenol. *ACS Sustain. Chem. Eng.* **2019**, *7*, 11662–11671. [[CrossRef](#)]
124. Qi, C.; Liu, X.; Lin, C.; Zhang, X.; Ma, J.; Tan, H.; Ye, W. Degradation of Sulfamethoxazole by Microwave-Activated Persulfate: Kinetics, Mechanism and Acute Toxicity. *Chem. Eng. J.* **2014**, *249*, 6–14. [[CrossRef](#)]
125. Rauf, M.A.; Ashraf, S.S. Fundamental Principles and Application of Heterogeneous Photocatalytic Degradation of Dyes in Solution. *Chem. Eng. J.* **2009**, *151*, 10–18. [[CrossRef](#)]
126. Mahdi, M.H.; Mohammed, T.J.; Al-Najar, J.A. Advanced Oxidation Processes (AOPs) for Treatment of Antibiotics in Wastewater: A Review. *IOP Conf. Ser. Earth Environ. Sci.* **2021**, *779*, 012109. [[CrossRef](#)]
127. Dewil, R.; Mantzavinos, D.; Poullos, I.; Rodrigo, M.A. New Perspectives for Advanced Oxidation Processes. *J. Environ. Manag.* **2017**, *195*, 93–99. [[CrossRef](#)] [[PubMed](#)]
128. Banerjee, S.; Pillai, S.C.; Falaras, P.; O'shea, K.E.; Byrne, J.A.; Dionysiou, D.D. New Insights into the Mechanism of Visible Light Photocatalysis. *J. Phys. Chem. Lett.* **2014**, *5*, 2543–2554. [[CrossRef](#)] [[PubMed](#)]
129. Vellanki, B.P.; Batchelor, B.; Abdel-Wahab, A. Advanced Reduction Processes: A New Class of Treatment Processes. *Environ. Eng. Sci.* **2013**, *30*, 264–271. [[CrossRef](#)]
130. Neta, P.; Huie, R.E.; Harriman, A. One-Electron-Transfer Reactions of the Couple SO<sub>2</sub>/SO<sub>2</sub><sup>−</sup> in Aqueous Solutions. *Pulse Radiolytic and Cyclic Voltammetric Studies. J. Phys. Chem.* **1987**, *91*, 1606–1611.
131. Ibrahim, I.; Athanasekou, C.; Manolis, G.; Kaltzoglou, A.; Nasikas, N.K.; Katsaros, F.; Devlin, E.; Kontos, A.G.; Falaras, P. Photocatalysis as an Advanced Reduction Process (ARP): The Reduction of 4-Nitrophenol Using Titania Nanotubes-Ferrite Nanocomposites. *J. Hazard. Mater.* **2019**, *372*, 37–44. [[CrossRef](#)]
132. Liu, X.; Vellanki, B.P.; Batchelor, B.; Abdel-Wahab, A. Degradation of 1,2-Dichloroethane with Advanced Reduction Processes (ARPs): Effects of Process Variables and Mechanisms. *Chem. Eng. J.* **2014**, *237*, 300–307. [[CrossRef](#)]

133. Cui, J.; Gao, P.; Deng, Y. Destruction of Per- and Polyfluoroalkyl Substances (PFAS) with Advanced Reduction Processes (ARPs): A Critical Review. *Environ. Sci. Technol.* **2020**, *54*, 3752–3766. [[CrossRef](#)]
134. Yu, H.; Nie, E.; Xu, J.; Yan, S.; Cooper, W.J.; Song, W. Degradation of Diclofenac by Advanced Oxidation and Reduction Processes: Kinetic Studies, Degradation Pathways and Toxicity Assessments. *Water Res.* **2013**, *47*, 1909–1918. [[CrossRef](#)]
135. Jeong, J.; Song, W.; Cooper, W.J.; Jung, J.; Greaves, J. Degradation of Tetracycline Antibiotics: Mechanisms and Kinetic Studies for Advanced Oxidation/Reduction Processes. *Chemosphere* **2010**, *78*, 533–540. [[CrossRef](#)] [[PubMed](#)]
136. Akerdi, A.G.; Bahrami, S.H. Application of Heterogeneous Nano-Semiconductors for Photocatalytic Advanced Oxidation of Organic Compounds: A Review. *J. Environ. Chem. Eng.* **2019**, *7*, 103283. [[CrossRef](#)]
137. Macedo, L.C.; Zaia, D.A.M.; Moore, G.J.; de Santana, H. Degradation of Leather Dye on TiO<sub>2</sub>: A Study of Applied Experimental Parameters on Photoelectrocatalysis. *J. Photochem. Photobiol. A Chem.* **2007**, *185*, 86–93. [[CrossRef](#)]
138. Wang, C.C.; Lee, C.K.; Lyu, M.D.; Juang, L.C. Photocatalytic Degradation of C.I. Basic Violet 10 Using TiO<sub>2</sub> Catalysts Supported by Y Zeolite: An Investigation of the Effects of Operational Parameters. *Dye. Pigment.* **2008**, *76*, 817–824. [[CrossRef](#)]
139. Zhang, Y.; Zhou, J.; Chen, X.; Wang, L.; Cai, W. Coupling of Heterogeneous Advanced Oxidation Processes and Photocatalysis in Efficient Degradation of Tetracycline Hydrochloride by Fe-Based MOFs: Synergistic Effect and Degradation Pathway. *Chem. Eng. J.* **2019**, *369*, 745–757. [[CrossRef](#)]
140. Antoniou, M.G.; Hey, G.; Rodríguez Vega, S.; Spiliotopoulou, A.; Fick, J.; Tysklind, M.; la Cour Jansen, J.; Andersen, H.R. Required Ozone Doses for Removing Pharmaceuticals from Wastewater Effluents. *Sci. Total Environ.* **2013**, *456–457*, 42–49. [[CrossRef](#)]
141. Lado Ribeiro, A.R.; Moreira, N.F.F.; Li Puma, G.; Silva, A.M.T. Impact of Water Matrix on the Removal of Micropollutants by Advanced Oxidation Technologies. *Chem. Eng. J.* **2019**, *363*, 155–173. [[CrossRef](#)]
142. Li, D.; Feng, Z.; Zhou, B.; Chen, H.; Yuan, R. Impact of Water Matrices on Oxidation Effects and Mechanisms of Pharmaceuticals by Ultraviolet-Based Advanced Oxidation Technologies: A Review. *Sci. Total Environ.* **2022**, *844*, 157162. [[CrossRef](#)]
143. Domingues, E.; Fernandes, E.; Gomes, J.; Martins, R.C. Advanced Oxidation Processes Perspective Regarding Swine Wastewater Treatment. *Sci. Total Environ.* **2021**, *776*, 145958. [[CrossRef](#)]
144. Kurian, M. Advanced Oxidation Processes and Nanomaterials: A Review. *Clean. Eng. Technol.* **2021**, *2*, 100090. [[CrossRef](#)]
145. Henglein, A. Small-Particle Research: Physicochemical Properties of Extremely Small Colloidal Metal and Semiconductor Particles. *Chem. Rev.* **1989**, *89*, 1861–1873. [[CrossRef](#)]
146. Adeleye, A.S.; Conway, J.R.; Garner, K.; Huang, Y.; Su, Y.; Keller, A.A. Engineered Nanomaterials for Water Treatment and Remediation: Costs, Benefits, and Applicability. *Chem. Eng. J.* **2016**, *286*, 640–662. [[CrossRef](#)]
147. Cai, Z.; Sun, Y.; Liu, W.; Pan, F.; Sun, P.; Fu, J. An Overview of Nanomaterials Applied for Removing Dyes from Wastewater. *Environ. Sci. Pollut. Res.* **2017**, *24*, 15882–15904. [[CrossRef](#)]
148. Lei, S.; Wang, S.; Gao, B.; Zhan, Y.; Zhao, Q.; Jin, S.; Song, G.; Lyu, X.; Zhang, Y.; Tang, Y. Ultrathin Dodecyl-Sulfate-Intercalated Mg-Al Layered Double Hydroxide Nanosheets with High Adsorption Capability for Dye Pollution. *J. Colloid Interface Sci.* **2020**, *577*, 181–190. [[CrossRef](#)]
149. Janson, O.; Unosson, E.; Strømme, M.; Engqvist, H.; Welch, K. Organic Degradation Potential of a TiO<sub>2</sub>/H<sub>2</sub>O<sub>2</sub>/UV-Vis System for Dental Applications. *J. Dent.* **2017**, *67*, 53–57. [[CrossRef](#)]
150. Massoudinejad, M.; Keramati, H.; Ghaderpoori, M. Investigation of Photo-Catalytic Removal of Arsenic from Aqueous Solutions Using UV/H<sub>2</sub>O<sub>2</sub> in the Presence of ZnO Nanoparticles. *Chem. Eng. Commun.* **2020**, *207*, 1605–1615. [[CrossRef](#)]
151. Hu, L.; Wang, P.; Liu, G.; Zheng, Q.; Zhang, G. Catalytic Degradation of P-Nitrophenol by Magnetically Recoverable Fe<sub>3</sub>O<sub>4</sub> as a Persulfate Activator under Microwave Irradiation. *Chemosphere* **2020**, *240*, 124977. [[CrossRef](#)]
152. Schröder, P.; Helmreich, B.; Škrbič, B.; Carballa, M.; Papa, M.; Pastore, C.; Emre, Z.; Oehmen, A.; Langenhoff, A.; Molinos, M.; et al. Status of Hormones and Painkillers in Wastewater Effluents across Several European States—Considerations for the EU Watch List Concerning Estradiols and Diclofenac. *Environ. Sci. Pollut. Res.* **2016**, *23*, 12835–12866. [[CrossRef](#)]
153. Sellaro, M.; Bellardita, M.; Brunetti, A.; Fontananova, E.; Palmisano, L.; Drioli, E.; Barbieri, G. CO<sub>2</sub> Conversion in a Photocatalytic Continuous Membrane Reactor. *RSC Adv.* **2016**, *6*, 67418–67427. [[CrossRef](#)]
154. Bellardita, M.; Camera-Roda, G.; Loddo, V.; Parrino, F.; Palmisano, L. Coupling of Membrane and Photocatalytic Technologies for Selective Formation of High Added Value Chemicals. *Catal. Today* **2020**, *340*, 128–144. [[CrossRef](#)]
155. Camera-Roda, G.; Santarelli, F.; Augugliaro, V.; Loddo, V.; Palmisano, G.; Palmisano, L.; Yurdakal, S. Photocatalytic Process Intensification by Coupling with Pervaporation. *Catal. Today* **2011**, *161*, 209–213. [[CrossRef](#)]
156. Molinari, R.; Lavorato, C.; Argurio, P. Recent Progress of Photocatalytic Membrane Reactors in Water Treatment and in Synthesis of Organic Compounds. A Review. *Catal. Today* **2017**, *281*, 144–164. [[CrossRef](#)]
157. Gopal, G.; Alex, S.A.; Chandrasekaran, N.; Mukherjee, A. A Review on Tetracycline Removal from Aqueous Systems by Advanced Treatment Techniques. *RSC Adv.* **2020**, *10*, 27081–27095. [[CrossRef](#)]
158. Emzhina, V.; Kuzin, E.; Babusenko, E.; Krutchinina, N. Photodegradation of Tetracycline in Presence of H<sub>2</sub>O<sub>2</sub> and Metal Oxide Based Catalysts. *J. Water Process Eng.* **2021**, *39*, 101696. [[CrossRef](#)]
159. Shi, W.; Fu, Y.; Hao, C.; Guo, F.; Tang, Y. Heterogeneous Photo-Fenton Process over Magnetically Recoverable MnFe<sub>2</sub>O<sub>4</sub>/MXene Hierarchical Heterostructure for Boosted Degradation of Tetracycline. *Mater. Today Commun.* **2022**, *33*, 104449. [[CrossRef](#)]
160. Davies, A.K.; McKellar, J.F.; Phillips, G.O.; Reid, A.G. Photochemical Oxidation of Tetracycline in Aqueous Solution. *J. Chem. Soc. Perkin Trans. 2* **1979**, 369–375. [[CrossRef](#)]

161. López-Peñalver, J.J.; Sánchez-Polo, M.; Gómez-Pacheco, C.V.; Rivera-Utrilla, J. Photodegradation of Tetracyclines in Aqueous Solution by Using UV and UV/H<sub>2</sub>O<sub>2</sub> Oxidation Processes. *J. Chem. Technol. Biotechnol.* **2010**, *85*, 1325–1333. [[CrossRef](#)]
162. Serrà, A.; Gómez, E.; Michler, J.; Philippe, L. Facile Cost-Effective Fabrication of Cu@Cu<sub>2</sub>O@CuO–Microalgae Photocatalyst with Enhanced Visible Light Degradation of Tetracycline. *Chem. Eng. J.* **2021**, *413*, 127477. [[CrossRef](#)]
163. Bautitz, I.R.; Nogueira, R.F.P. Degradation of Tetracycline by Photo-Fenton Process-Solar Irradiation and Matrix Effects. *J. Photochem. Photobiol. A Chem.* **2007**, *187*, 33–39. [[CrossRef](#)]
164. Yamal-Turbay, E.; Jaén, E.; Graells, M.; Pérez-Moya, M. Enhanced Photo-Fenton Process for Tetracycline Degradation Using Efficient Hydrogen Peroxide Dosage. *J. Photochem. Photobiol. A Chem.* **2013**, *267*, 11–16. [[CrossRef](#)]
165. Zhuang, Y.; Liu, Q.; Kong, Y.; Shen, C.; Hao, H.; Dionysiou, D.D.; Shi, B. Enhanced Antibiotic Removal through a Dual-Reaction-Center Fenton-like Process in 3D Graphene Based Hydrogels. *Environ. Sci. Nano* **2019**, *6*, 388–398. [[CrossRef](#)]
166. Liu, S.; Zhao, X.R.; Sun, H.Y.; Li, R.P.; Fang, Y.F.; Huang, Y.P. The Degradation of Tetracycline in a Photo-Electro-Fenton System. *Chem. Eng. J.* **2013**, *231*, 441–448. [[CrossRef](#)]
167. Ao, X.; Sun, W.; Li, S.; Yang, C.; Li, C.; Lu, Z. Degradation of Tetracycline by Medium Pressure UV-Activated Peroxymonosulfate Process: Influencing Factors, Degradation Pathways, and Toxicity Evaluation. *Chem. Eng. J.* **2019**, *361*, 1053–1062. [[CrossRef](#)]
168. Nasser, S.; Mahvi, A.H.; Seyedsalehi, M.; Yaghmaei, K.; Nabizadeh, R.; Alimohammadi, M.; Safari, G.H. Degradation Kinetics of Tetracycline in Aqueous Solutions Using Peroxydisulfate Activated by Ultrasound Irradiation: Effect of Radical Scavenger and Water Matrix. *J. Mol. Liq.* **2017**, *241*, 704–714. [[CrossRef](#)]
169. Hou, L.; Zhang, H.; Xue, X. Ultrasound Enhanced Heterogeneous Activation of Peroxydisulfate by Magnetite Catalyst for the Degradation of Tetracycline in Water. *Sep. Purif. Technol.* **2012**, *84*, 147–152. [[CrossRef](#)]
170. Ji, Y.; Shi, Y.; Dong, W.; Wen, X.; Jiang, M.; Lu, J. Thermo-Activated Persulfate Oxidation System for Tetracycline Antibiotics Degradation in Aqueous Solution. *Chem. Eng. J.* **2016**, *298*, 225–233. [[CrossRef](#)]
171. Zhang, X.; Deng, H.; Zhang, G.; Yang, F.; Yuan, G.E. Natural Bornite as an Efficient and Cost-Effective Persulfate Activator for Degradation of Tetracycline: Performance and Mechanism. *Chem. Eng. J.* **2020**, *381*, 122717. [[CrossRef](#)]
172. Yang, Q.; Yang, X.; Yan, Y.; Sun, C.; Wu, H.; He, J.; Wang, D. Heterogeneous Activation of Peroxymonosulfate by Different Ferromanganese Oxides for Tetracycline Degradation: Structure Dependence and Catalytic Mechanism. *Chem. Eng. J.* **2018**, *348*, 263–270. [[CrossRef](#)]
173. Guan, R.; Yuan, X.; Wu, Z.; Wang, H.; Jiang, L.; Zhang, J.; Li, Y.; Zeng, G.; Mo, D. Accelerated Tetracycline Degradation by Persulfate Activated with Heterogeneous Magnetic Ni<sub>x</sub>Fe<sub>3-x</sub>O<sub>4</sub> Catalysts. *Chem. Eng. J.* **2018**, *350*, 573–584. [[CrossRef](#)]
174. Gao, Y.; Cong, S.; He, Y.; Zou, D.; Liu, Y.; Yao, B.; Sun, W. Study on the Mechanism of Degradation of Tetracycline Hydrochloride by Microwave-Activated Sodium Persulfate. *Water Sci. Technol.* **2020**, *82*, 1961–1970. [[CrossRef](#)] [[PubMed](#)]
175. Khan, M.H.; Bae, H.; Jung, J.Y. Tetracycline Degradation by Ozonation in the Aqueous Phase: Proposed Degradation Intermediates and Pathway. *J. Hazard. Mater.* **2010**, *181*, 659–665. [[CrossRef](#)] [[PubMed](#)]
176. Wang, Y.; Zhang, H.; Zhang, J.; Lu, C.; Huang, Q.; Wu, J.; Liu, F. Degradation of Tetracycline in Aqueous Media by Ozonation in an Internal Loop-Lift Reactor. *J. Hazard. Mater.* **2011**, *192*, 35–43. [[CrossRef](#)]
177. Wang, Y.; Zhang, H.; Chen, L. Ultrasound Enhanced Catalytic Ozonation of Tetracycline in a Rectangular Air-Lift Reactor. *Catal. Today* **2011**, *175*, 283–292. [[CrossRef](#)]
178. Gómez-Pacheco, C.V.; Sánchez-Polo, M.; Rivera-Utrilla, J.; López-Peñalver, J. Tetracycline Removal from Waters by Integrated Technologies Based on Ozonation and Biodegradation. *Chem. Eng. J.* **2011**, *178*, 115–121. [[CrossRef](#)]
179. Hou, L.; Zhang, H.; Wang, L.; Chen, L. Ultrasound-Enhanced Magnetite Catalytic Ozonation of Tetracycline in Water. *Chem. Eng. J.* **2013**, *229*, 577–584. [[CrossRef](#)]
180. Wang, Y.; Zhang, H.; Chen, L.; Wang, S.; Zhang, D. Ozonation Combined with Ultrasound for the Degradation of Tetracycline in a Rectangular Air-Lift Reactor. *Sep. Purif. Technol.* **2012**, *84*, 138–146. [[CrossRef](#)]
181. Safari, G.H.; Hoseini, M.; Seyedsalehi, M.; Kamani, H.; Jaafari, J.; Mahvi, A.H. Photocatalytic Degradation of Tetracycline Using Nanosized Titanium Dioxide in Aqueous Solution. *Int. J. Environ. Sci. Technol.* **2015**, *12*, 603–616. [[CrossRef](#)]
182. Wang, P.; Yap, P.S.; Lim, T.T. C-N-S Tridoped TiO<sub>2</sub> for Photocatalytic Degradation of Tetracycline under Visible-Light Irradiation. *Appl. Catal. A Gen.* **2011**, *399*, 252–261. [[CrossRef](#)]
183. Mohammadi, M.; Sabbaghi, S.; Binazadeh, M.; Ghaedi, S. Chemosphere Type-1  $\alpha$ -Fe<sub>2</sub>O<sub>3</sub>/TiO<sub>2</sub> Photocatalytic Degradation of Tetracycline from Wastewater Using CCD-Based RSM Optimization. *Chemosphere* **2023**, *336*, 139311. [[CrossRef](#)]
184. Sharma, M.; Mandal, M.K.; Pandey, S.; Kumar, R.; Dubey, K.K. Visible-Light-Driven Photocatalytic Degradation of Tetracycline Using Heterostructured Cu<sub>2</sub>O-TiO<sub>2</sub> Nanotubes, Kinetics, and Toxicity Evaluation of Degraded Products on Cell Lines. *ACS Omega* **2022**, *7*, 33572–33586. [[CrossRef](#)] [[PubMed](#)]
185. Ahmadi, M.; Ramezani Motlagh, H.; Jaafarzadeh, N.; Mostoufi, A.; Saeedi, R.; Barzegar, G.; Jorfi, S. Enhanced Photocatalytic Degradation of Tetracycline and Real Pharmaceutical Wastewater Using MWCNT/TiO<sub>2</sub> Nano-Composite. *J. Environ. Manag.* **2017**, *186*, 55–63. [[CrossRef](#)] [[PubMed](#)]
186. Wang, W.; Fang, J.; Shao, S.; Lai, M.; Lu, C. Compact and Uniform TiO<sub>2</sub>@g-C<sub>3</sub>N<sub>4</sub> Core-Shell Quantum Heterojunction for Photocatalytic Degradation of Tetracycline Antibiotics. *Appl. Catal. B* **2017**, *217*, 57–64. [[CrossRef](#)]
187. Phakathi, N.A.; Tichapondwa, S.M.; Chirwa, E.M.N. Photocatalytic Degradation of Tetracycline Using Visible-Light-Driven Porous g-C<sub>3</sub>N<sub>4</sub> Nanosheets Catalyst. *Chem. Eng. Trans.* **2022**, *96*, 391–396. [[CrossRef](#)]

188. Gaffar, S.; Kumar, A.; Alam, J.; Riaz, U. Efficient Visible Light-Induced Photocatalytic Degradation of Tetracycline Hydrochloride Using  $\text{CuFe}_2\text{O}_4$  and PANI/ $\text{CuFe}_2\text{O}_4$  Nanohybrids. *Environ. Sci. Pollut. Res.* **2023**, *30*, 108878–108888. [CrossRef] [PubMed]
189. Liu, W.; Wei, C.; Peng, R.; Chu, R.; Sun, H.; Zhang, X.; Xie, F. Persulfate Assisted Photocatalytic Degradation of Tetracycline by Bismuth Titanate under Visible Light Irradiation. *New J. Chem.* **2022**, *46*, 10854–10862. [CrossRef]
190. Kaushal, S.; Kumar, A.; Bains, H.; Singh, P.P. Photocatalytic Degradation of Tetracycline Antibiotic and Organic Dyes Using Biogenic Synthesized  $\text{CuO}/\text{Fe}_2\text{O}_3$  Nanocomposite: Pathways and Mechanism Insights. *Environ. Sci. Pollut. Res.* **2023**, *30*, 37092–37104. [CrossRef]
191. Semeraro, P.; Bettini, S.; Sawalha, S.; Pal, S.; Licciulli, A.; Marzo, F.; Lovergine, N.; Valli, L.; Giancane, G. Photocatalytic Degradation of Tetracycline by  $\text{ZnO}/\gamma\text{-Fe}_2\text{O}_3$  Paramagnetic Nanocomposite Material. *Nanomaterials* **2020**, *10*, 1458. [CrossRef]
192. Nguetsa Kuate, L.J.; Chen, Z.; Lu, J.; Wen, H.; Guo, F.; Shi, W. Photothermal-Assisted Photocatalytic Degradation of Tetracycline in Seawater Based on the Black  $\text{g-C}_3\text{N}_4$  Nanosheets with Cyano Group Defects. *Catalysts* **2023**, *13*, 1147. [CrossRef]
193. Chen, F.; Yang, Q.; Sun, J.; Yao, F.; Wang, S.; Wang, Y.; Wang, X.; Li, X.; Niu, C.; Wang, D.; et al. Enhanced Photocatalytic Degradation of Tetracycline by  $\text{AgI}/\text{BiVO}_4$  Heterojunction under Visible-Light Irradiation: Mineralization Efficiency and Mechanism. *ACS Appl. Mater. Interfaces* **2016**, *8*, 32887–32900. [CrossRef]
194. Jia, X.; Wang, F.; Xu, X.; Liu, C.; Zhang, L.; Jiao, S.; Zhu, G.; Wang, X.; Yu, G. Highly Efficient Photocatalytic Degradation of Tetracycline by Modifying UiO-66 via Different Regulation Strategies. *ACS Omega* **2023**, *8*, 27375–27385. [CrossRef]
195. Oluwole, A.O.; Olatunji, O.S. Photocatalytic Degradation of Tetracycline in Aqueous Systems under Visible Light Irradiation Using Needle-like  $\text{SnO}_2$  Nanoparticles Anchored on Exfoliated  $\text{g-C}_3\text{N}_4$ . *Environ. Sci. Eur.* **2022**, *34*, 5. [CrossRef]
196. Zhang, X.X.; Wang, X.J.; Niu, Y.Y. Photocatalytic Degradation of Tetracycline by Supramolecular Materials Constructed with Organic Cations and Silver Iodide. *Catalysts* **2022**, *12*, 1581. [CrossRef]
197. Doosti, M.; Jahanshahi, R.; Laleh, S.; Sobhani, S.; Sansano, J.M. Solar Light Induced Photocatalytic Degradation of Tetracycline in the Presence of  $\text{ZnO}/\text{NiFe}_2\text{O}_4/\text{Co}_3\text{O}_4$  as a New and Highly Efficient Magnetically Separable Photocatalyst. *Front. Chem.* **2022**, *10*, 1013349. [CrossRef]
198. Li, S.; Wang, C.; Liu, Y.; Cai, M.; Wang, Y.; Zhang, H.; Guo, Y.; Zhao, W.; Wang, Z.; Chen, X. Photocatalytic Degradation of Tetracycline Antibiotic by a Novel  $\text{Bi}_2\text{Sn}_2\text{O}_7/\text{Bi}_2\text{MoO}_6$  S-Scheme Heterojunction: Performance, Mechanism Insight and Toxicity Assessment. *Chem. Eng. J.* **2022**, *429*, 132519. [CrossRef]
199. Huang, J.; Xue, P.; Wang, S.; Han, S.; Lin, L.; Chen, X.; Wang, Z. Fabrication of Zirconium-Based Metal-Organic Frameworks@tungsten Trioxide ( $\text{UiO-66-NH}_2@\text{WO}_3$ ) Heterostructure on Carbon Cloth for Efficient Photocatalytic Removal of Tetracycline Antibiotic under Visible Light. *J. Colloid Interface Sci.* **2022**, *606*, 1509–1523. [CrossRef]
200. Palominos, R.A.; Mondaca, M.A.; Giraldo, A.; Peñuela, G.; Pérez-Moya, M.; Mansilla, H.D. Photocatalytic Oxidation of the Antibiotic Tetracycline on  $\text{TiO}_2$  and  $\text{ZnO}$  Suspensions. *Catal. Today* **2009**, *144*, 100–105. [CrossRef]
201. Wang, X.; Wang, A.; Ma, J. Visible-Light-Driven Photocatalytic Removal of Antibiotics by Newly Designed  $\text{C}_3\text{N}_4@\text{MnFe}_2\text{O}_4$ -Graphene Nanocomposites. *J. Hazard. Mater.* **2017**, *336*, 81–92. [CrossRef] [PubMed]
202. Alyani, S.J.; Pirbazari, A.E.; Khalilsaraei, F.E.; Kolur, N.A.; Gilani, N. Growing Co-Doped  $\text{TiO}_2$  Nanosheets on Reduced Graphene Oxide for Efficient Photocatalytic Removal of Tetracycline Antibiotic from Aqueous Solution and Modeling the Process by Artificial Neural Network. *J. Alloys Compd.* **2019**, *799*, 169–182. [CrossRef]
203. Song, J.; Wu, X.; Zhang, M.; Liu, C.; Yu, J.; Sun, G.; Si, Y.; Ding, B. Highly Flexible, Core-Shell Heterostructured, and Visible-Light-Driven Titania-Based Nanofibrous Membranes for Antibiotic Removal and E. *Coil Inactivation*. *Chem. Eng. J.* **2020**, *379*, 122269. [CrossRef]
204. Wang, Q.; Li, P.; Zhang, Z.; Jiang, C.; Zuojiào, K.; Liu, J.; Wang, Y. Kinetics and Mechanism Insights into the Photodegradation of Tetracycline Hydrochloride and Ofloxacin Mixed Antibiotics with the Flower-like  $\text{BiOCl}/\text{TiO}_2$  Heterojunction. *J. Photochem. Photobiol. A Chem.* **2019**, *378*, 114–124. [CrossRef]
205. Wierzbicka, E.; Altomare, M.; Wu, M.; Liu, N.; Yokosawa, T.; Fehn, D.; Qin, S.; Meyer, K.; Unruh, T.; Spiecker, E.; et al. Reduced Grey Brookite for Noble Metal Free Photocatalytic  $\text{H}_2$  evolution. *J. Mater. Chem. A Mater.* **2021**, *9*, 1168–1179. [CrossRef]
206. Belhouchet, N.; Hamdi, B.; Chenchouni, H.; Bessekhoud, Y. Photocatalytic Degradation of Tetracycline Antibiotic Using New Calcite/Titania Nanocomposites. *J. Photochem. Photobiol. A Chem.* **2019**, *372*, 196–205. [CrossRef]
207. Lakhera, S.K.; Hafeez, H.Y.; Veluswamy, P.; Ganesh, V.; Khan, A.; Ikeda, H.; Neppolian, B. Enhanced Photocatalytic Degradation and Hydrogen Production Activity of in Situ Grown  $\text{TiO}_2$  Coupled  $\text{NiTiO}_3$  Nanocomposites. *Appl. Surf. Sci.* **2018**, *449*, 790–798. [CrossRef]
208. Yang, Q.; Wang, S.; Chen, F.; Luo, K.; Sun, J.; Gong, C.; Yao, F.; Wang, X.; Wu, J.; Li, X.; et al. Enhanced Visible-Light-Driven Photocatalytic Removal of Refractory Pollutants by  $\text{Zn}/\text{Fe}$  Mixed Metal Oxide Derived from Layered Double Hydroxide. *Catal. Commun.* **2017**, *99*, 15–19. [CrossRef]
209. Galedari, M.; Mehdipour Ghazi, M.; Rashid Mirmasoomi, S. Photocatalytic Process for the Tetracycline Removal under Visible Light: Presenting a Degradation Model and Optimization Using Response Surface Methodology (RSM). *Chem. Eng. Res. Des.* **2019**, *145*, 323–333. [CrossRef]
210. Yu, J.; Kiwi, J.; Zivkovic, I.; Rønnow, H.M.; Wang, T.; Rtimi, S. Quantification of the Local Magnetized Nanotube Domains Accelerating the Photocatalytic Removal of the Emerging Pollutant Tetracycline. *Appl. Catal. B* **2019**, *248*, 450–458. [CrossRef]

211. Hong, Y.; Li, C.; Yin, B.; Li, D.; Zhang, Z.; Mao, B.; Fan, W.; Gu, W.; Shi, W. Promoting Visible-Light-Induced Photocatalytic Degradation of Tetracycline by an Efficient and Stable Beta-Bi<sub>2</sub>O<sub>3</sub>@g-C<sub>3</sub>N<sub>4</sub> Core/Shell Nanocomposite. *Chem. Eng. J.* **2018**, *338*, 137–146. [CrossRef]
212. Tun, P.P.; Wang, J.; Khaing, T.T.; Wu, X.; Zhang, G. Fabrication of Functionalized Plasmonic Ag Loaded Bi<sub>2</sub>O<sub>3</sub>/Montmorillonite Nanocomposites for Efficient Photocatalytic Removal of Antibiotics and Organic Dyes. *J. Alloys Compd.* **2020**, *818*, 152836. [CrossRef]
213. Heidari, S.; Haghghi, M.; Shabani, M. Sono-Photodeposition of Ag over Sono-Fabricated Mesoporous Bi<sub>2</sub>Sn<sub>2</sub>O<sub>7</sub>-Two Dimensional Carbon Nitride: Type-II Plasmonic Nano-Heterojunction with Simulated Sunlight-Driven Elimination of Drug. *Chem. Eng. J.* **2020**, *389*, 123418. [CrossRef]
214. Wang, C.Y.; Zhang, X.; Qiu, H.B.; Huang, G.X.; Yu, H.Q. Bi<sub>24</sub>O<sub>31</sub>Br<sub>10</sub> Nanosheets with Controllable Thickness for Visible-Light-Driven Catalytic Degradation of Tetracycline Hydrochloride. *Appl. Catal. B* **2017**, *205*, 615–623. [CrossRef]
215. Ha, G.H.; Mohan, H.; Oh, H.S.; Kim, G.; Seralathan, K.K.; Shin, T. Photocatalytic Degradation of Tetracycline Using Hybrid Ag/Ag<sub>2</sub>S@BiOI Nanowires: Degradation Mechanism and Toxicity Evaluation. *Chemosphere* **2022**, *303*, 135091. [CrossRef] [PubMed]
216. Ye, J.; Liu, J.; Huang, Z.; Wu, S.; Dai, X.; Zhang, L.; Cui, L. Effect of Reduced Graphene Oxide Doping on Photocatalytic Reduction of Cr(VI) and Photocatalytic Oxidation of Tetracycline by ZnAlTi Layered Double Oxides under Visible Light. *Chemosphere* **2019**, *227*, 505–513. [CrossRef]
217. Yu, F.; Li, Y.; Han, S.; Ma, J. Adsorptive Removal of Antibiotics from Aqueous Solution Using Carbon Materials. *Chemosphere* **2016**, *153*, 365–385. [CrossRef] [PubMed]
218. Bai, X.; Wang, Y.J.; Li, Y.; Wang, X.J. Adsorption-Photocatalytic Remediation for Series of Tetracycline Contaminants with BiOCl-CdS Composite under Simulated Sunlight. *J. Taiwan Inst. Chem. Eng.* **2019**, *104*, 94–105. [CrossRef]
219. Méndez-Arriaga, F.; Torres-Palma, R.A.; Pétrier, C.; Esplugas, S.; Gimenez, J.; Pulgarin, C. Ultrasonic Treatment of Water Contaminated with Ibuprofen. *Water Res.* **2008**, *42*, 4243–4248. [CrossRef]
220. Lee, Y.; Lee, S.; Cui, M.; Ren, Y.; Park, B.; Ma, J.; Han, Z.; Khim, J. Activation of Peroxodisulfate and Peroxymonosulfate by Ultrasound with Different Frequencies: Impact on Ibuprofen Removal Efficient, Cost Estimation and Energy Analysis. *Chem. Eng. J.* **2021**, *413*, 127487. [CrossRef]
221. da Luz, V.C.; Bazoti, S.F.; Behling, L.; Dalla Rosa, C.; Pasquali, G.D.L. Enhanced UV Direct Photolysis and UV/H<sub>2</sub>O<sub>2</sub> for Oxidation of Triclosan and Ibuprofen in Synthetic Effluent: An Experimental Study. *Water Air Soil Pollut.* **2022**, *233*, 126. [CrossRef]
222. Adityosulindro, S.; Julcour, C.; Barthe, L. Heterogeneous Fenton Oxidation Using Fe-ZSM5 Catalyst for Removal of Ibuprofen in Wastewater. *J. Environ. Chem. Eng.* **2018**, *6*, 5920–5928. [CrossRef]
223. Adityosulindro, S.; Julcour, C.; Riboul, D.; Barthe, L. Degradation of Ibuprofen by Photo-Based Advanced Oxidation Processes: Exploring Methods of Activation and Related Reaction Routes. *Int. J. Environ. Sci. Technol.* **2022**, *19*, 3247–3260. [CrossRef]
224. Méndez-Arriaga, F.; Esplugas, S.; Giménez, J. Degradation of the Emerging Contaminant Ibuprofen in Water by Photo-Fenton. *Water Res.* **2010**, *44*, 589–595. [CrossRef]
225. Quero-Pastor, M.J.; Garrido-Perez, M.C.; Acevedo, A.; Quiroga, J.M. Ozonation of Ibuprofen: A Degradation and Toxicity Study. *Sci. Total Environ.* **2014**, *466–467*, 957–964. [CrossRef]
226. Almeida, V.M.; Orge, C.A.; Pereira, M.F.R.; Soares, O.S.G.P. O<sub>3</sub> Based Advanced Oxidation for Ibuprofen Degradation. *Chin. J. Chem. Eng.* **2022**, *42*, 277–284. [CrossRef]
227. Rao, Y.F.; Xue, D.; Pan, H.; Feng, J.; Li, Y. Degradation of Ibuprofen by a Synergistic UV/Fe(III)/Oxone Process. *Chem. Eng. J.* **2016**, *283*, 65–75. [CrossRef]
228. Li, X.; Wang, Y.; Yuan, S.; Li, Z.; Wang, B.; Huang, J.; Deng, S.; Yu, G. Degradation of the Anti-Inflammatory Drug Ibuprofen by Electro-Peroxone Process. *Water Res.* **2014**, *63*, 81–93. [CrossRef] [PubMed]
229. Miranda, M.O.; Cabral Cavalcanti, W.E.; Barbosa, F.F.; Antonio De Sousa, J.; Ivan Da Silva, F.; Pergher, S.B.C.; Braga, T.P. Photocatalytic Degradation of Ibuprofen Using Titanium Oxide: Insights into the Mechanism and Preferential Attack of Radicals. *RSC Adv.* **2021**, *11*, 27720–27733. [CrossRef] [PubMed]
230. Candido, J.P.; Andrade, S.J.; Fonseca, A.L.; Silva, F.S.; Silva, M.R.A.; Kondo, M.M. Ibuprofen Removal by Heterogeneous Photocatalysis and Ecotoxicological Evaluation of the Treated Solutions. *Environ. Sci. Pollut. Res.* **2016**, *23*, 19911–19920. [CrossRef]
231. Khalaf, S.; Shoqeir, J.H.; Lelario, F.; Scrano, L.; Bufo, S.A.; Karaman, R. TiO<sub>2</sub> and Active Coated Glass Photodegradation of Ibuprofen. *Catalysts* **2020**, *10*, 560. [CrossRef]
232. Agócs, T.Z.; Puskás, I.; Varga, E.; Molnár, M.; Fenyvesi, É. Stabilization of Nanosized Titanium Dioxide by Cyclodextrin Polymers and Its Photocatalytic Effect on the Degradation of Wastewater Pollutants. *Beilstein J. Org. Chem.* **2016**, *12*, 2873–2882. [CrossRef]
233. Jallouli, N.; Pastrana-Martínez, L.M.; Ribeiro, A.R.; Moreira, N.F.F.; Faria, J.L.; Hentati, O.; Silva, A.M.T.; Ksibi, M. Heterogeneous Photocatalytic Degradation of Ibuprofen in Ultrapure Water, Municipal and Pharmaceutical Industry Wastewaters Using a TiO<sub>2</sub>/UV-LED System. *Chem. Eng. J.* **2018**, *334*, 976–984. [CrossRef]
234. Jiménez-Salcedo, M.; Monge, M.; Tena, M.T. Photocatalytic Degradation of Ibuprofen in Water Using TiO<sub>2</sub>/UV and g-C<sub>3</sub>N<sub>4</sub>/Visible Light: Study of Intermediate Degradation Products by Liquid Chromatography Coupled to High-Resolution Mass Spectrometry. *Chemosphere* **2019**, *215*, 605–618. [CrossRef]

235. Li, F.; Kang, Y.; Chen, M.; Liu, G.; Lv, W.; Yao, K.; Chen, P.; Huang, H. Photocatalytic Degradation and Removal Mechanism of Ibuprofen via Monoclinic BiVO<sub>4</sub> under Simulated Solar Light. *Chemosphere* **2016**, *150*, 139–144. [[CrossRef](#)] [[PubMed](#)]
236. Alhumade, H.; Akhtar, J.; Al-Shahrani, S.; Moujдин, I.A.; Tahir, M.B. Ozonation of Ibuprofen in Presence of SrWO<sub>4</sub>/ZnO Photo-Catalyst. *Emerg. Contam.* **2022**, *8*, 391–399. [[CrossRef](#)]
237. Fidelis, M.Z.; Favaro, Y.B.; dos Santos, A.S.G.G.; Pereira, M.F.R.; Brackmann, R.; Lenzi, G.G.; Soares, O.S.G.P.; Andreo, O.A.B. Enhancing Ibuprofen and 4-Isobutylacetophenone Degradation: Exploiting the Potential of Nb<sub>2</sub>O<sub>5</sub> Sol-Gel Catalysts in Photocatalysis, Catalytic Ozonation, and Photocatalytic Ozonation. *J. Environ. Chem. Eng.* **2023**, *11*, 110690. [[CrossRef](#)]
238. Espindola, J.C.; Cristóvão, R.O.; Mendes, A.; Boaventura, R.A.R.; Vilar, V.J.P. Photocatalytic Membrane Reactor Performance towards Oxytetracycline Removal from Synthetic and Real Matrices: Suspended vs Immobilized TiO<sub>2</sub>-P25. *Chem. Eng. J.* **2019**, *378*, 122114. [[CrossRef](#)]
239. Sun, H.; Zhou, T.; Kang, J.; Zhao, Y.; Zhang, Y.; Wang, T.; Yin, X. High-Efficient Degradation of Oxytetracycline by Visible Photo-Fenton Process Using MnFe<sub>2</sub>O<sub>4</sub>/g-C<sub>3</sub>N<sub>4</sub>: Performance and Mechanisms. *Sep. Purif. Technol.* **2022**, *299*, 121771. [[CrossRef](#)]
240. Zhang, Z.; Du, C.; Zhang, Y.; Yu, G.; Xiong, Y.; Zhou, L.; Liu, Y.; Chi, T.; Wang, G.; Su, Y.; et al. Degradation of Oxytetracycline by Magnetic MOFs Heterojunction Photocatalyst with Persulfate: High Stability and Wide Range. *Environ. Sci. Pollut. Res.* **2022**, *29*, 30019–30029. [[CrossRef](#)]
241. Ma, Y.; Wang, R.; Gao, C.; Han, R. Carbon Nanotube-Loaded Copper-Nickel Ferrite Activated Persulfate System for Adsorption and Degradation of Oxytetracycline Hydrochloride. *J. Colloid Interface Sci.* **2023**, *640*, 761–774. [[CrossRef](#)]
242. Li, K.; Yediler, A.; Yang, M.; Schulte-Hostede, S.; Hung, M. Ozonation of Oxytetracycline and Toxicological Assessment of Its Oxidation By-Products. *Chemosphere* **2008**, *72*, 473–478. [[CrossRef](#)]
243. Do Vinh, T.; Nguyen, D.; Nguyen Trung, K.; Le, P. TiO<sub>2</sub> and Au-TiO<sub>2</sub> Nanomaterials for Rapid Photocatalytic Degradation of Antibiotic Residues in Aquaculture Wastewater. *Materiasl* **2019**, *12*, 2434. [[CrossRef](#)]
244. Augugliaro, V.; García-López, E.; Loddo, V.; Malato-Rodríguez, S.; Maldonado, I.; Marci, G.; Molinari, R.; Palmisano, L. Degradation of Lincomycin in Aqueous Medium: Coupling of Solar Photocatalysis and Membrane Separation. *Sol. Energy* **2005**, *79*, 402–408. [[CrossRef](#)]
245. Deng, Y.; Liu, J.; Huang, Y.; Ma, M.; Liu, K.; Dou, X.; Wang, Z.; Qu, S.; Wang, Z. Engineering the Photocatalytic Behaviors of g/C<sub>3</sub>N<sub>4</sub>-Based Metal-Free Materials for Degradation of a Representative Antibiotic. *Adv. Funct. Mater.* **2020**, *30*, 2002353. [[CrossRef](#)]
246. Kontogiannis, A.; Evgenidou, E.; Nannou, C.; Bikiaris, D.; Lambropoulou, D. MOF-Based Photocatalytic Degradation of the Antibiotic Lincomycin Enhanced by Hydrogen Peroxide and Persulfate: Kinetics, Elucidation of Transformation Products and Toxicity Assessment. *J. Environ. Chem. Eng.* **2022**, *10*, 108112. [[CrossRef](#)]
247. Tan, J.X.; Chen, Z.Y.; Chen, C.H.; Hsieh, M.F.; Lin, A.Y.C.; Chen, S.S.; Wu, K.C.W. Efficient Adsorption and Photocatalytic Degradation of Water Emerging Contaminants through Nanoarchitectonics of Pore Sizes and Optical Properties of Zirconium-Based MOFs. *J. Hazard. Mater.* **2023**, *451*, 131113. [[CrossRef](#)]
248. Farhadian, N.; Akbarzadeh, R.; Pirsasheb, M.; Jen, T.C.; Fakhri, Y.; Asadi, A. Chitosan Modified N, S-Doped TiO<sub>2</sub> and N, S-Doped ZnO for Visible Light Photocatalytic Degradation of Tetracycline. *Int. J. Biol. Macromol.* **2019**, *132*, 360–373. [[CrossRef](#)]
249. Çağlar Yılmaz, H.; Akgeyik, E.; Bougarrani, S.; El Azzouzi, M.; Erdemoğlu, S. Photocatalytic Degradation of Amoxicillin Using Co-Doped TiO<sub>2</sub> Synthesized by Reflux Method and Monitoring of Degradation Products by LC-MS/MS. *J. Dispers. Sci. Technol.* **2020**, *41*, 414–425. [[CrossRef](#)]
250. Balarak, D.; Mengelizadeh, N.; Rajiv, P.; Chandrika, K. Photocatalytic Degradation of Amoxicillin from Aqueous Solutions by Titanium Dioxide Nanoparticles Loaded on Graphene Oxide. *Environ. Sci. Pollut. Res.* **2021**, *28*, 49743–49754. [[CrossRef](#)]
251. Aba-Guevara, C.G.; Medina-Ramírez, I.E.; Hernández-Ramírez, A.; Jáuregui-Rincón, J.; Lozano-Álvarez, J.A.; Rodríguez-López, J.L. Comparison of Two Synthesis Methods on the Preparation of Fe, N-Co-Doped TiO<sub>2</sub> Materials for Degradation of Pharmaceutical Compounds under Visible Light. *Ceram. Int.* **2017**, *43*, 5068–5079. [[CrossRef](#)]
252. Al-Musawi, T.J.; Yilmaz, M.; Ramírez-Coronel, A.A.; Al-Awsi, G.R.L.; Alwaily, E.R.; Asghari, A.; Balarak, D. Degradation of Amoxicillin under a UV or Visible Light Photocatalytic Treatment Process Using Fe<sub>2</sub>O<sub>3</sub>/Bentonite/TiO<sub>2</sub>: Performance, Kinetic, Degradation Pathway, Energy Consumption, and Toxicology Studies. *Optik* **2023**, *272*, 170230. [[CrossRef](#)]
253. Zhou, L.; Guo, X.; Lai, C.; Wang, W. Electro-Photocatalytic Degradation of Amoxicillin Using Calcium Titanate. *Open Chem.* **2018**, *16*, 949–955. [[CrossRef](#)]
254. Elmolla, E.S.; Chaudhuri, M. Comparison of Different Advanced Oxidation Processes for Treatment of Antibiotic Aqueous Solution. *Desalination* **2010**, *256*, 43–47. [[CrossRef](#)]
255. Ashraf, A.; Liu, G.; Yousaf, B.; Arif, M.; Ahmed, R.; Rashid, A.; Riaz, L.; Rashid, M.S. *Phyto-Mediated Photocatalysis: A Critical Review of in-Depth Base to Reactive Radical Generation for Erythromycin Degradation*; Springer: Berlin/Heidelberg, Germany, 2022; Volume 29, ISBN 0123456789.
256. Chu, L.; Zhuang, R.; Chen, D.; Wang, J.; Shen, Y. Degradation of Macrolide Antibiotic Erythromycin and Reduction of Antimicrobial Activity Using Persulfate Activated by Gamma Radiation in Different Water Matrices. *Chem. Eng. J.* **2019**, *361*, 156–166. [[CrossRef](#)]
257. Albornoz, L.L.; da Silva, S.W.; Bortolozzi, J.P.; Banús, E.D.; Brussino, P.; Ulla, M.A.; Bernardes, A.M. Degradation and Mineralization of Erythromycin by Heterogeneous Photocatalysis Using SnO<sub>2</sub>-Doped TiO<sub>2</sub> Structured Catalysts: Activity and Stability. *Chemosphere* **2021**, *268*, 128858. [[CrossRef](#)] [[PubMed](#)]

258. Xekoukoulotakis, N.P.; Xinidis, N.; Chroni, M.; Mantzavinos, D.; Venieri, D.; Hapeshi, E.; Fatta-Kassinos, D. UV-A/TiO<sub>2</sub> Photocatalytic Decomposition of Erythromycin in Water: Factors Affecting Mineralization and Antibiotic Activity. *Catal. Today* **2010**, *151*, 29–33. [[CrossRef](#)]
259. Vignesh, K.; Rajarajan, M.; Suganthi, A. Photocatalytic Degradation of Erythromycin under Visible Light by Zinc Phthalocyanine-Modified Titania Nanoparticles. *Mater. Sci. Semicond. Process* **2014**, *23*, 98–103. [[CrossRef](#)]
260. Li, G.; Wang, B.; Zhang, J.; Wang, R.; Liu, H. Rational Construction of a Direct Z-Scheme g-C<sub>3</sub>N<sub>4</sub>/CdS Photocatalyst with Enhanced Visible Light Photocatalytic Activity and Degradation of Erythromycin and Tetracycline. *Appl. Surf. Sci.* **2019**, *478*, 1056–1064. [[CrossRef](#)]
261. Mohsin, M.; Bhatti, I.A.; Iqbal, M.; Naz, S.; Ashar, A.; Nisar, J.; Al-Fawzan, F.F.; Alissa, S.A. Oxidative Degradation of Erythromycin Using Calcium Carbonate under UV and Solar Light Irradiation: Condition Optimized by Response Surface Methodology. *J. Water Process Eng.* **2021**, *44*, 102433. [[CrossRef](#)]
262. Fakhri, A.; Rashidi, S.; Tyagi, I.; Agarwal, S.; Gupta, V.K. Photodegradation of Erythromycin Antibiotic by  $\gamma$ -Fe<sub>2</sub>O<sub>3</sub>/SiO<sub>2</sub> Nanocomposite: Response Surface Methodology Modeling and Optimization. *J. Mol. Liq.* **2016**, *214*, 378–383. [[CrossRef](#)]
263. Baran, W.; Adamek, E.; Sobczak, A.; Makowski, A. Photocatalytic Degradation of Sulfa Drugs with TiO<sub>2</sub>, Fe Salts and TiO<sub>2</sub>/FeCl<sub>3</sub> in Aquatic Environment-Kinetics and Degradation Pathway. *Appl. Catal. B* **2009**, *90*, 516–525. [[CrossRef](#)]
264. Mendiola-Alvarez, S.Y.; Palomino-Cabello, C.; Hernández-Ramírez, A.; Turnes-Palomino, G.; Guzmán-Mar, J.L.; Hinojosa-Reyes, L. Coupled Heterogeneous Photocatalysis Using a P-TiO<sub>2</sub>-AFe<sub>2</sub>O<sub>3</sub> Catalyst and K<sub>2</sub>S<sub>2</sub>O<sub>8</sub> for the Efficient Degradation of a Sulfonamide Mixture. *J. Photochem. Photobiol. A Chem.* **2020**, *394*, 112485. [[CrossRef](#)]
265. Wang, N.; Li, X.; Yang, Y.; Zhou, Z.; Shang, Y.; Zhuang, X. Photocatalytic Degradation of Sulfonamides by Bi<sub>2</sub>O<sub>3</sub>-TiO<sub>2</sub>/PAC Ternary Composite: Mechanism, Degradation Pathway. *J. Water Process Eng.* **2020**, *36*, 101335. [[CrossRef](#)]
266. Batista, A.P.S.; Nogueira, R.F.P. Parameters Affecting Sulfonamide Photo-Fenton Degradation—Iron Complexation and Substituent Group. *J. Photochem. Photobiol. A Chem.* **2012**, *232*, 8–13. [[CrossRef](#)]
267. Pelalak, R.; Alizadeh, R.; Gharehabani, E.; Heidari, Z. Degradation of Sulfonamide Antibiotics Using Ozone-Based Advanced Oxidation Process: Experimental, Modeling, Transformation Mechanism and DFT Study. *Sci. Total Environ.* **2020**, *734*, 139446. [[CrossRef](#)]
268. Du, J.; Ma, S.; Yan, Y.; Li, K.; Zhao, F.; Zhou, J. Corn-Silk-Templated Synthesis of TiO<sub>2</sub> Nanotube Arrays with Ag<sub>3</sub>PO<sub>4</sub> Nanoparticles for Efficient Oxidation of Organic Pollutants and Pathogenic Bacteria under Solar Light. *Colloids Surf. A Physicochem. Eng. Asp.* **2019**, *572*, 237–249. [[CrossRef](#)]
269. Liu, Z.; Liu, X.; Lu, Q.; Wang, Q.; Ma, Z. TiOF<sub>2</sub>/TiO<sub>2</sub> Composite Nanosheets: Effect of Hydrothermal Synthesis Temperature on Physicochemical Properties and Photocatalytic Activity. *J. Taiwan Inst. Chem. Eng.* **2019**, *96*, 214–222. [[CrossRef](#)]
270. El-Kemary, M.; El-Shamy, H.; El-Mehasseb, I. Photocatalytic Degradation of Ciprofloxacin Drug in Water Using ZnO Nanoparticles. *J. Lumin.* **2010**, *130*, 2327–2331. [[CrossRef](#)]
271. Wen, X.J.; Niu, C.G.; Zhang, L.; Liang, C.; Guo, H.; Zeng, G.M. Photocatalytic Degradation of Ciprofloxacin by a Novel Z-Scheme CeO<sub>2</sub>-Ag/AgBr Photocatalyst: Influencing Factors, Possible Degradation Pathways, and Mechanism Insight. *J. Catal.* **2018**, *358*, 141–154. [[CrossRef](#)]
272. Yu, X.; Zhang, J.; Zhang, J.; Niu, J.; Zhao, J.; Wei, Y.; Yao, B. Photocatalytic Degradation of Ciprofloxacin Using Zn-Doped Cu<sub>2</sub>O Particles: Analysis of Degradation Pathways and Intermediates. *Chem. Eng. J.* **2019**, *374*, 316–327. [[CrossRef](#)]
273. Yang, L.; Xiang, Y.; Jia, F.; Xia, L.; Gao, C.; Wu, X.; Peng, L.; Liu, J.; Song, S. Photo-Thermal Synergy for Boosting Photo-Fenton Activity with RGO-ZnFe<sub>2</sub>O<sub>4</sub>: Novel Photo-Activation Process and Mechanism toward Environment Remediation. *Appl. Catal. B* **2021**, *292*, 120198. [[CrossRef](#)]
274. Ge, X.; Meng, G.; Liu, B. Ultrasound-Assisted Preparation of LaFeO<sub>3</sub>/Polystyrene for Efficient Photo-Fenton Degradation of Ciprofloxacin Hydrochloride. *J. Ind. Eng. Chem.* **2022**, *115*, 390–401. [[CrossRef](#)]
275. Gupta, A.; Garg, A. Degradation of Ciprofloxacin Using Fenton's Oxidation: Effect of Operating Parameters, Identification of Oxidized by-Products and Toxicity Assessment. *Chemosphere* **2018**, *193*, 1181–1188. [[CrossRef](#)] [[PubMed](#)]

**Disclaimer/Publisher's Note:** The statements, opinions and data contained in all publications are solely those of the individual author(s) and contributor(s) and not of MDPI and/or the editor(s). MDPI and/or the editor(s) disclaim responsibility for any injury to people or property resulting from any ideas, methods, instructions or products referred to in the content.